*inorganics*

MDPI

*Review*

# Halogen Bonding: A Halogen-Centered Noncovalent Interaction Yet to Be Understood

**Pradeep R. Varadwaj [1,2,*], Arpita Varadwaj [1,2] and Helder M. Marques [3]**

1 Department of Chemical System Engineering, School of Engineering, The University of Tokyo 7-3-1, Tokyo 113-8656, Japan; varadwaj.arpita@gmail.com
2 The National Institute of Advanced Industrial Science and Technology (AIST), Tsukuba 305-8560, Japan
3 Molecular Sciences Institute, School of Chemistry, University of the Witwatersrand, Johannesburg 2050, South Africa; helder.marques@wits.ac.za
* Correspondence: pradeep@t.okayama-u.ac.jp or pradeep@tcl.t.u-tokyo.ac.jp or prv.aist@gmail.com

Received: 6 January 2019; Accepted: 26 February 2019; Published: 12 March 2019


**Abstract:** In addition to the underlying basic concepts and early recognition of halogen bonding, this paper reviews the conflicting views that consistently appear in the area of noncovalent interactions and the ability of covalently bonded halogen atoms in molecules to participate in noncovalent interactions that contribute to packing in the solid-state. It may be relatively straightforward to identify Type-II halogen bonding between atoms using the conceptual framework of σ-hole theory, especially when the interaction is linear and is formed between the axial positive region (σ-hole) on the halogen in one monomer and a negative site on a second interacting monomer. A σ-hole is an electron density deficient region on the halogen atom X opposite to the R–X covalent bond, where R is the remainder part of the molecule. However, it is not trivial to do so when secondary interactions are involved as the directionality of the interaction is significantly affected. We show, by providing some specific examples, that halogen bonds do not always follow the strict Type-II topology, and the occurrence of Type-I and -III halogen-centered contacts in crystals is very difficult to predict. In many instances, Type-I halogen-centered contacts appear simultaneously with Type-II halogen bonds. We employed the Independent Gradient Model, a recently proposed electron density approach for probing strong and weak interactions in molecular domains, to show that this is a very useful tool in unraveling the chemistry of halogen-assisted noncovalent interactions, especially in the weak bonding regime. Wherever possible, we have attempted to connect some of these results with those reported previously. Though useful for studying interactions of reasonable strength, IUPAC's proposed "less than the sum of the van der Waals radii" criterion should not always be assumed as a necessary and sufficient feature to reveal weakly bound interactions, since in many crystals the attractive interaction happens to occur between the midpoint of a bond, or the junction region, and a positive or negative site.

**Keywords:** halogen bonding; noncovalent interactions; Type-I, -II and -III contacts; σ-hole concepts and controversies; MESP and electron density models; crystalline structures; IGM analysis

## 1. Introduction

There is much ongoing discussion on halogen-centered noncovalent interactions and many interesting papers [1–3] and reviews [4–7] have appeared. Essentially, these seek to provide a fundamental understanding of their characteristic signatures [8,9], the underlying physical chemistry involved, and the way they drive packing between molecules of interest in the development of engineered crystals [10].

There are two notable reasons for the copious exploration of this area. One arises partly from disagreement on the fundamental nature (origin) of these interactions, with conflicting viewpoints being advanced [4,11–17]. The other undoubtedly stems from the widespread occurrence of these interactions

in highly specific recognition processes, occurring in many areas of science and engineering, including drug design [18], crystallography [19], biology [9], catalysis [1], supramolecular chemistry [20], molecular recognition [21], physics, and chemistry [10]. The conflicting viewpoints arise not only from attempts at interpreting and understanding the sets of observed data at an individual level, but also from attempts to identify the characteristic signatures that vary on a system-by-system basis.

Some contend that certain theoretical approaches and the descriptors derived from them are sufficiently robust to reveal the chemistry of noncovalent interactions involving halogen derivatives [22–30], whereas others found them to perform well for specific systems but not for all [6,31,32]. For instance, many density functionals have previously been proposed to be sufficiently robust for the study of noncovalent interactions [23,24], but these either fail to identify, overestimate, or underestimate such interactions for the other systems [33–35]. For weakly bound $Ne_2$ and $He_2$ (but not $Ar_2$), the density functional ωB97x-D gives numerically reasonable results when compared to CCSD(T)/aug-cc-pV5Z, but it underestimates all three interactions [33]. The M05-2X, PBE0, B2PLYP-D, X3LYP, ωB97x-D, and M06L functionals also give reasonable results; in descending order, M06, M06-2X, M05, B3LYP, B2PLYP, and B97-D do the worst. Of these, the density functionals significantly overestimate, while the two traditional functionals not specifically parameterized significantly underestimate the interactions [33]. Similarly, some have observed that the functionals with high exact exchange or long-range corrections (such as M06-2X, ωB97XD, and double hybrids) were suitable for the study of the noncovalent chemistry of some halogen bonded dimers [23,24], whereas these perform differently in other systems [35–37]. To this end, there has always been a quest for new functionals, supporting the assertion of Ayers and Parr "it is not impossible to find a universal density functional; it is just that may be well hidden" [38].

It is our view, and that of others [39], that this type of ongoing critical discussion and evaluation enables one to validate previously proposed definitions, hypotheses, and characteristics of noncovalent interactions. Yet there are others who, either directly or indirectly, reject such proposals, or discard the proposed characteristics as standalone criteria for identifying a noncovalent interaction [6,12,31,32,40–50]. Some believe that the definitions proposed for the study of such intermolecular interactions are rather poor, far from complete, and the characteristics recommended are insufficient and misleading [32,40,41,49,51–53]. For instance, the so-called (revised) first criterion proposed by the International Union of Pure and Applied Chemistry (IUPAC) for recognizing a hydrogen bond in 2011 [54] is "The forces involved in the formation of a hydrogen bond include those of an electrostatic origin, those arising from charge transfer between the donor acceptor leading to partial covalent bond formation between H and Y, and those originating from dispersion." Although a similar (but not exact) view was provided for halogen bonding in many contexts, Clark expostulated that this IUPAC criterion for hydrogen bonding is meaningless from a purist quantum chemical viewpoint [55]. Similarly, giving a possible explanation of the context when a hydrogen bond becomes a van der Waals interaction, Tantardini [50] has stressed that there is a fallacy in the geometric definition of hydrogen bonding provided by Arunan et al. [54].

Views that hydrogen bonds are seen experimentally, that the halogen bond has been defined, and that carbon bonding has been proposed to characterize chemical systems, have been provided [56,57]. While making these statements, one might recall Coulson's statement (quoted in [58]), "Sometimes it seems to me that a bond between two atoms has become so real, so tangible, so friendly, that I can almost see it. Then I awake with a little shock, for a chemical bond is not a real thing. It does not exist. No one has ever seen one. No one ever can. It is a figment of our own imagination." Similarly, Hoffmann commented (quoted in [58]) "My advice is this: Push the concept to its limits. Be aware of the different experimental and theoretical measures out there. Accept that at the limits a bond will be a bond by some criteria, may be not others. Respect chemical tradition, relax, and instead of wringing your hands about how terrible it is that this concept cannot be unambiguously defined, have fun with the fuzzy richness of the idea.".

That a hydrogen bond can be experimentally visualized is against the firm belief that a chemical bond is not an observable, nor is it associated with any quantum mechanical operator (so there

are no real bonds—only bonding [59]); thus, a bond cannot be seen experimentally as purportedly shown using extensive manipulation of high-resolution spatial images [57,60]. Even so, the ability to experimentally observe chemical bonds is believed to be a potential breakthrough of the atomic force microscopy (AFM) and scanning tunneling microscopy (STM) techniques. As commented by Ritter [58], "Coulson's prediction of never being able to see a bond is becoming frayed at the edges, thanks to the exquisite touch of the atomic force microscope (AFM).".

That "a bond is seen" is to be viewed in the same light as the claim that orbitals are observable experimentally [61,62]. Whilst some have reported experimental observations of orbitals [61,62], yet there are arguments that this sort of claim is physically meaningless [55,63,64]. Others [27] have reasoned that "orbitals are simply mathematical constructs that are used to obtain an approximate solution of the multi-electron Schrödinger equation. They have no physical reality [65], nor does the orbital overlap accordingly. Finally, the wave function should be designed in such a manner as not to neglect the instantaneous correlation between the electrons' movements in response to their mutual electrostatic repulsions." Although this is the argument advanced in that study [27], Ivanov et al. [66] demonstrated that the frontier orbitals are game makers in that the extent of orbital overlap greatly assists in the rationalization of the role played by polaron localization and delocalization, a topic of significant interest in the rational design of novel charge-transfer materials [67–70].

Similarly, as above, the concept of charge transfer is also well-established [71–74]. Like others [43,44,75], Legon and coworkers discussed its deterministic importance extensively [76–83]. They largely focused on the determination of quadrupole coupling constants associated with non-spherical atom (especially involving N, Cl, Br, and I atoms) in complexes; from this they calculated charge transfer, hence suggesting that charge transfer is a valuable tool in understanding intermolecular interactions [78,82–88]. However, there are views that charge transfer accompanying complex formation is merely a form of polarization, and that dispersion is an integral part of an electrostatic interaction that is Coulombic in origin and is not a separate interaction [27]. To quote the authors, "Exchange, Pauli repulsion, orbitals and correlation are all very important components of the mathematics of arriving at a satisfactory wave function and the resulting electronic density. However, they do not contribute directly to the physical forces (Coulombic attractions) that hold the system together, . . . , the key point is that dispersion—whether involving dipole/dipole or nuclear/electronic interactions—is Coulombic; it is simply part of polarization. It is not a separate interaction.".

According to Clark et al. [89], the neglect of polarization, or attributing its effects to charge transfer, often leads to the incorrect assertion that purely electrostatic interpretations are inadequate. Their argument is that polarization is an intrinsic part of an electrostatic interaction, and must be considered to yield the correct results. Polarization is measurable and an integral part of Coulomb interactions that must be considered in a complete electrostatic model. Politzer and coworkers commented that "The illusion of charge transfer is in the model; the reality of polarization is in the electronic density, the physical observable" [27]. They also point out that it was Feynman who noted that the Hellmann–Feynman theorem shows rigorously that both intra- and intermolecular interactions are purely Coulombic. This conclusion, which includes polarization and dispersion as well as static charge distributions, follows directly from the fact that the potential energy terms in the Hamiltonian operator are all Coulombic (charge transfer is sometimes invoked as an additional factor, but it is increasingly recognized that charge transfer, in noncovalent interactions, is just a mathematical representation of the actual physical effect, which is polarization) [26]. The authors argued further that the formation of complexes involves the transfer of some fraction of an electron from an occupied orbital on an "electron donor" (the negative site) to an empty orbital, usually antibonding, of an "electron acceptor" (the molecule with a positive σ-hole). However, this explanation [27] ignores the inconvenient truths that (1) electrons are indivisible and cannot be fractioned and (2) that orbitals have no physical existence. Strictly speaking, these arguments are not in line with the charge transfer perspectives of those that discuss intermolecular bonding interactions are a result of charge transfer from bonding orbital and/or lone pairs to the electron deficient regions [90–92].

On the other hand, there are many others who affirm that polarization, charge transfer and dispersion as separate components of an interaction allows one to better understand the system being studied [40,41]. In particular, Oliveira and coworkers argue that to learn about the mechanistic details of noncovalent interactions it is useful to refer to quantum chemical models, and in this sense, orbital theory is useful to describe the covalent interactions between the monomers and single out the charge transfer between their specific orbitals [93,94]. Řezáč and de la Lande argue that it is intuitive to separate the changes in the electronic structure within the molecular fragments (induction or polarization) from charge transfer across the border between these fragments [95]. The problem is that this border has to be drawn arbitrarily and the results of further analysis depend strongly on its definition. Some approaches rely on the definition of charge transfer in terms of orbitals—polarization is a rearrangement of electrons within orbitals localized on one molecule and charge transfer is the transfer of an electron from one molecule to unoccupied orbitals on the other [95]. Similarly, Varadwaj et al. showed that charge transfer is a factor controlling the equilibrium constants of late first-row transition metal complexes (the so-called Irving–Williams series) [96], and have suggested it to be a major driving force to provide geometrical stability to organic–inorganic perovskites in gas-phase adducts [97–99]. Given the conflicting views on charge transfer emerging from various groups, and given that the concepts of charge transfer, charge separation, as well as charge recombination, have been widely utilized to develop a variety of donor–acceptor functional materials (e.g., organic photovoltaics) [71,100–104], it seems to us from the various conflicting arguments summarized above that the concept of charge transfer is yet to be fully understood. There is clearly a pressing need for rigorous methodical developments to resolve the issue.

It was argued that moderate-to-strong intermolecular interactions in chemical systems contain partial-to-significant covalency [14,93,105–107], a concept that was discussed by Ruedenberg several decades ago [108]. According to him, "The wave mechanical kinetic behavior, which differs typically from the classical behavior and is characterized by the cue 'uncertainty principle', is a fundamentally essential element of covalent bonding. Any explanation of chemical bonding based essentially on an electrostatic, or any other kinetic concept, misses the very reason why quantum mechanics can explain chemical bonding, whereas classical mechanics cannot." The specific cause for covalent bonding is realized provided that "as the electron is pulled towards the attractive center(s), the kinetic energy of the shared electron increases less rapidly than that of the unshared electron. As a consequence, the shared electron can cluster around each of the two nuclei more tightly before the kinetic energy reaches half of the potential energy." Because the magnitude of the former is smaller than the latter, the total energy would be more negative, hence stabilizing the interaction. These views are in agreement with Oliveira et al. [90], who have recently examined a total of 202 halogen bonded complexes, wherein a total of 10 different electronic effects have been identified that contribute to halogen bonding and that explain the variation in their intrinsic strengths. Among others, it was shown that covalent contributions to halogen bonds always have to be considered, and explaining these interactions merely by the so-called the σ-hole concept [109] is an oversimplification; a σ-hole is a tiny electron deficient region on bound halogen in molecules in its covalent bond extension. For the understanding of the covalent contribution one must keep in mind that the lone pair orbital directly donates charge to the σ-hole in halogen bonded systems. The covalent contribution can be quantified by the nature and predominance of the kinetic and potential energy densities, which can be evaluated using the Quantum Theory of Atoms in Molecules (QTAIM) [110–113]. The total energy density, which is the sum of these two energy density properties, is not necessarily a minimum at the position of a σ-hole, and the electrostatic potential is inadequate to provide the potential covalent character of halogen bonding. The review of Grabowski provides rigorous insights into covalency in noncovalent interactions [114].

That charge transfer accompanies the formation of binary complexes was also shown by Alkorta and coworkers [115]. They have suggested that significant charge (up to 0.4*e*) has to be transferred from the $XNH_3^+$ unit to the electron donor molecule to form an $[NH_3^+,N]:ClNH_3^+$ complex, and due

to the strong overlap between them, they form covalent bonds [115]. Similar results have also been reported by Varadwaj and coworkers for organic–inorganic lead halide perovskite complexes [96–99].

The above views are against the contention of others that the notion of covalency is vague since there is no unique definition of covalency [116,117]. It is therefore understandable that some theoreticians, imbued with the exotic mysteries of quantum mechanics, are taken aback when informed that the chemical bond can be explained rigorously in terms of classical physics (Coulomb's Law). What does this do, for example, to the electrostatics vs. covalency debate [27]? The authors further stated that since covalency is purely conceptual and any attempt to quantify it is necessarily arbitrary, this is a quintessential academic debate: it cannot be resolved and can (and will) continue indefinitely. Clearly, in our view, there is no consensus on the precise mathematical "translation" between the divergent conceptual frameworks emerging from various research groups and thus it is rather difficult to clarify the exact terms of disagreement.

Another point worthy of consideration concerns the total binding energy (also called interaction energy, formation energy, and so on) of complex systems, which is generally used to quantify the strength of an intermolecular interaction. It has been argued that since it is determined by quantum mechanical methods, it is a physically observable property [118–120]. By contrast, Cremer and coworkers [121,122] discussed, on a number of occasions, that the dissociation energies (or interaction energies) only give rather limited insight into the true intrinsic strength of a chemical bond. The geometric and electronic rearrangements of the fragments associated with a bond breaking process have an energetic cost which is not related to the intrinsic strength of a bond; the same is true for noncovalent interactions. These authors have suggested that the vibrational motions of a molecule in its equilibrium state or during a chemical reaction provide a wealth of information about its structure, stability, and reactivity. They then connected force constants to the intrinsic bond dissociation energy of a bond and, accordingly, showed that these are excellent descriptors of bond order and bond strength. They further argued that bond dissociation energies, bond lengths, or bond densities, are not directly related to the bond strength because they also depend on quantities other than just the bond strength: the bond dissociation energy on the stabilization energies of the fragments, the bond length on the compressibility limit distance between the atoms; the bond stretching frequency on the atom masses, and so on.

In similar vein, a comment has been made [27] that "a frequently used analytical technique is 'interaction energy decomposition', whereby the interaction (stabilization) energy of a noncovalent complex is somehow separated into a set of supposedly fundamental contributions. There is no general consensus as to what these fundamental contributions are; different researchers invoke different subsets of a group that includes electrostatics, charge transfer, polarization, correlation, dispersion, exchange, Pauli repulsion, orbital interaction, distortion, etc. There is no physically meaningful way to separate these, since they are not independent of each other. This has the advantage that everyone can invent his/her own procedure, and none can be shown to be more incorrect than any other" [27]. Contrary to this view, Zhu et al., in a recent study, proposed a method called self-attractive Hartree (SAH) decomposition to unravel pairs of electrons directly from the electron density, which, unlike molecular orbitals, is claimed to be a well-defined observable that can be accessed experimentally [123]. The key idea is to partition the density into a sum of one-electron fragments that simultaneously maximize the self-repulsion and maintain regular shapes. This leads to a set of rather unusual equations in which every electron experiences self-attractive Hartree potential in addition to an external potential common for all the electrons. Interestingly, however, Wick et al. [124] state that the interaction energies of DFT-SAPT also provide a well-defined partitioning of formal bonding contributions (SAPT refers to Symmetry Adapted Perturbation Theory [125]). Esterhuysen et al. [126] argued that interactions with nucleophiles, such as the trifluoromethyl groups in molecules, are predominantly dispersion driven, enabled by strong polarization of the $CF_3$-group to decrease Coulomb repulsion, resulting in the formation of intermolecular complexes. They showed that SAPT provides accurate results comparable to high level CCSD(T) results. In our view, if dispersion, like exchange and Pauli repulsions, is not a

real force and is not a separate entity, is an illusion of a real interaction, and has no meaning outside the mean-field theories, then why is there a need to invoke it in a variety of contexts to explain a wide range of intermolecular interactions? If there is a need for exchange and Pauli repulsion terms to satisfy quantum mechanical requirements to obtain the energy of a chemical system, what is the point of ignoring these and considering only electrostatic (and polarization) effects to explain what happens in reality? What does this have to do with the so-called "technically important" ("mathematical model" and "real physical effect") debate?

In fact, there have been hundreds of papers published that view London dispersion as a separate entity. This is not surprising given it is described by $r^{-6}$ radial dependences and is indeed different from charge–charge type Coulombic interactions that follow $r^{-1}$ radial dependence; dipole–dipole, ion–dipole interactions, etc., are also Coulombic interactions that have fundamentally different radial dependence. Note that the Hartree–Fock self-consistent field treatment fully accounts for the Coulombic (electrostatic plus polarization) interactions, as do many DFT functionals such as the most popular B3LYP and PBE. However, these fail to provide a correct description of bonding interactions in most delocalized systems, as well in systems where dynamic charge density fluctuations in the bonding region plays the role. In response to this, many dispersion-corrected functionals have been developed with an empirical procedure to account for dispersion. Some of these dispersion corrected functionals are appropriate for some systems, yet inadequate for the other. Inclusion of dispersion as an empirical term in DFT functionals does explain why, for instance, the $(C_{60})_2$ fullerene dimer has a bound state, and why the interaction between the $C_{60}$ monomers in the dimer is unusually long-ranged [127]. Clark added that our mathematical models (usually either HF or DFT mean-field theories) need to be corrected in order to make neutral atoms or nonpolar molecules bind weakly to each other, so that dispersion, like exchange, is technically important [55].

Despite these recent advances, there are many [128–130] who neglect the importance of the various factors noted above and employ an individualistic approach when looking at the chemistry of the systems they study. For instance, and in contrast with the suggestions of Ref. [27], Oliveira and coworkers suggested that halogen bonding in 36 YX$\cdots$AR$_m$ (X: F, Cl, Br; Y: donor group; AR$_m$ acceptor group) complexes is the result of electrostatic and strong covalent contributions. It can be strengthened by H-bonding or lone pair delocalization. The covalent character of a halogen bond increases in the way 3c-4e (three-center-four-electron) bonding becomes possible [93]. Wang et al. [51] have shown that for the FNSi$\cdots$BrF complex, and similar others, the energy decomposition approach based on the block-localized wave function (BLW) energy method (BLW-ED) can partition the overall stability gained on the formation of intermolecular noncovalent interaction into several physically meaningful components. The electrostatic repulsion in these counterintuitive cases is overwhelmed by the stabilizing polarization, dispersion interaction, and most importantly, the charge transfer interaction, resulting eventually counterintuitively in an overall attraction. Similarly, the high-level ab initio and symmetry adapted perturbation theory (SAPT) [131] calculations on close B–H$\cdots\pi$ contacts, which have been observed in crystallographic structures of Ir–dithiolene–phosphine complexes containing a boron hydride cluster [132], have reinterpreted the nature of B–H$\cdots\pi$ contacts in this system. Although the characteristics of the B–H$\cdots\pi$ interaction have been known for decades, these authors argued that they disproved the widely-accepted view that these are attractive electrostatic interactions that arise as a consequence of the intermolecular interaction. They then have redefined the B–H$\cdots\pi$ contacts as being nonspecific dispersion-driven interactions. The argument that supports this view originated from the electrostatic energy component of the interaction which was found to be weak and in which dispersion makes enormous contribution. Hence, in their view, the crystallographically-observed B–H$\cdots\pi$ interactions do not constitute a novel type of hydrogen bonding of boron hydride clusters. Although this was the central part of the study, there are many others that are skeptical of SAPT, for instance, who would claim that this is physically meaningless since one cannot dissect the interaction energy this way; its components are not quantum mechanically separable, and hence the complainants prefer the traditional interpretation of the nature of the B–H$\cdots\pi$

interaction in boron clusters. The studies of Zou et al. [133] and Zhang et al. [134] provide rigorous insight into the chemistry of these interactions.

The complex controversies associated with halogen-centered noncovalent interactions have recently been pointed out by Saha and coworkers [11]. These contrasting views are indeed useful because they not only shed light on some of the fundamental issues involved, but also assist in the development of new formalisms for the exploration of noncovalent interactions. The question that arises is: if all energy components of the intermolecular interaction (exchange, polarization, charge transfer, dispersion, electrostatic effects, etc.) cannot be treated as separate entities to interpret an intermolecular interaction, why have there been so many energy decomposition procedures developed from time-to-time and proposed? Why have these been shown to be robust in their own way? Why has this trend persisted? Will this kind of practice, with the appearance of new proposals from time-to-time, continue indefinitely? These questions can be answered in many different ways depending on one's interest and level of understanding of the problem. We leave this for the readers to judge for themselves.

A major issue in the area of halogen-centered noncovalent interactions is that there have been many crystal structures reported [135] in which the intermolecular interactions are short and highly directional, and are demonstrably responsible for the emergence of the solid-state structures. In doing so, the importance of most of the secondary and other primary interactions responsible for packing is sometimes completely neglected (see discussions given below with examples). This is in agreement with the view of Mackenzie and coworkers [136], who, quoting Desiraju, assert that there is a "compelling need . . . to be able to visualize a crystal structure in its entirety, not just look at selected intermolecular interactions which have been deemed to be important," and of Nangia and Desiraju (quoted in [136]), who commented that "a detailed understanding of crystal packing and crystal design depends very substantially on viewing the molecule as an organic whole," and have suggested to view molecules as "organic wholes", thereby fundamentally altering the discussion of intermolecular interactions through the use of a variety of novel computational and graphical tools.

In this short review, we aim to provide a brief overview of the advances of the underlying concepts of halogen bonding and halogen-centered noncovalent interactions including those involving fluorine. A few exemplar crystal systems (taken from Cambridge Structure Database (CSD) [135]) involving these interactions, which have been known from the mid to the late 20th century, are used to illustrate the way these preliminary studies guided the development of the conceptual framework of halogen-centered noncovalent bonding interactions, and to show that there are many systems like them deposited in the CSD that have not been well understood. The latter part of the review comprises several examples from more recent literature highlighting the fact that Type-II interactions are not the only interactions to be assumed when examining the emergence of the entire geometry of many crystals. There are many other interactions involved between the interacting monomers locally, which may or may not be the forced consequences of the primary interactions. These interactions contribute in part to the packing of molecules and hence cannot simply be overlooked. The Type-I interactions are shown to occur in a variety of situations, especially in crowded halogen-substituted environments. Their presence cannot and should not be neglected if the nature of the intermolecular interactions at play and their characterizations are the central focus of discussion in attempting to arrive at an understanding of molecular packing and crystal formation.

## 2. Geometry-Based Identification of Halogen Bonding

Halogen bonding is a noncovalent interaction. It is formed by the group 17 elements of the periodic table in molecules upon their attractive engagement with a negative site. The negative site can be any (main group) element of the periodic table that is able to donate at least some partial electron density. The lateral portions of covalently bonded atoms such as N, S, F, P, O, Se, Te, Cl, Br, I, etc.; aromatic rings (as in benzene); ions (viz. $X^-$, $X_3^-$ (X = F, Cl, Br, I), and 1-carba-closo-$[CHB_{11}I_{11}]^-$; among many others, are generally observed as negative sites and have been historically recognized as electron donors.

As with a hydrogen bond [54], which has been recognized for a long time, a halogen bond in chemical systems is effectively identified through two of its primary geometrical properties. The first is the A···X bond distance between atoms A and X, where A is the halogen bond acceptor (an electron density donor) and X is the halogen derivative (X = F, Cl, Br, I, At), that is, the halogen bond donor (an electron density acceptor). The second is the directionality, defined by the angle ∠A···X–R, which can be either linear or near-linear, and R is the fragment covalently bound to X. These geometry-based features are similar to the criteria generally used for identifying hydrogen bonding, A···H–R.

It is often asserted that halogen bonding shares many characteristics with hydrogen bonding [54]. If taken literally this is misleading: it is only the nature of some characteristics (viz. intermolecular distance, directionality, and bond strength) that are somehow similar to both types of bonding interactions, which is why halogen bonding (or even other noncovalent interactions) is often considered to have a familial relationship with hydrogen bonding.

Apart from these fundamental features above, there have been many additional signatures proposed IUPAC) [39], which are a consequence of the electronic structure changes associated with the halogen bond donor fragment X–R, including vibrational frequency shift (IR/Raman), chemical shift (NMR), electron density topological signatures, and so on. Clearly, these characteristics aid in detecting the A···X–R halogen bonding topology in molecules, clusters, and solids, and the more signatures present, the greater the level of confidence in identifying the interaction involved.

These geometric, electronic, vibrational, NMR, and charge density topological features are applicable to a number of noncovalent interactions that have been known over decades, yet named relatively recently [78,137]. These are formed by the elements of Groups of 14, 15, and 16 of the periodic table, and have been referred to as tetrel bonding, pnictogen bonding, and chalcogen bonding, respectively [78]. There are also other geometrically and energetically similar interactions, comparable to hydrogen bonds and other σ-hole interactions, called aerogen bonding [138], magnesium bonding [4,139], lithium bonding [4,140], and so on. Depending on the nature of the interacting fragments in forming these interactions, these could be highly directional, or less so, deviating appreciably from 180°. These interactions are all consequences of attraction between sites of opposite charge polarities. Lump–hole interactions [47,49,141,142] also have similar bonding characteristics. The difference is that these are manifest when, for instance, two atomic sites of identical polarity but with marginal or appreciable differences in charge density interact with each other.

Clearly, there is no need for new proposals and for another IUPAC definition for identifying and characterizing these interactions, although naming them as a separate interaction type, such as aerogen bonding [138], magnesium bonding [4,139], lithium bonding [4,140,142], and so on, will be useful as this will discriminate which atom type in the molecule has the electrophile on it that causes the attractive engagement with the negative site. In fact, all these interaction types above have been known crystallographically for decades. Their chemistry is fundamentally virtually similar, although characteristics might vary. The novelty that has been shown from time-to-time is the way they drive the rational design of materials, and the circumstances under which they appear to violate the rules in various chemical systems. Some accept this sort of observation and characterization as novel, whereas others do not find them so—commenting, for example, that "this is nothing new and so on." This debate has continued since definitions for the hydrogen bond were given [54,143–145] (there are over 50 definitions proposed so far) and will safely continue for the foreseeable future.

### *2.1. Early Recognition*

The possibility of a halogen bond in $H_3N\cdots I_2$ has been known since 1814 [146,147]. The same system was further analyzed in 1863 [148], and later by many other researchers. By the mid-20th century, several adducts containing the halogen bond had been reported [149]. For example, in 1959, Strømme reported the single crystal structure of trimethylamine···iodine ($(CH_3)_3N\cdots I_2$) [150], and Hassel and Strømme reported the single crystal structures of 1,4-dioxane···chlorine ($C_4H_8O_2\cdots Cl_2$) [151] and acetone··· adducts ($C_3H_6O\cdots Br_2$) [152]. Since then, several hundreds of

thousands of crystal structures containing the halogen bond have been deposited in the CSD. However, the fundamental bonding abilities of halogen in most of these crystals were only partially understood during this time. In 1969, Hassel was awarded the Nobel Prize in Chemistry for his outstanding discovery that halogens in molecules can be potentially able to self-assemble, and directionally organize to form charge-transfer complexes in the crystalline phase (in presence of electron donors) [153]. In 1978, Dumas and coworkers reported complexes of $CCl_4$, $CBr_4$, $SiCl_4$, and $SiBr_4$ with tetrahydrofuran, tetrahydropyran, pyridine, anisole, and di-*n*-butyl ether in organic solvents [154]. Even by then the term "halogen bond" had not been coined, nor its characteristics fully appreciated.

Figure 1a shows a seemingly counterintuitive scenario in which the covalently bound halogen atom in $Br_2$ resides in close proximity to the predominantly electronegative O atom in an acetone molecule, thereby forming the $Br_2 \cdots OC_3H_6$ crystal [152]; the positions of the H atoms are missing in the cif (crystal information file) retrieved from the CSD. The perdeuteroacetone crystal structure of the same system was subsequently reported several times, viz. by Marshall et al. in 2013 (CSD ref: ACETBR04) [155], by Jones et al. in 2014 (CSD ref: ACETBR01–03), and by Marshall et al. in 2018 (CSD ref: ACETBR05–07) [156]. The crystal structure of perdeuteroacetone bromide is given in Figure 1b, showing the possibility of an attractive contact between a Br atom in $Br_2$ and the O and D atoms of the perdeuteroacetone moiety. The intermolecular distance between them is reasonably short and the O$\cdots$Br–Br angle is more linear than the Br$\cdots$D–C angle. It is evident that the crystal is locally stabilized by two interaction types involving O$\cdots$Br(–Br) and Br$\cdots$D(–C), thereby this system may not be invoked as exemplar that is stabilized with halogen bonds only as the deuterium bond plays a crucial role as well. The argument is also applicable to the acetone–bromine system, wherein the Br$\cdots$H(–C) hydrogen bonding should also play a critical role.

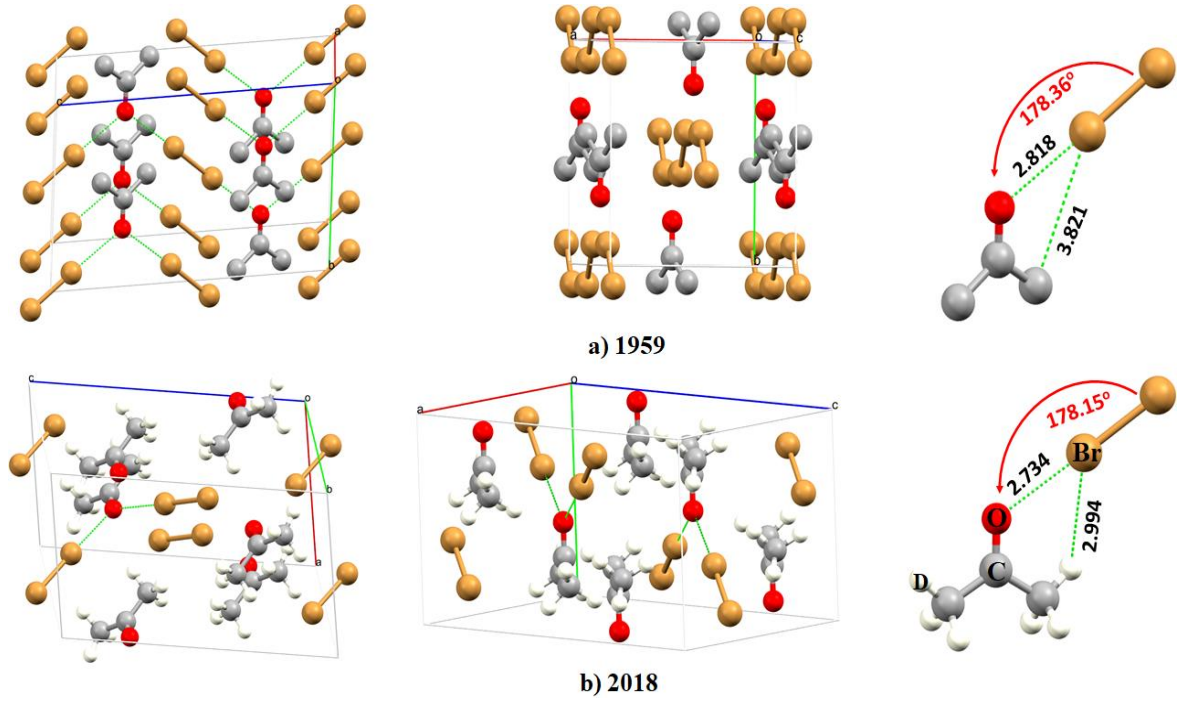


**Figure 1.** Various views of the ball-and-stick models of the unit cell of the (**a**) acetone–bromine (CSD ref: ACETBR) and (**b**) perdeuteroacetone bromide (CSD ref: ACETBR06) crystals. Atom type is marked in (**b**). Selected bond distances and angles are in Å and degrees, respectively. The dotted lines between atoms indicate intermolecular interactions. Year of publication shown both in (**a**,**b**). The H atoms of acetone–bromine are missing in the crystal information file and are not shown.

Similar early studies, where the counterintuitive bonding interactions of the halogen are evident, are shown in Figure 2. These show the electronegative atoms such as O, N S, Se, I, and P in

molecules are in a quasilinear arrangement with the diatomic halogen molecules. Except for the 1-diphenylphosphino-2-methyl-1,2-dicarbadodecaborane(10) hemikis(iodine) geometry (CSD ref: ECISIT), the A···X intermolecular distances in all other adducts are very short. For example, the N···I distance in the trimethylamine–iodine adduct is 2.271 Å, and suggests a potentially strong interaction that might contain an appreciable amount of covalency (in what is supposedly an ion pair). The three atoms involving the atom D and the dihalogen molecule $X_2$ (X = Cl, I) in these systems form an angle that is ranging between 173.81° and 179.40°.

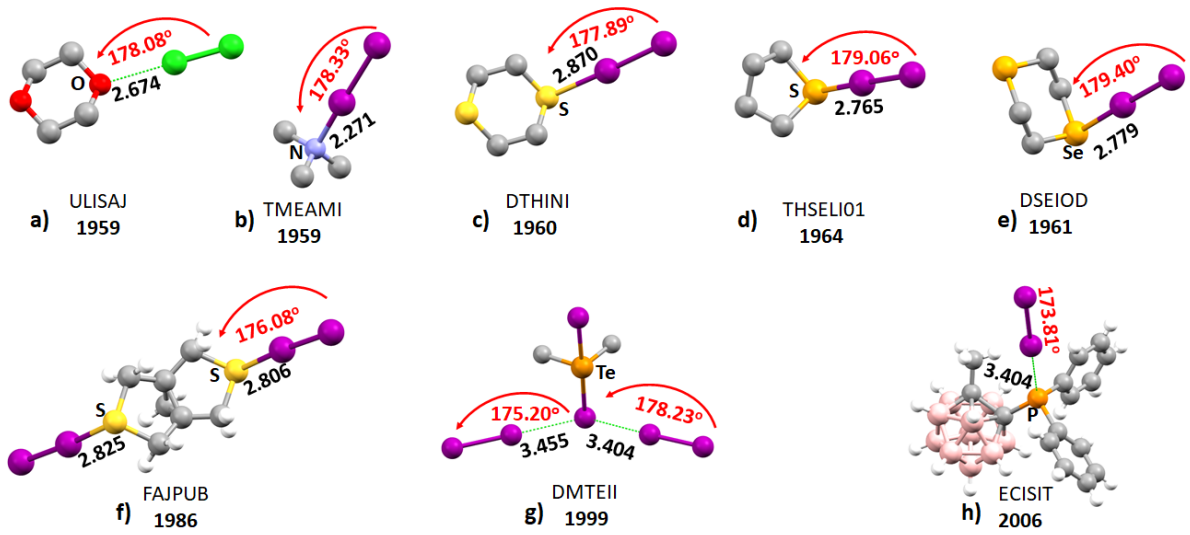


**Figure 2.** The ball-and-stick and space-filling models of some selected solid-state adducts reported between the middle of the 20th and early this century. These include (**a**) 1,4-Dioxane chlorine (ULISAJ), (**b**) Trimethylamine–iodine (TMEAMI), (**c**) 1,4-Dithiane bis(iodine) (DTHINI), (**d**) Tetrahydroselenophene iodine (THSELI01), (**e**) 1,4-Diselenane bis(iodine) (DSEIOD), (**f**) Dithia(3.3.1)propellane bis(iodine) (FAJPUB), (**g**) Dimethyl-di-iodo-tellurium iodine (DMTEII), and (**h**) 1-Diphenylphosphino-2-methyl-1,2-dicarbadodecaborane(10) hemikis(iodine) (ECISIT). The CSD reference codes and year of publication are indicated for each case: hydrogen in white-gray, oxygen in red, carbon in gray, nitrogen in blue, sulfur in yellow, selenium in light-orange, chlorine in green, iodine in purple, boron in light-pink and phosphorous in orange. The H atoms in several of these adducts are missing in the crystal information file, and hence are not shown.

To rationalize the intermolecular interaction in these systems, we recall that halides have been traditionally assigned an electronic charge of −1. Because of this, and because of their high electronegativity, they have been viewed traditionally as loci of negative charge in molecules, which explains why halogens they are often invoked as exemplar Lewis bases. This purported nature of a halogen does not explain the geometrical arrangement observed between the halogen and the negative atoms in the adducts shown in Figures 1 and 2. The arrangement is surprising as one might expect centers of negative charge localized on the interacting atoms in these adducts to be electrostatically repelled (Coulomb's law). The underlying physical chemistry behind this puzzling phenomenon (i.e., the attraction between two negative sites) was not appreciably articulated until the 1990s.

### *2.2. The Birth of Halogen Bonding and the σ-Hole Concept*

The greater availability of computational resources from the 1990s has provided the means of elucidating the versatile bonding abilities of halogen in molecules. Specifically, it was argued that the assignment of a single negative charge to halogen atoms is misleading since the outer surfaces of the halogens Cl, Br, and I in molecules feature an anisotropic distribution of charge density. There is a tiny region on the outer surface of the halogen, opposite to the covalent σ-bond it forms with other atom(s),

that is positive, while the lateral portions of the atom, dominated by electron lone pair densities, is negative. The positive site on the halogen derivative has the ability to attract the negative site on an interacting species, leading to the formation of an adduct between them (as in some complexes in Figure 2). Nevertheless, the term "halogen bond" was not used in the 1990s, nor was the concept of a halogen bond defined. In 2007 the term "σ-hole" was coined [109], and its underlying conceptual framework was introduced.

A "σ-hole" on a halogen X, and especially on the heavier halogens in molecules, was shown to appear along the outermost extension of a covalent σ-bond. The term "σ-hole" refers to the electrostatic region on X that is electron density deficient; it therefore has literally nothing to do with a "hole", and it is also called an "electrophilic cap". The strength of the σ-hole is often quantified by the local maximum of electrostatic potential, $V_{S,max}$, often evaluated on the 0.001 a.u. isodensity envelope. Because $V_{S,max}$ on the halogen derivative (especially the latter halogens) in most of the halogen-substituted molecules was calculated to be positive, the σ-hole was traditionally regarded as a region of positive electrostatic potential [120]. By contrast, the lateral sides of the halogen derivative is often characterized with the local minimum of electrostatic potential, $V_{S,min}$, which generally corresponds regions of richer electron density. Figure 3a,b illustrates, for example, regions described by $V_{S,max}$ and $V_{S,min}$ for $SF_4$ and $SF_6$, respectively; Figure 3c–f displays the 3D view of Molecular Electrostatic Surface Potential (MESP) plots for $SF_4$, $SF_6$, and $CX_4$ (X = F, Cl, Br) molecules.

Because the σ-hole is positive, in most cases it leaves the equatorial portions of the halogen negative such that the equatorial portion has a higher electron density than the axial site. This difference in the nature of the distribution of the electron density between the axial and equatorial sites has led to the development of the concept of charge density anisotropy and explains why many describe the nature of a covalently bonded halogen in a complex as having "amphoteric" character. Because of this kind of charge density profile, a halogen in molecules does serve both as an acceptor and a donor of electron density; the (relatively) positive axial portion of the covalently bound halogen would behave as an electrophile and the (relatively) negative lateral portion as a nucleophile towards sites of opposite polarity. This behavior of the halogen can be inferred from Figure 1b, in which the axial site on the Br atom in $Br_2$ serves as Lewis acid for the O atom, and the equatorial site on the same atom as a Lewis base for the D atom, thus forming O$\cdots$Br–Br and Br$\cdots$D–C halogen- and deuterium-bonded contacts, respectively. This partly explains the underlying physical chemistry behind the packing of the molecules and the consequent evolution of the crystal structure of the perdeuteroacetone bromide adduct.

Nevertheless, a σ-hole is generally quantified with the 0.0010 a.u (electrons bohr$^{-3}$) isodensity envelope mapped surface maxima of electrostatic potential, $V_{S,max}$. We stress that the choice of this envelope is arbitrary [44], although it encloses about 96–97% of the properties of the atom in molecules [25]. There are others who have argued that this isodensity envelope is not ideal (as is arbitrary [44]) and the use of an isodensity envelope with values between 0.0014 and 0.0020 a.u. will assist in recovering the true nature of the reactive surface as these encompass >> 96–97% of the electron density, thus reconciling the expectations of chemical intuition with the outputs of computational calculations [52,157,158]. The underlying reason behind the suggestion to use an isodensity envelope with a value between 0.0014 and 0.0020 a.u. was that the nature of the electrostatic potentials that emerges from the mapped 0.0010 a.u. isodensity envelope does not always provide correct insight into why, for instance, the F and Cl atoms in $CF_4$ [158] and $CH_3Cl$ [52], respectively, attract the entirely negative nitrogen or oxygen bases in the molecules in close proximity.

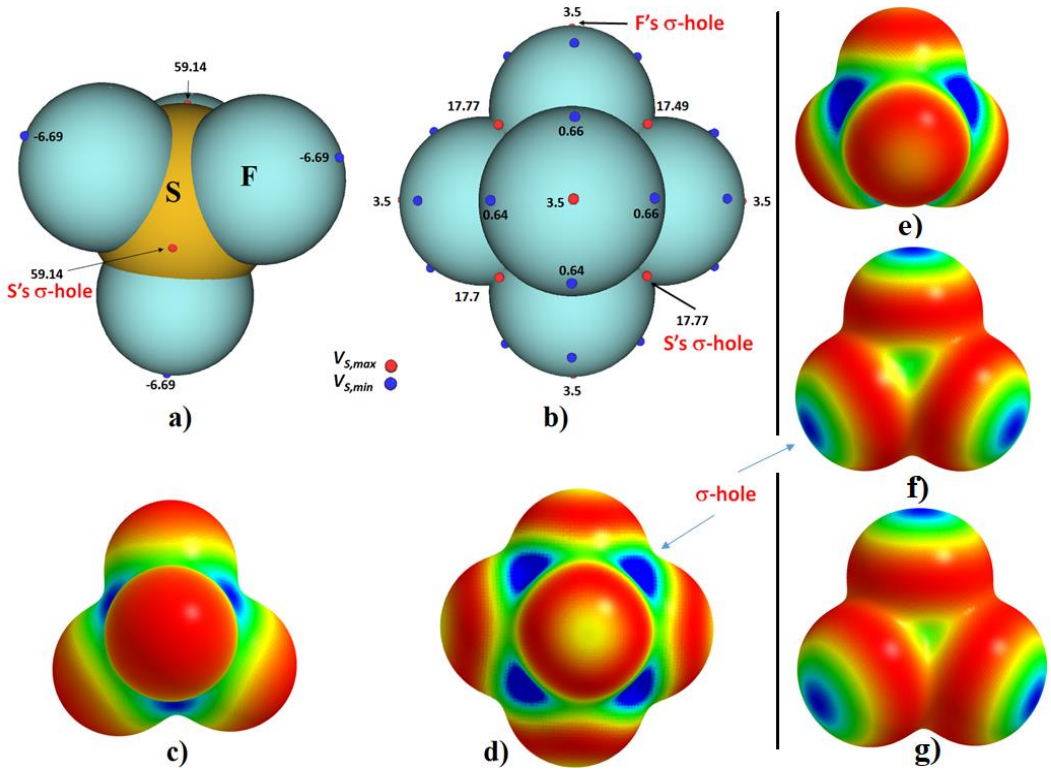


**Figure 3.** M06-2X/aug-cc-pVTZ level 0.0020 a.u. mapped potential on the electrostatic surface of (**a**) $SF_4$ and (**b**) $SF_6$ (this work). The atom–atom overlapping model is shown in (**a**,**b**), whereas the 3D model of the corresponding species is illustrated in (**c**,**d**), respectively. Values, which refer to extrema of electrostatic potential, are in kcal $mol^{-1}$. The S atom's σ-hole regions marked in (**a**,**b**) refer to the triangular blue regions in (**c**,**d**), whereas the σ-hole of the F atom refers the circular yellowish region on the fluorine's outer surface in (**d**), and is not evident of the same atom in (**c**). Included are also the 0.001 a.u. envelope mapped MESP plots for (**e**) $CF_4$, (**f**) $CCl_4$, and (**g**) $CBr_4$ (this work). Color: blue: strongly positive; red: strongly negative.

One might argue that choosing a > 0.0014 a.u. envelope means moving closer to the nucleus of the atom in a molecule, and one might then come up with a tiny electron density deficient surface. While this might be so for some systems, its use assists in extricating the missing potential extrema on the 0.001 a.u. mapped isodensity envelope (as shown below, Figure 4). Furthermore, we note that the two contour values (0.0010 and 0.0020 a.u.), as originally recommended by Bader et al. [159], are large enough to encompass ≈ 96% of a molecule's electronic charge. The selection of either of these envelopes depends on the nature and size of the constituents of a molecule; this determines their overall volumes, polarities, and so on. Interestingly, this observation of Bader et al. has often been referred to validate the claim that the 0.0010 a.u. (but not 0.0020 a.u.) envelope of the electronic density is the ideal molecular surface on which to compute the electrostatic potential [25]. However, our argument above is not only consistent with Bader et al. [159] but also with the recent suggestion of Bauzá and coworkers [157]. In the latter study, it was argued that the 0.0020 a.u. envelope, which encloses >99% of the electron density, is ideal for mapping of the potential.

In a recent study [141], we discussed the nature of $V_{S,max}$ computed on the 0.0010 and 0.0020 a.u. isodensity envelope for several fluorinated monomers. We found that the σ-holes on the fluorine atoms along the outer extensions of the Cl–F, Cl–F, and S–F bonds in the molecules $ClF_3$, $ClF_2Br$, and $F_2SO$, respectively, are all negative, computed using the 0.0020 a.u. isodensity envelope. This means that the σ-holes are neither absent nor neutral, as found on the 0.0010 a.u. isodensity envelope. For instance, the 0.0020 a.u. mapped $V_{S,max}$ was −22.12 kcal $mol^{-1}$ on the fluorine along the outermost extension of the Cl–F bond in $ClF_2Br$. It is −13.75 and −3.50 kcal $mol^{-1}$ on the fluorine atom along the extensions of

the Cl–F and S–F bonds in $ClF_3$ and $F_2SO$, respectively. Similarly, the $V_{S,max}$ associated with the σ-hole on the fluorine in $FNO_2$ was not negative as found on the 0.0010 a.u. isodensity mapped potential surface, but positive, with $V_{S,max}$ = +1.69 kcal mol$^{-1}$ (hence displaying a positive σ-hole on the surface of the fluorine).

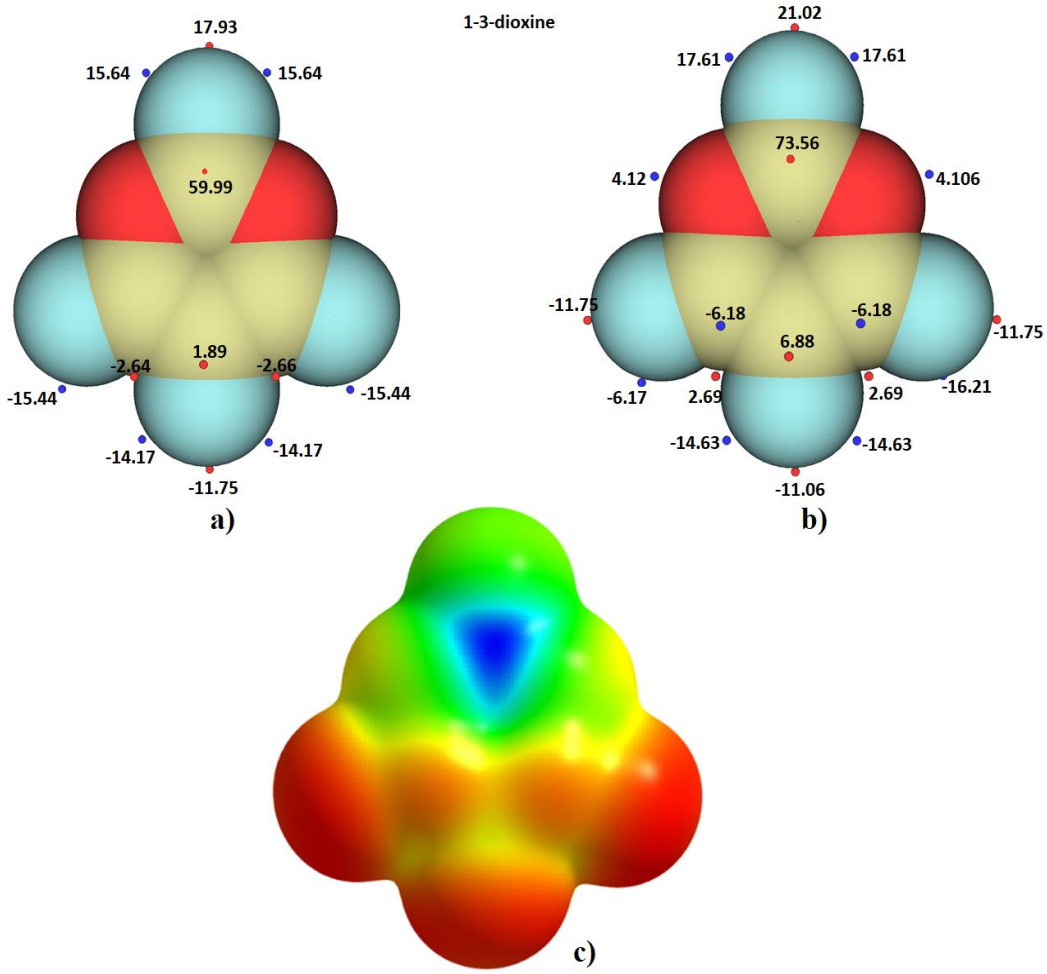


**Figure 4.** (**a**) 0.0010 a.u. and (**b**) 0.0020 a.u. isodensity envelopes with mapped potential extrema on the molecular electrostatic surface of (space-filled) fully fluorinated 1,3-dioxine ($C_4F_4O_2$), obtained with M06-2X/aug-cc-pVTZ (this work). Filled blue and red circles represent $V_{S,min}$ and $V_{S,max}$, respectively, and are in kcal mol$^{-1}$. (**c**) The 0.002 a.u. mapped electrostatic surface potential of 1,3-dioxine, in which, the orientation of atoms constituting the molecule is same as those shown (**a**,**b**) (this work). Color: blue—strongly positive; red—strongly negative.

It is believed that a high isoelectron density value results in a more contracted surface (i.e., lower internal volume). Because the surface will be closer to the nucleus and encompass less electron density inside (i.e., the nucleus will be less shielded) it is expected that regions of positive electrostatic potential will become more positive and region of negative potential will become less negative (or even positive). If this this the case, how does one gain insight into the true nature of the surface reactivity? To further demonstrate this matter, and the unreliability of the 0.0010 a.u. isodensity envelope, given that it is in any event arbitrary [44], we have chosen the $F_2SO$ system as a prototype, and have listed in Table 1 the $V_{S,max}$ on F computed on various isodensity envelopes for $F_2SO$, with values starting from 0.0010 a.u. up to 0.0055 a.u. As is apparent from the data, the surface of bonded fluorine along the S–F bond extensions does not enclose a σ-hole when the potential is mapped with 0.0010–0.0015 a.u. isodensity envelopes; this would lead to the conclusion that the F's σ-hole is neutral. However, choosing isodensity envelopes > 0.0015 a.u. leads to the appearance of $V_{S,max}$ on F atoms along the

S–F bond extensions. The sign of the $V_{S,max}$, which is associated with the F's σ-hole, remains negative passing from the 0.00165 a.u. to the 0.0050 a.u. isodensity envelopes, and becomes positive only when the 0.0055 a.u. isodensity surface is used. These variations are certainly not the effect of polarization, confirming further the arbitrariness of the 0.0010 au isodensity envelope [44].

**Table 1.** Dependence of M06-2X/6–311++G(2d,2p) electrostatic potential $V_{S,max}$ of F along the S–F bond extension in $SOF_2$ ($V_{S,max}$ values in bottom row in kcal mol$^{-1}$) on the nature of the isodensity envelope (values in top row).

| 0.0010 | 0.0015 | 0.00165 | 0.0017 | 0.0018 | 0.0020 | 0.0025 | 0.0030 | 0.0035 | 0.0040 | 0.0050 | 0.0055 |
|---|---|---|---|---|---|---|---|---|---|---|---|
| - [a] | - [a] | −3.72 | −3.70 | −3.64 | −3.50 | −3.10 | −2.60 | −2.10 | −1.52 | −0.25 | +0.41 |

[a] No extrema of electrostatic potential found on the F atoms when mapped on these envelopes [141].

These views above are consonant with those that appeared in a recent contribution of Lange et al. [160]. The authors used 30 nitrogen-bearing heterocycles, halogenated systematically by chlorine, bromine, or iodine, yielding 468 different ligands, to explore scaffold effects on halogen bonding strength. As a template interaction partner, they chose *N*-methylacetamide, representative of a protein backbone. Adduct formation energies were obtained at a MP2/TZVPP level of theory. They evaluated $V_{S,max}$ altering the isodensity values from 0.0010 a.u. to 0.050 a.u. The effect of secondary interactions was neglected. They found no direct linear relationship between $V_{S,max}$ and the formation energy as often claimed in other studies. Rather, the best overall fit between these quantities was found to be a third-order polynomial function ($R^2$ = 0.99), with the $V_{S,max}$ calculated using an isodensity surface of 0.014 a.u.

Figure 4 illustrates another example of this type. Two of the four F atoms in tetrafluoro-1,3-dioxane show the presence σ-holes on the 0.0010 a.u. isodensity envelope, and the remaining two lacks this (Figure 4a). One might conclude that the σ-hole on the latter two F atoms are neutral, as was done previously for $CH_3F$ [161], which is not true [12]. Others would suggest that there could be an anomeric effect that strengthens polar flattening and allows facile polarization to give a "neutral σ-hole", as done in previous studies for the fragment –$CF_3$, in molecules that act as hotspots for dispersion interactions [126,162]. This conclusion is misleading, as relatively higher values of the isodensity envelope for mapping the potential provides a completely opposite perspective on the nature of the surface reactivity (Figure 4b). For instance, an increase of the isodensity envelope values to 0.0015 and 0.0020 a.u. resulted in various minima and maxima of electrostatic potential for fully fluorinated 1,3-dioxine that were absent on the 0.0010 a.u. isodensity mapped surface. The missing σ-holes on the two F atoms on the C–F bond extensions were found to be negative, with the $V_{S,max}$ values being −11.95 and −11.75 kcal mol$^{-1}$ for the 0.0015 and 0.0020 a.u. envelopes, respectively. The outer surface of the two O atoms were now turned out to be positive, described by $V_{S,min}$ values of +3.67 and +4.12 kcal mol$^{-1}$ on the 0.0015 and 0.0020 a.u. mapped surfaces, respectively, meaning that the O atom in this molecule might be able to attract a negative site to form chalcogen bonding! Details of other potential extrema found with a 0.0020 a.u. mapped electrostatic surface are shown in Figure 4b. Clearly, these results confirm the importance of using isodensity values other than the often suggested 0.0010 a.u. envelope on which to compute the electrostatic potential.

Nevertheless, it has been said [25,26,52] that the seminal work of 2007 [109] resulted in the true birth of halogen bonding. Since then several thousands of research articles dealing with the topic either theoretically or experimentally, or both, have appeared, which have followed the definition and several characteristics proposed by IUPAC [39] to identify the occurrence of a halogen bond in the solid-state or in gas phase adducts. Many of the theoretical studies focus only on binary complexes or slightly larger systems, limited by issues of computational efficiency and resources. In many of these studies the results obtained suggest a close agreement between the gas and solid-state properties of the bonding interactions. Legon and coworkers [78,83,88], using Fourier transform microwave spectroscopy, performed a significant number of studies on a wide variety of halogen-bonded adducts

in the gas phase. Their results on the intermolecular geometries and the nature of charge-distributions and charge-transfers accompanying the formation of these systems reveal some close similarities between the properties of the gas phase binary adducts and the adducts synthesized and studied in the condensed phase. These demonstrate that lattice and solvent effects have a marginal influence on basic halogen bond features, a view that has been advanced in a recent review [10].

### *2.3. Classification of Halogen Bonding*

Halogen bonding has been classified as Type-I and Type-II. Traditionally, this classification is based on the nature of the intermolecular angle of interaction observed in a variety of geometries in the crystalline phase that emerged from a database survey. For instance, in 1994, Pedireddi et al. [163] examined 1051 contacts in crystals, which led them to divide these mainly into two categories depending upon the values of the two C–X···X angles $\theta_1$ and $\theta_2$ around the X atoms in a fragment of the type C–X···X–C. As such, Type-I contacts were defined as those in which $\theta_1 \approx \theta_2 << 180°$, while Type-II were defined as those in which $\theta_1 \cong 90°$ and $\theta_2 \cong 180°$. There are several other such studies reported [9–11,19,164–169] that show halogen-centered Type-I and Type-II interactions that can be approximated with those illustrated in Scheme 1a,b, in which, $90° < \theta_2,\theta_2 \leq 150°$ and $160° < \theta_2 \leq 180°$, respectively. Note that the angular ranges given above for these two types of interactions are tentative. Depending on the involvement of secondary interactions, or the nature of the interacting sites, these can be significantly off. For instance, there are many occasions reported crystallographically, in which, Type-II contacts have been observed in the range of $140° < \theta_2 \leq 160°$. The same directionality condition is applicable to any other noncovalent interaction formed by tetrel, pnictogen, and chalcogen atoms in molecules.

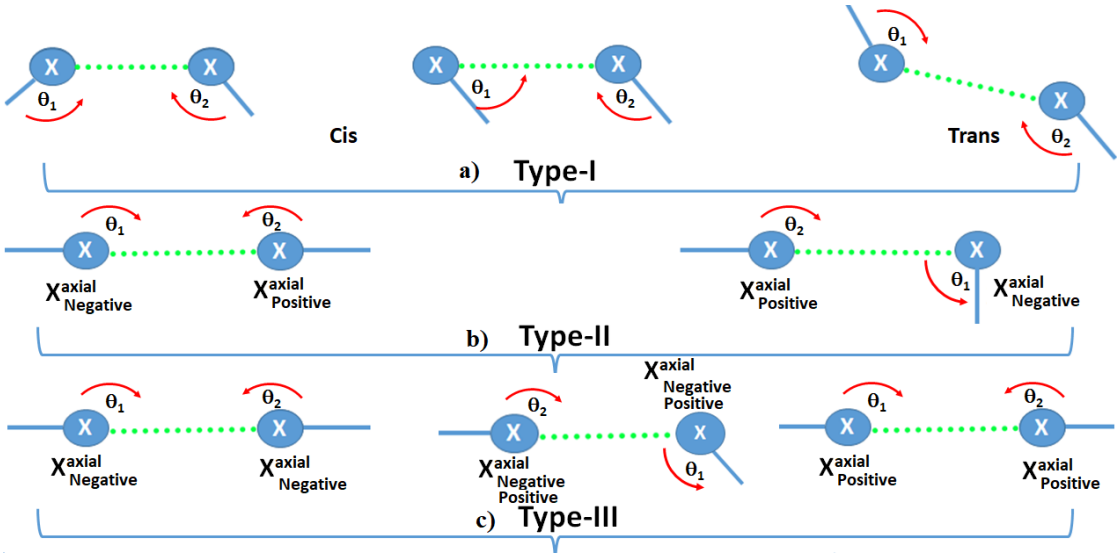


**Scheme 1.** (**a**) Type-I halogen···halogen bonding, (**b**) Type-II halogen bonding, and (**c**) Type-III halogen···halogen bonding.

In addition to angle as a constraint, another requirement to confirm the formation of a Type-II halogen bonding is that the covalently bound halogen atom must enclose a positive site, either along the bond extension or around it. This site must engage in an attractive interaction with a negative site. It must be kept in mind that all Type-II halogen-centered interactions are not halogen bonds. Examples of systems are known where there is no requirement for negative and positive sites to be involved in the attractive engagement to sustain a Type-II topology. In such cases, the interacting sites on the halogen atoms can be both positive (or both negative) in the monomer [47,141]. This means that the definition of Type-II halogen bonding illustrated in Scheme 1b is not applicable to such intermolecular interactions. We have recently proposed that these be referred to as *σ-σ centered type-II halogen-centered noncovalent bonding* [141]. Interactions involving a Type-II (geometric) topology of bonding, but do/do

not involve a positive site, could be referred to as Type-III *halogen*· · ·*halogen bonding*, Scheme 1c. In fact, this terminology is specifically applicable to interactions formed between two atomic sites of similar or dissimilar electrostatic potential in interacting monomer molecules in which the interacting sites conceive σ-holes that are either both positive or both negative. Also, the angle $\theta_2$ is close to that of Type-II since there are many occasions in which the position of σ-hole does not show up exactly along the outer extension of the covalent bond. One such instance is illustrated in Figure 5 (see the $(C_6F_6)_2$ dimer).

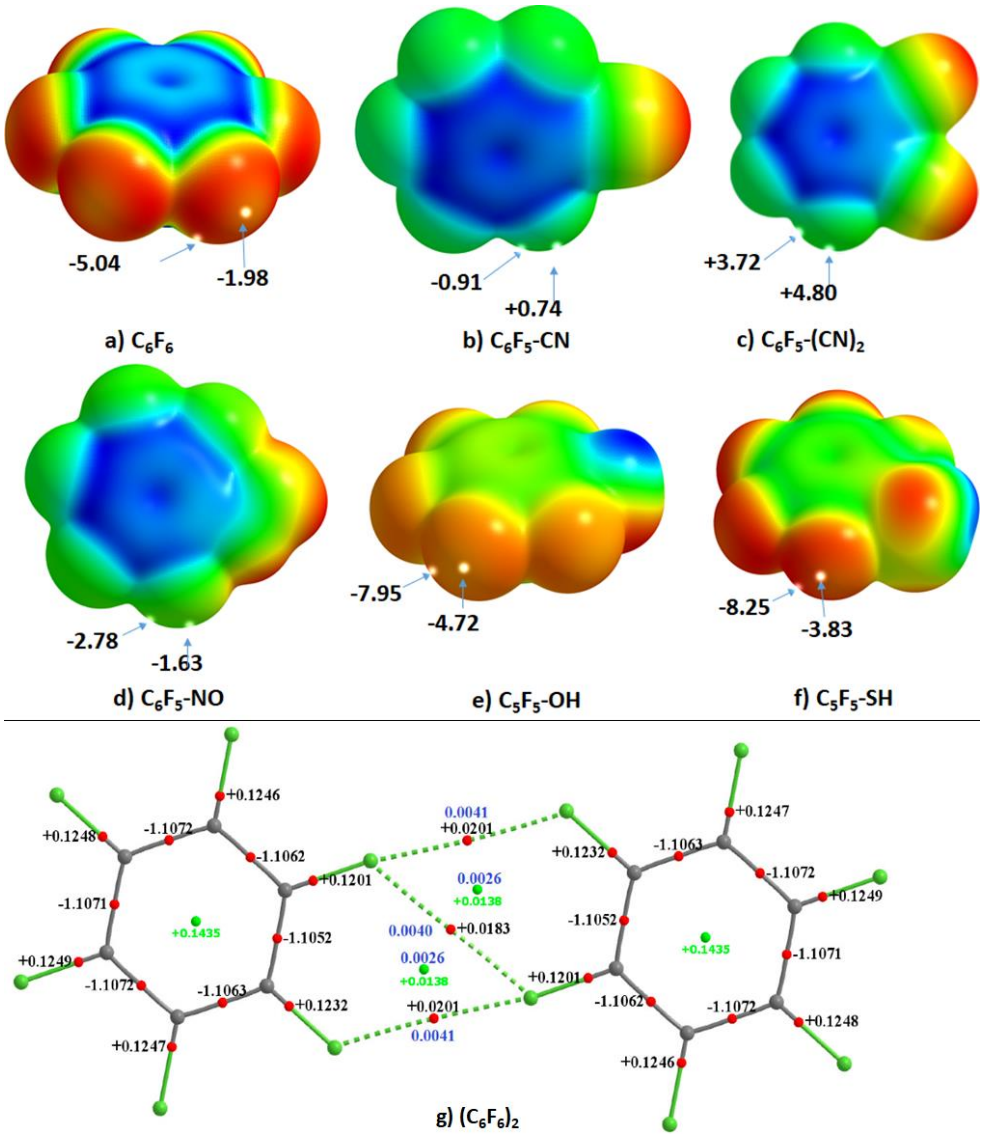


**Figure 5.** (**a**–**f**) PBE/6-311++G(2d,2p) level 0.0010 a.u. isodensity mapped molecular electrostatic surface potential of some partially and fully fluorinated aromatic compounds. The maximum and minimum ($V_{s,max}$ and $V_{s,min}$ (in kcal mol$^{-1}$), respectively) of MESP are shown on some fluorine atoms in a few of these compounds, demonstrating anisotropy in the charge density. For clarity, yellow dots representing $V_{s,max}$ and $V_{s,min}$ are shown only for a few cases (Color: blue—strongly positive; red—strongly negative). (**g**) The MP2/cc-pVTZ level QTAIM molecular graph of the $(C_6F_6)_2$ homomolecular dimer [49], formed even when the fluorine in the $C_6F_6$ monomer is entirely negative. The charge density ($\rho_b$/a.u., blue) at selected F· · ·F bcps and rcps, and the Laplacian of the charge density ($\nabla^2\rho_b$/a.u., black) at all bcps and rcps are shown. Bcps: tiny red spheres; rcps (ring critical points): tiny green spheres; bond paths: solid and dotted lines in atom color; solid and dotted lines represent the open- and closed-shell interactions, respectively.

The above requirements for Type-II and -III halogen bonding are, however, not necessary for the formation of Type-I halogen···halogen bonding, Scheme 1a. The halogen atoms forming this topology can be either entirely negative or entirely positive, and the angles of interaction are generally significantly off from 180° (90° < $\theta_2$,$\theta_2 \leq$ 150°). For the $(NF_3)_2$ dimer geometry discussed elsewhere [141], for example, ∠F···F−N = 116.2°; this involves a Type-I halogen···halogen bonding topology. Its formation is due to the attraction between the negative equilateral sites localized on the fluorine atoms in $NF_3$, which are likely to be driven by dispersion.

### *2.4. The Many-fold Controversy*

There is a myriad of contradictory views expressed in the literature dealing with noncovalent interactions (some are referred to in the Introduction) and it is not possible to summarize all of them here; we outline only a few of them below.

#### 2.4.1. Is an Atom–Atom Contact a Bond (or an Interaction)?

Although significant progress has been made in the area of noncovalent interactions, Dunitz [170] has recently questioned whether interatomic short contacts in intermolecular regions of crystals should be regarded as bonding interactions. The open questions were, to quote: "Should the observation of short distances between pairs of atoms on the peripheries of different molecules in crystals be regarded as evidence of specific intermolecular bonding between the atoms concerned? And if the answer is not yes but no or perhaps or sometimes: how are we to distinguish the bonding atom–atom interaction from the energetically neutral or antibonding type? Do we need another IUPAC commission to decide?" Alternative viewpoints have been provided to clarify the meaning of atom–atom short contacts associated with chemical interactions [171,172]. In an answer, Lecomte et al. [171] argued that individual atom–atom pair interactions (of atoms in a crystal) are structure determining, and thus are responsible for the entire structure of the chemical system being examined. In our view, which may be in accord with that of Desiraju [173], the packing between molecular domains in crystals is closely related with the atom–atom contact distances; this, together with the directionalities involved, collectively determine the energies of these contacts. Clearly, these three features, together with lattice forces, and sometimes solvation, are often examined to determine the way and the extent to which an intermolecular interaction drives packing of molecules in a crystal. In addition, we should remember that charge density topologies between atomic domains provide an effective means of rationalizing the presence of atom–atom interactions in chemical systems [174]. The usefulness of the application of charge density models while examining bonding interactions should not be underestimated by any chance. Note that the one-electron density obtained from DFT calculations contain the information needed to define molecular structure and most atomic properties. But approximate functionals often fail in describing weak interactions, in which, a part of this failure could be in reproducing the exact density in diffuse regions. The inconsistency in the topological properties of the valence-shell charge depletion of atoms arises when basis sets and/or functionals are changed. Experimentally, there is less scattering and thus more error in this region.

#### 2.4.2. How to Define a Bond?

Debate is ongoing to validate the IUPAC recommended characteristics [39,40,50,55] of halogen bonding, the underlying concepts of σ-hole theory [16,49,51], the origin of directionality [175–177], and the geometric definition by which halogen bonding (and other σ-hole interactions) may be identified [49,169]. For instance, it was suggested that a minimum of four atoms or group of atoms should be considered to define a hydrogen bond (or a halogen bond) [39,177]. This is because each part (donor and acceptor fragments) affects the other parts and is also affected by them. McAllister argued that the term "halogen bond", represented by the three dots as in R–X···Y, is a controversial statement because the whole fragment R–X···Y constitutes a bond [178]; a similar view is provided for hydrogen bonds elsewhere that suggests a bond could be traceable between two atoms [99]. The geometric

criterion for a halogen bond, requiring the involvement of at least four atoms, is different to the way a chemical bond is traditionally viewed.

A bond (or an atom–atom contact) [99,170–172] is usually taken to be formed if, and only if, the nuclei of two atoms are linked, as in diatomic $H_2$, $O_2$, and $X_2$ (X = F, Cl, Br) molecules, for example. This is true regardless of the nature of bond, i.e., whether it is a covalent bond in molecules, an ionic bond in NaCl, or a coordinate bond in a transition metal complex. As Lecomte et al. [171] noted elsewhere, atom–atom contacts, irrespective of their nature (covalent, ionic, metal–metal, metal–ligand, hydrogen, halogen, chalcogen, van der Waals, halogen$\cdots$halogen, hydrogen$\cdots$hydrogen (H$\cdots$H), etc.), follow this bonding rule. When QTAIM based bond paths and bond critical points of charge density $\rho$(r) are observed where classical models prohibit bonding, these cases may indicate a failure of these models to encapsulate unusual bonding situations for which they were never designed [171,179].

Clearly, no matter how many atoms constitute a molecule, a bond is effectively realized between two atoms. By doing so, the role of all other neighboring bonds comprising the molecular system is neglected. For instance, the substitution effect of halides in a benzene molecule causes the formation of halobenzene derivatives, $C_6H_{6-n}X_n$. In this example, the C–X bond is formed through the replacement of the C–H bonds in $C_6H_6$. Because of this, the C–C bond distances of the aromatic moiety are directly linked with the C–X fragment of the molecule and are also geometrically affected. Accordingly, the electronic structure and vibrational characteristics of the C–C bonds in $C_6X_6$ also change compared to those in the $C_6H_6$ molecule. Surely this does not need to be taken into account when recognizing C–X as a bond. Equivalently, it is then inappropriate to suggest that a minimum of four atoms or group of atoms to be essentially required to define a noncovalent interaction, such as a hydrogen bond, a halogen bond, a chalcogen bond, a pnictogen bond, or any other (σ-hole) bonding interaction. Of course, provided one is required to define the directionality constraints of these interactions, a minimum of three atoms are required. If a minimum of four atoms are required to define a halogen bond, does this require the geometric constraints on the dihedral angle to be defined as a feature for recognizing a halogen bond? What if an interaction is formed between the electron acceptor fragment of a molecule and an anion $X^-$ (X = F, Cl, Br, I), for example? In this case, the electron donor fragment does not comprise more than one atom. How does one fulfill the constraint of a minimum of four atoms to define a noncovalent interaction? Should this be treated as a special case? In our view, prescriptions such as this are baseless and add nothing to the understanding of the physical chemistry of the interaction. The donor and acceptor fragments might be required to provide additional insight into the electronic and vibrational changes [39,54] accompanying the formation of an adduct; however these are certainly not a necessary prerequisite to define the geometry of an atom–atom (bonded) interaction.

#### 2.4.3. Is the Concept of Atomic Charge Meaningful?

The concept of charge on an atom in a molecule is a useful property with a long history [180,181]. Its determination has been devised over thirty theoretical and experimental approaches [180]. According to Meister and Schwarz [180], effective partial charges are assigned to atoms in molecules and crystals in order to economically describe the ionicity and polarity of chemical bonds. Volkov et al. observed that the QTAIM allows a rigorous definition of the charges of the atoms in molecules and provides a realistic basis for comparison between molecules and between experiment and theory [182]. Bader and Matta [183] contend that the charge on an atom in a molecule is defined by QTAIM as the (average) expectation value of the number operator, a Dirac observable. An atomic charge is measurable and it, together with its change, contributes to numerous measurable properties: to all molecular moments; molecular polarizability; intensities of electronic, infrared, and Raman absorption intensities; and to the polarization of a dielectric. Matczak noted that the accurate reproduction of molecular dipole moments by partial atomic charges is an important factor contributing to the reliable determination of intermolecular interactions in simulations [181]. Nevertheless, because the nature and magnitude of atomic charges vary with respect to the definition devised by different models, these sometimes do not match with each other. Politzer and coworkers [89,184,185] have called this

"a fallacy of atomic charges", and contend that a single positive or negative charge cannot be assigned to an atoms in molecules. Such a perspective emerged from the notion that σ-hole bonding between like atoms resulting in "like–like" interactions could not be understood in terms of atomic charges assigned by any of the usual procedures, which view a bonded atom as being entirely positive or entirely negative. In this context, the importance of electrostatic potential has often been stressed to be unique, an experimentally measurable property [186–188]; it could explain the bonding scenario between like atoms of dissimilar site polarities in molecules. There are others who have observed that there is significant ambiguity in the determination of electrostatic potential itself [189]; this was shown using several molecules of different degree of degeneracy, quasidegeneracy, and symmetry, leading to the conclusion that molecular electrostatic potential is ill-defined for degenerate ground states due to the ill-defined nature of the electron density.

Verstraelen et al. have claimed that for the development of ab initio derived force fields, atomic charges must be computed from electronic structure computations, such that (i) they accurately describe the molecular electrostatic potential and (ii) they are transferable to the force field application of interest [130]. Ionescu and coworkers [190] argued that partial atomic charges are a well-established concept and are very useful in understanding and modeling the chemical reactivity behavior of molecules, ranging from simple compounds, to crystals, to large drug-like molecules, to biomacromolecular complexes with hundreds of thousands of atoms. Hamad et al. [191] found that knowledge of atomic charges on specific systems is important, and that they are useful in gaining insight into metal–organic frameworks (MOFs). The strategy, which is applicable to other porous materials, paves the way for large-scale computational screening of MOFs for specific applications as well as contributing to a better understanding of the structure–property relationships for MOFs, eventually assisting in their development and application [192]. In molecular simulations with fixed-charge force fields, the choice of partial atomic charges influences numerous computed physical properties, including binding free energies. Mobley and coworkers [193] commented that the past decades have witnessed simulations employing carefully parameterized fixed-charge force fields that can provide useful insights into biological and chemical questions. Their overview focuses on the four major force field families, i.e., AMBER, CHARMM, GROMOS, and OPLS, which are based on the same classical functional form and are being continuously improved to the present day. In molecular dynamics or Monte Carlo simulations, the interactions between the particles (atoms) in the system are described by a force field. The empirical functional form of classical fixed-charge force fields dates back to 1969 and remains essentially unchanged. In a fixed-charge force field, the polarization is not modeled explicitly, i.e., the effective partial charges do not change depending on conformation and environment [194].

Whereas the determination of atomic charge by theoretical methods is not unified, attempts to find a robust method for its determination have been made from time-to-time. For instance, Stasyuk and coworkers [104], as well as several others [195], have recently proposed new models for evaluating charges that could be utilized for arriving at a fundamental understanding of some chemical systems, including endohedral fullerenes. Evidently, atomic charge is certainly a valuable property [196] that will continue to play a crucial role in the understanding systems in diverse areas of science.

#### 2.4.4. Is the Directionality Feature in Halogen-Centered Noncovalent Interactions Understood?

Scholfield et al. [197] examined the structure and stability of proteins that were characterized by a series of weak noncovalent electrostatic, van der Waals, and hydrogen bond (HB) interactions. In the $Y18^{br}F$ system, the bromine was within van der Waals distance of the Glu11 oxygen (~100% of the sum of the van der Waals radii, $\sum R_{vdW}$), but at an angle of approach of 142.7° from the oxygen of Glu11. Because this angle was nonlinear relative to the C–Br bond, it was then suggested that for these geometries the bromine is not making a halogen bond, or at least not a very strong one. Interestingly, however, the angle of approach was 150.0° for the Glu11 oxygen toward the I–C bond. This led to the interpretation that this angular restriction places it within the same category as the electropositive

σ-hole of iodine [198], and that iodine is more ideal for making halogen bond in the Y18$^{i}$F construct leading to a stronger interaction than the analogous interaction in the Y18$^{br}$F construct. This leads to the conclusion that the angle of interaction is a factor when deciding whether a halogen atom makes a halogen bond.

It is often suggested that the directionality of halogen bonds is electrostatically driven [53,186,199–202]. This is applicable to Type-II halogen bonds that are linear or quasilinear. Type-I halogen bonds have been regarded as nondirectional because they do not obey the guiding principles of σ-hole theory. Even in this case the anisotropic nature of the charge density leading to the so-called "fallacy of atomic charges" does not hold since there are many occasions in which halogen atoms forming this bonding topology are entirely negative (or entirely positive). Factors influencing the origin of both these topologies of bonding have been significantly debated over the last five years, leading to diverse opinions, and no specific agreement has yet been reached on the exact nature of their origin. Some have argued that a positive σ-hole is not a prerequisite for a molecule to participate in a halogen bond as a halogen donor [115]. Many believe that this view is not (always) true, as charge transfer, induction, dispersion, and exchange repulsions play the dominant role in determining the directionality of halogen bonds at equilibrium geometry of a complex. For instance, Huber and coworkers [175] examined linear (most stable) and perpendicular complexes theoretically, and suggested that charge-transfer interactions and Pauli repulsion are the driving forces for the directionality of halogen bonds. A similar perspective was provided by Stone who found that while electrostatics are the largest attractive term in halogen bonding, the propensity of halogen bonds to be linear is dominated by the exchange-repulsion term as it acts as an effective barrier when halogen bonds are forced away from collinearity [13]. Riley et al. suggested that the C–Br$\cdots$Cl angles for some halogen bonded complexes with cationic halogen bond donors the secondary interaction that occurs between $Cl^-$ and the cation ammonium group (angles greater than ~120°) enhances exchange repulsion associated with the halogen's oblate shape, which is probably chiefly responsible for halogen bond directionality, as has been found for neutral halogen bonds [203]. Others argued that the contribution due to electrostatics may be significant in some complexes, as significant as dispersion and exchange in the others, but the equilibrium geometry of a complex system that is stabilized by a noncovalent interaction (no matter what type of bond it is) is always driven by all of them [12,45,47,49,51,52,204]. This suggests that the directionality of the interaction is simply a representation of the delicate balance between all component interactions acting on the nuclei of atoms. From the various arguments given above, it is clear that the origin of the directional feature of a halogen bond is yet to be fully understood; for this, many other systems need to be examined, focusing particularly on directionality. This is consistent with the view of others [205], i.e., in order to more effectively exploit the use of halogens in rational ligand design, it is necessary to quantify the detailed nature of these interactions, including their energetic contributions and their orientation dependence.

#### 2.4.5. Polarization Induced σ-Hole: Is It Real or a Provocation?

Why is it that a σ-hole is not found when X = F, as well as in some other cases, such as $CH_3Cl$? This question was asked and answered in 2007 [109]. Specifically, it was argued that the σ-hole on the halogen in these systems is not found because of the higher electronegativity of fluorine (or chlorine) that gives it a disproportionately large share of the σ bonding electrons, which helps to neutralize the σ-hole. Alternatively, it was argued that if the electron-attracting power of X is greater than that of the remaining part R of its molecule R–X, then the halogen atom may gain enough electronic charge to neutralize the σ-hole [109]. It was also suggested that there could be an anomeric effect that strengthens polar flattening and allows facile polarization to give a "neutral σ-hole" (as has been done for the molecular fragment $–CF_3$) that acts as a hotspot for dispersion interactions [126,162]. These views continued to be held [206], even though it has been shown in several instances that these and similar systems do have σ-holes on the outer extensions of C–X bonds [12,45–47,49,52]. In fact, in 2008, ab initio calculations by Riley and Hobza [207], for instance, have shown that the

complex $H_3C–Cl\cdots O{=}CH_2$ is bound despite the chlorine in $H_3C–Cl$ lacking a significant positive potential. In many studies this has often been used as an example of the failure of σ-hole theory: "The proponents of σ-hole theory regard this interpretation of the 'failure of the electrostatic interpretation' to be incorrect and suggest it is because the potential on the chlorine prior to interaction does not reflect the polarization caused by the electric field of the oxygen in $O{=}CH_2$" [89]. In fact, there have been many different studies appeared in the last 10 years that show that $O{=}CH_2$ induces a positive potential on Cl on this molecule [25,27,89,208]. To exaggerate this, a charge of $-0.27629e$ was placed at a distance of 3 Å from the chlorine nucleus along the extension of the C–Cl bond; this resulted in a positive (σ-hole) potential on the chlorine [202]. This is also against the argument of the same authors that electrons are indivisible and cannot be fractioned [27], so the placement of a fractional charge is misleading and unrealistic. The placement of a negative (or positive) test charge at a distance from an atom in a molecule actually makes the entire system anionic (or cationic), and the computed electrostatic potential will undoubtedly be negative (or positive) everywhere on the surface of the resulting molecular species. Is it due to induction? The answer is presumably "no". Even if one does so in models, it will significantly perturb the electronic structure of the $CH_3Cl$ molecule. For instance, provided a charge of $-1$ is placed at a distance of 3.0 Å from Cl in $CH_3Cl$, and provided the geometry of the entire system is energy-minimized at a specific level of theory, this will completely dissociate the C–Cl bond and results in the entire system becoming an ion pair. Although some firmly rely on this to contend that a σ-hole can be induced, others believe that a σ-hole is an inherent property of bound atoms in molecules that cannot be induced [209].

Varadwaj et al. [52] have shown that the local maximum of the electrostatic potential, $V_{s,max}$, on the surface of the chlorine along the outermost extension of the C–Cl bond in $CH_3Cl$ would vary dramatically from slightly negative to slightly positive values with respect to the basis set sizes and correlation methods employed. The strength of the Cl's σ-hole potential in $CH_3Cl$, mapped on the 0.001 a.u. isodensity envelope, was approximately +1.0 kcal $mol^{-1}$ at the best level of theory employed, CCSD/6-311++G(3d,2p). From this result, it is clear that the electric field of $O{=}CH_2$ does not induce a positive σ-hole on Cl. Thus the claims in [25,27,89,202] are refuted as Cl's σ-hole in $CH_3Cl$ is inherently positive; this is only apparent when appropriate theoretical methods are employed since the molecule contains a heavier halogen that requires additional diffuse functions for the proper correlated description of the system's properties. The positive σ-hole on Cl explains why it is competent to participate in an attractive engagement with the negative site on several bases.

One can always argue that the formation of the $O\cdots Cl$ interaction in $H_3C–Cl\cdots O{=}CH_2$ is a consequence of mutual polarization that happens when $O{=}CH_2$ approaches the Cl and is strong enough to pull electron density away from the Cl, leaving a more positive σ-hole. In fact, mutual polarization is indeed an essential feature that drives the formation of many complexes. However, the interacting atoms in the two monomers have already overlapped in the complex; hence the transformation of the nature of Cl's σ-hole from negative to positive within the equilibrium geometry of the complex cannot be extrapolated by introducing the concept of polarization.

If one accepts that polarization induces a positive σ-hole on Cl in $H_3C–Cl$, is the occurrence of the same phenomenon possible for other molecules as well? We have not found any realistic example in the literature where a σ-hole could be induced on an atom in a molecule through the electric field of a partner molecule which can then potentially attract the negative site in the partner molecule to form an intermolecular contact between them. As summarized in Table 1 for $F_2SO$, and shown for many other systems such as 1,3-dioxine (Figure 4) and $CF_4$ [158], as well as in many halogen-substituted systems discussed elsewhere [12,47,49,141], the nature of σ-hole on atoms in molecules is an inherent property which can be traced provided an appropriate theoretical method is chosen for the study. This will be appreciated when examining the dimers of fluorine-substituted benzene derivatives shown in Figure 5g and Section 4.1. The negative σ-hole on the F atom in one of the monomers cannot be turned positive by the electric field of a similar atom in another similar molecule. Indeed, the effect of polarization is important for the monomers to interact attractively, but certainly the inherently

negative nature of the σ-hole does not turn positive during the course of interaction. Irrespective of the functional and basis set used, the nature of the F's σ-hole in $C_6F_6$ does not change sign from negative to positive.

Whilst the suggestion that a positive σ-hole can be induced on Cl in $H_3C$–Cl is thought-provoking, it creates a great deal of confusion unnecessarily. It would therefore be interesting to see in future investigations whether the entirely negative σ-hole on the F atom along the C–F bond extension in $H_3C$–F can be turned to become positive by placing a relatively more negative site in another molecule (but certainly not a charged species) in its close vicinity so that they attract each other, leading to the formation of a binary complex. Will the topology of the resulting interaction be directional? What is the strength of such an interaction? An answer to these questions may assist in resolving the aforesaid controversy (at least partially). Note that the potentials of $CH_3F$ (and $CF_4$) were shown to be indicative of fluorine interacting only with electrophiles [161], yet some of us have disproved it in other studies since the fluorine in $CF_4$ does show significant ability to attract nucleophiles [158].

#### 2.4.6. Is the σ-Hole Model a Unified Model?

It has also been shown on several occasions that the σ-hole model apparently fails to explain Type-I [210] and Type-III halogen···halogen interactions [12,16,17,45,46,49] between molecules. The conceptual framework of a σ-hole developed from an electrostatic potential does not work in these systems; neither does the concept of polarization completely explains this kind of interaction since both sites that attract each other when forming a Type-I topology have nearly similar electrostatic potentials. There are also instances where the electrostatic potential model cannot be utilized to account for directional bonding between electrophilic or between nucleophilic regions [12,16,17,45,46,49]. This is in agreement with the views of Bayse [14] that even though halogen bonding interactions are often discussed in terms of an area of positive electrostatic potential on the halogen center along the outer portion of the bond axis, there are several others who have noted a lack of completeness in this model. This is also in agreement with Wang et al. [51], who view the intermolecular attractive interaction between electrophilic (σ-hole) sites as a counterintuitive phenomenon because the electrostatic component of the interaction is repulsive and plays a destabilizing role. Using the block-localized wave function (BLW) energy decomposition method [211], they demonstrated that charge transfer seemingly plays the main role, and that the predicted bonding sites related with the "hole" concept are universally insufficient to describe the noncovalent interactions in these counterintuitive complexes. Because other stabilizing factors contribute to the stability, and sometimes play even bigger roles than electrostatic interaction, these are consequently considered to be important in governing the structure of complexes. In essence, these studies unequivocally suggest that the σ-hole model and its concepts do not form a unified model, nor it is universal. It works for some systems, but fails for others, and cannot explain Type-I and -III halogen···halogen bonding interactions.

### *2.5. The Topology of Fluorine Centered Bonding*

As indicated above, and in a perspective article published in Science in 2017 [206], it was noted that "the σ-hole is more marked for Br and I than for Cl; for F, the lightest halogen, with its tightly bound electrons, ostensibly no σ-hole and no-halogen bonding would be formed." Identical views have been expressed by others [16]; many of these were based on the misleading results of the seminal study published in 2007 [109], as well as from the notion that views σ-holes "as regions of positive molecular electrostatic potential collinear with and opposite to covalent bonds to atoms of Groups IV–VII" [120]. This is incorrect, as can be deduced from surveying the literature published in this area over the last five years, which shows that the fluorine atoms in most fluorine-containing molecules do have a σ-hole [142,212–215]. Depending on the electron withdrawing ability of the remaining part of the fluorinated molecule, an electron deficient region may develop on the axial portion of the fluorine atom. Given that the nature of the σ-hole is determined by the sign of $V_{S,max}$, the σ-hole could be positive or negative [12,45–47,49,142,158,212–215]. That is, when $V_{S,max} > 0$ on the F atom, it is referred to as a positive σ-hole, and when $V_{S,max} < 0$,

it is called a negative σ-hole. For instance, the 0.0010 a.u. mapped fluorine σ-hole potential in $CH_3F$ ($V_{S,max}$ = −23.89 kcal mol$^{-1}$ with M06-2X/6-311++G(2d,2p) [12]), $C_6H_5F$ ($V_{S,max}$ = −15.4 kcal mol$^{-1}$ PBE/6-311++G(2d,2p) [49]), and $C_6F_6$ ($V_{S,max}$ = –4.8(−5.1) kcal mol$^{-1}$ with M06-2X/6-311++G(d,p) (PBE/6-311++G(2d,2p) [49])) are negative, whereas that in $CF_4$ ($V_{S,max}$ = +1.77 kcal mol$^{-1}$ with QCISD(full)/6-311++G(2d,2p) [12]) and FCN ($V_{S,max}$ = +14.88 kcal mol$^{-1}$ M06-2X/6–311++G(2d,2p), this study) are positive. Figure 5a–f presents yet another set of examples in which the σ-hole on the F atom on the outermost C–F bond extensions can either be positive or negative [17]. This effectively means the σ-hole on the fluorine has the ability to make noncovalent contacts with other atoms in interacting molecules (albeit weakly). These and other recent studies provide detailed insight into the nature of σ-hole profile of fluorine in a variety of molecules [12,17,45–47,49,158,212–215]. Figure 5g confirms that the negative σ-hole on fluorine in $C_6F_6$ can attract a negative site to form the $(C_6F_6)_2$ dimer [49], which involves both Type-III and Type-I topologies of bonding (Scheme 1).

Unlike for the heavier halogens, both the noncovalent chemistry and reactivity profiles of fluorine in molecules are yet to be fully delineated. This is understandable because there are relatively very few theoretical studies reported highlighting the reactive nature of the fluorine participating in attractive interactions that may be intuitively obvious or indeed counterintuitive [32,142,214–216]. Because the reactive behavior of fluorine in molecules is more difficult to predict [12,32,45–47,49,216] (which is not always the case for the heavier halogens), it is rather difficult to make standalone conclusions about the nature of fluorine's σ-hole in molecules, although it is more likely (not always) to be negative than positive in small molecules.

The positive (or negative) fluorine atom in molecules attracts a positive (or negative) site on the partner molecule to form complexes. This is observed experimentally [16] and was proved theoretically; in such cases either the fluorine atoms are both positive or both negative [12,17,45–47,49,158]. The intermolecular bonding pattern in these complex systems are of σ···σ type (Type-III), yet these violate the requirement of polarities on the halogen atom that is essential for halogen bond formation. This means that a bonding pattern similar to that of a halogen bond is not necessarily a halogen bond. Hence, a Type-II bonding pattern between two negative sites, or that between two positive sites, is not necessarily a halogen bond [49], even though it was said Type-II halogen···halogen contacts are halogen bonds [144].

Kawai and coworkers [16] have experimentally examined the bonding affinities of F atoms in some perfluorobenzene derivatives. They suggested that the F···F directional interactions are the consequence of halogen bonding. In our view, this is misleading given the underlying definition for halogen bonding put forwarded by IUPAC [39] is taken into account. That is to say, in order to form a halogen bond between fluorine atoms one requires the attractive engagement of a positive site on one fluorine atom along the C–F bond extension with a negative site on another fluorine atom on the C–F fragment of another interacting monomer.

Figure 6 illustrates one such perfluoro compound examined by Kawai et al. [16]: phenyleneethynylene(bis(2,3,5,6-tetrafluoro-4-(2,3,4,5,6-pentafluorophenylethynyl)phenyl)-ethyne (BPEPE-F18)). Our calculation on this molecule shows that the $V_{S,max}$ values associated with the fluorine's σ-hole vary between −3.63 and −7.71 kcal mol$^{-1}$. These negative sites in the monomer molecule have actually attracted the negative sites on another same molecule(s) to form ordered 2D supramolecular architecture on some metal surfaces reported by Kawai and coworkers [16]. Our calculation suggests that the F atoms in these monomers attract each other to form dimers and trimers in the gas phase as well, analogous to what has been shown in other studies for $C_6F_6$ [45]. Clearly, appropriate care has to be exercised to separate Type-II halogen bonding from Type-I and Type-III halogen···halogen interactions, as they are not the same, and the significance of both has been discussed several times [17,19,212,213,217,218]. It is therefore imperative to understand what is in a name [97,177,219].

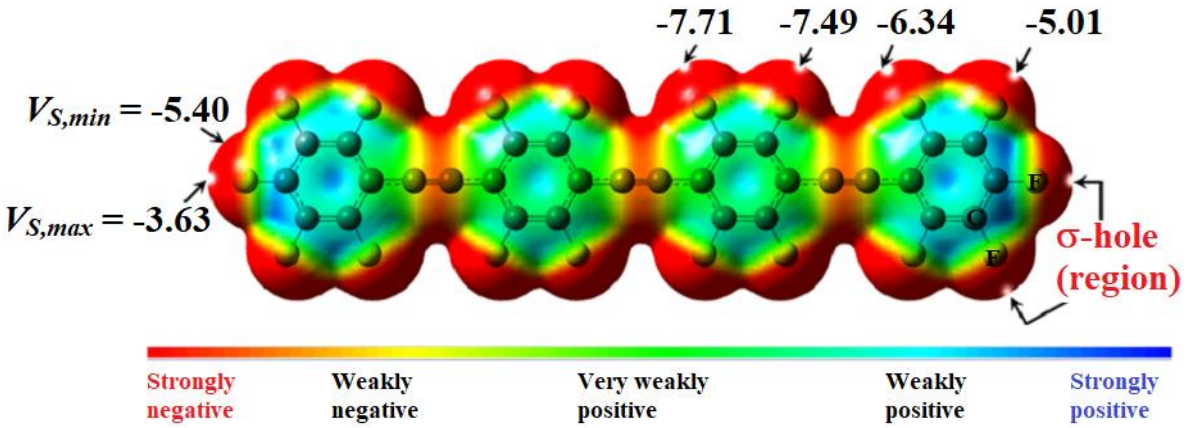


**Figure 6.** M062X/6-311++G(d,p) level 0.0010 a.u. isodensity mapped molecular electrostatic surface potential of BPEPE-F18. The maximum and minimum ($V_{S,max}$ and $V_{S,min}$, respectively) of MESP around some fluorine atoms in this compound are displayed, showing the presence of σ-holes with $V_{S,max} < 0$ along the outermost extensions of the C–F bonds. Values are in kcal mol$^{-1}$.

### *2.6. The $X_3$ Synthon in Crystals*

The $X_3$ (X = Cl, Br, I) synthon in crystals has been known for some time [167]. It has a windmill-like geometrical architecture, regarded as a building block in the development of network structures. The topology is illustrated in Figures 7 and 8 as found in the single crystals of 1,3,5-trichloro-2,4,6-trifluorobenzene [217] and hexaiodobenzene [220], reported in 1981 and 2007, respectively; although the same topology in the latter compound was known from earlier studies [221,222]. Whereas the $X_3$ topology is common in many halogenated aromatic crystal geometries, Kawai et al. [16] and Han et al. [223] have suggested in separate studies that they were the first to show an approximate windmill-like $X_3$ synthon between the perfluoro aromatic compounds that feature a (Type-II) halogen bonding pattern. The angular deviation of the Type-II bonding from the ideal value of 180° in these systems was attributed to the effect of the substrate (*viz.* the Ag(110) surface). In fact, this sort of angular deviation was also found in perfluorobenzene complexes (and other similar complexes) in the gas phase [17,45,49]; the deviation is clearly not an effect of the substrate. In any case, the same pattern, which was more pronounced with respect to the directional behavior, was also evident between the clusters in $C_6Br_6$ islands adsorbed on a Ag(110) surface [223]. In the case of the 1,3.5-trifluorobenze island, however, half of the unit cell revealed an $F_3$ pattern analogous to that found for adsorbed $C_6F_6$ [223]. Liu et al. [224] reported a "windmill" pattern in the cyclic halogen polymers $(XBr)_3$ (X = Cl, Br, I) and $(BrY)_n$ ($n$ = 3–6, Y = Cl, Br, I).

In a following section, we show that the $X_3$ topology between the fluorine atoms is evident in several cases, including the crystal structure of perfluoromethane ($CF_4$), that between the Cl atoms in perchloromethane $CCl_4$.

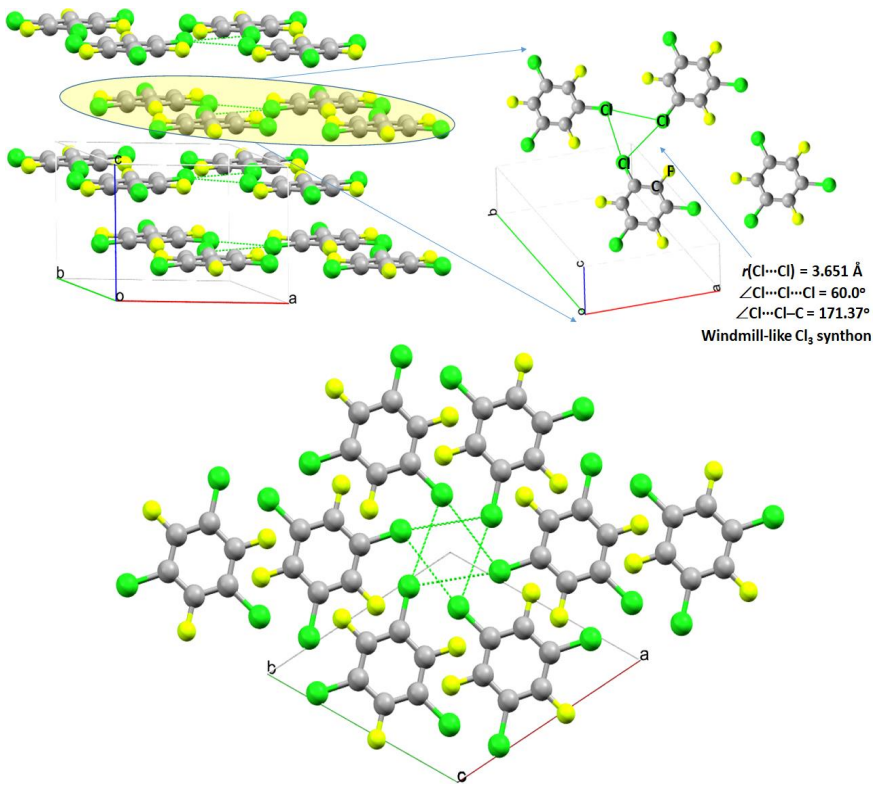


**Figure 7.** The windmill-like $X_3$ topology found in the structure of the crystal of 1,3,5-Trichloro-2,4,6-trifluorobenzene (CSD ref: BARBO). The Cl atom in each molecule in the crystal engages with another two Cl atoms of two neighboring same molecules to form the synthon, responsible for the formation of 2D layer structure.

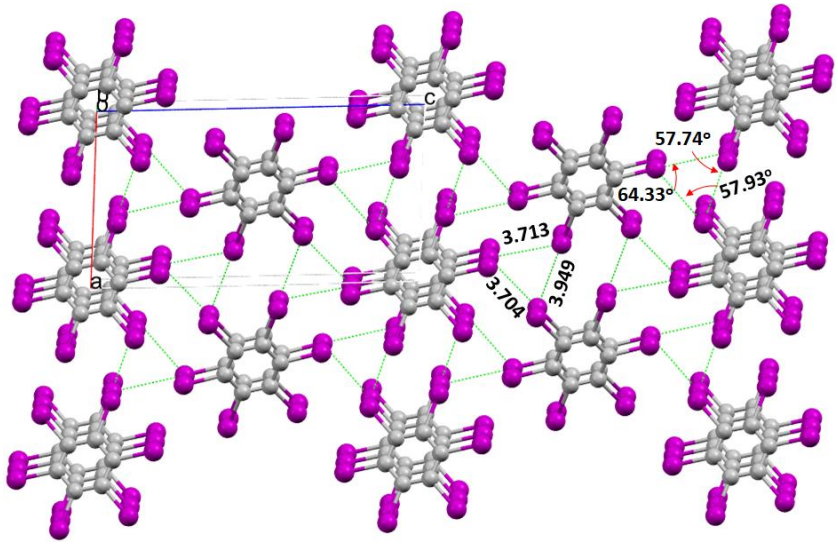


**Figure 8.** The triangular windmill-like $X_3$ topology in the structure of the crystal of hexaiodobenzene ($C_6I_6$) (CSD ref: HIBENZ11 (2007)). The other two crystals of the same system displaying the same topology catalogued in CSD to have the reference codes HIBENZ01 (1970) and HIBENZ10 (1968). The $\angle X\cdots X\cdots X$ angle associated with the $X_3$ windmill is distorted from an ideal value of 60°, yet the three I atoms forming this are in the same plane. The intermolecular $I\cdots I$ distance accompanied with the $X_3$ windmill varies between 3.704 and 3.949 Å. The three $\angle I\cdots I$–C Type-II associated with the three halogen bonds that are linked with the triangular $I_3$ synthon are 173.59, 174.24, and 178.26°. The numerous Type-I interactions feasible in the crystal are not displayed. The C and I atoms are in grey and purple, respectively.

## 3. Charge Density Models for Visualizing Noncovalent Interactions

In addition to the innovative QTAIM approach originally developed by Bader [110–113,225], the literature has witnessed the development of several charge density based models during last 10 years [226–229]. All these approaches have assisted in a way in exploring the chemistry of noncovalent interactions regardless of their type.

QTAIM is based on the zero-flux condition ($\nabla\rho(r).\hat{n} = 0$)) that defines the boundary of an atom in molecules or solids through the space partitioning approach [230,231], where $\rho$ represents the electron density and $\nabla\rho$ is the electron density gradient vector. Within the model [110–113,225], several signatures have been suggested for the identification and subsequent characterization of chemical bonding between atomic basins. Although there are many of them, two of the fundamental (minimal) bonding signatures are (i) the presence of a (3,−1) bond critical point (bcp) and (ii) the presence of bond path between bonded atomic basins. These are collectively useful, visualizable through modern computational tools such as AIMAll [232], and are often used in inferring the presence of possible bonding interactions in chemical systems. Bader suggested that the presence of a bond path is a universal indicator of a bonded interaction [233], but is not a chemical bond by itself [59]. In our opinion, these two statements refer to the same thing. The first indicates that bond paths signal the possibility of an interaction between atoms in molecules and the second cautions that one should not equate bond paths with chemical bonds (as are only indicators). We believe these statements are not contradictory, as claimed elsewhere [124].

Many studies, ranging from dimers to solid-state structures, invoke these two signatures to provide arguments in support of their observations of bonding interactions as these signatures often are consonant with chemical intuition and rationalize experimental observations [234]. In several instances these signatures assist in identifying interactions that are classically forbidden—or are at least unexpected—but are adequate to explain the underlying chemistry of the materials in question [235–238]. Interestingly, their absence between atomic domains in some systems has been led to comments about "the failure of the theory". For instance, recently, Escudero-Adán et al. [239] found a weak triel bond with no bond path connecting the bonding atoms (the electron density path was deflected to a nearby atom) and then claimed that the Bader analysis may not be a reliable tool for very weak interactions. Other reports along similar lines have appeared [210,240,241]. In our perspective, the absence of these minimal features of QTAIM should not be taken as evidence of the failure of the entire theory. As Lane et al. pointed out [240,241], the absence of these specific signatures is because the QTAIM criteria for bonding are somewhat stringent. We believe there are several other descriptors in the theory which should be examined before dismissing the entire theory. Two such important descriptors in the theory are the delocalization index [242–245] and the source function [246,247]. These have been shown to be adequate for the exploration of bonding, especially when bond path and critical point topologies are absent. Tantardini [50] has recently shown that the limit of long-range weakly bound interactions can be found through an analysis of the atomic source function. As long ago as 1985, Bader and MacDougall [248] provided an insightful description of how the critical point topologies of the Laplacian of the charge density can predict directions of bonding interactions, which should also be considered before arriving at a specific conclusion.

The sign and magnitude of the Laplacian of the charge density ($\nabla^2\rho_b$) and the total energy density ($H_b$), where $H_b$ is the sum of the potential energy density ($V_b$) and the gradient kinetic energy density ($G_b$) at the bcp, provide additional information about the ionic and covalent (closed- and open-shell) nature of the interaction involved, respectively. The Laplacian of the density may not be an appropriate measure for covalent bonding because it misses the kinetic energy part. An accepted measure on the nature of bonding is perhaps the Cremer and Kraka criterion [133,249–251]. A necessary condition is the existence of a bond path and a bcp between the two atoms under consideration; a sufficient condition is a negative value of the local energy density $H(\mathbf{r}) = V(\boldsymbol{r}) + G(\boldsymbol{r})$ at the bcp, which implies a dominating potential energy $V(\boldsymbol{r})$ (always negative, stabilizing) over the kinetic energy $G(\boldsymbol{r})$ (always positive, destabilizing), and is indicative of a covalent interaction. These signatures are not only true

for hydrogen bonds [252], but also for halogen bonds, tetrel bonds, chalcogen bonds, pnictogen bonds, and any other noncovalent interaction, and including metal–ligand coordinate interactions of various types [253,254].

The Reduced Density Gradient (RDG) model [226], on the other hand, is another charge density based approach for exploring chemical bonding. It relies on the sign of the second eigenvalue $\lambda_2$ of the Hessian second derivative charge density matrix to characterize the bond type and the charge density $\rho$ for estimating the strength of the interaction. These are collected at each point of a grid encompassing the two interacting molecular systems. This model has already gained significant popularity since it is transferable to systems in diverse areas of the chemical, physical, biological and materials sciences, and engineering. Later, the Density Overlap Regions Indicator (DORI) [227] approach was proposed that assists with revealing the regions of space where the total electron density results from a strong overlap of shell, atomic, or molecular densities, and hence, is an effective tool in extricating the nature of covalent and noncovalent interactions in molecules, molecular complexes and solids. Both RDG and DORI approaches use isosurfaces in three dominant colors to discriminate strong, weak, and van der Waals interactions, which are not indifferent from repulsive ones. For instance, the regions of space colored as blue (green and light-green) and red (yellow and orange) are used for distinguishing attractive interactions from repulsive ones. One of the main differences between RDG and QTAIM methods is that the former predicts the nonlocal nature of charge density distributions between atomic basins, whereas the latter concentrates locally on the critical points of $\rho(\boldsymbol{r})$ but not on the nonlocal nature of the surrounding regions. RDG does detect noncovalent interactions regardless of the presence and absence of bcps as it accounts for the nonlocal nature of $\nabla\rho(\boldsymbol{r})$ in regions in the close vicinity to bcps ($\nabla\rho(\boldsymbol{r}).\hat{n} = 0$). Equation (1) represents the formulation governing RDGs:

$$s = \frac{|\nabla\rho(r)|}{2(3\pi^2)^{\frac{1}{3}}\rho(r)^{\frac{4}{3}}} \tag{1}$$

Equation (1) suggests that in the high density region $\rho^{4/3}$ dominates over $|\nabla\rho|$ and $s(\rho)$ decreases steadily. As $|\nabla\rho|$ approaches zero at a bcp, $s(\rho)$ goes to zero. However, as the term $\rho^{4/3}$ approaches zero more rapidly than $|\nabla\rho|$, their ratio grows exponentially in the atomic tail, so that it tends to zero at low density values. Therefore, the 2D plot of $s(\rho)$ displays features that are representative of interactions. RDG isosurfaces are generally colored red and blue-green, indicative of repulsive and attractive interactions, respectively, since these correspond to $\lambda_2 > 0$ and $\lambda_2 < 0$, respectively.

According to Lefebvre et al. [255,256], there are several limitations and drawbacks of the RDG model. In the model it is difficult to separate out intermolecular interactions in large systems, such as, for example, in biological protein–ligand systems. In such systems, the protein itself features internal hydrogen bonds and van der Waals interactions within its framework, which makes it difficult to separate them out from those occurring between the protein and the ligand. Lefebvre et al. have therefore proposed a modified version of the RDG model, which they called the Independent Gradient Model (IGM). It is a model for the automatic identification of intermolecular interactions using promolecular density (or even using relaxed densities calculated from a wave function) [255,256], significantly reducing the computation time but losing no information about the chemistry of the interactions. It is based on a reference electron density featuring an exponential decay characteristic for non-interacting atoms, and the expression of the electron density gradient (EDG) in terms of atomic components furnishes the basis for the model. The model provides a way of identifying and quantifying the net EDG attenuation due to interactions.

In the RDG model the monomer densities are used as a reference, which is not well-defined for heterodimers. From Equation (1), it is obvious that in regions between two atomic or molecular domains the total gradient $|\nabla\rho|$ attenuates and falls to zero at the bcp and, hence, $s$ suddenly drops. In IGM, and as indicated above, promolecular atomic electron densities are summed up, but the associated atomic gradients are not allowed to interfere. This is achieved by using absolute

values when summing atomic gradients, which erases any electron density contra-gradient feature. This artifice brings the system into a virtual state in which individual gradients can be added without affecting the true electron density. The resulting total gradient $|\nabla\rho^{IGM}|$ is treated as an upper limit of the true gradient, and the difference between them, $\delta g$ ($\delta g = |\nabla\rho^{IGM}| - |\nabla\rho|$), measures the net EDG collapse due to interactions, and hence identifies the presence of opposite signs in the components of the total EDG $|\nabla\rho(r)|$ due to interactions.

A descriptor of the model, $\delta g^{\text{inter}}$ ($=|\nabla\rho^{IGM,inter}| - |\nabla\rho|$) uniquely defines intermolecular interaction regions, thus generating data composed solely of intermolecular interactions for drawing the corresponding 3D isosurface representations. The exponent "*IGM,inter*" ensures that the interactions within the user-defined fragments in chemical systems are cancelled, while preserving the interaction inside these fragments, and hence is effective in extracting the desired interaction present in $|\nabla\rho|$.

The IGM-based isosurfaces between the interacting atomic domains are, in a sense, analogous to those of the coloring schemes used for the RDG and DORI approaches. In these, by definition, the isosurfaces enclose the bcp: this means they are centered around the bcp and so describing interactions not only at the bcp, but also around it. The reason for this is that the sign of the second eigenvalue $\lambda_2$ is used to differentiate between attractive and repulsive domains in regions where $\delta g^{\text{inter}}$ dominates, thereby isolating regions occupied by charge concentration ($\lambda_2 < 0$) and charge depletion ($\lambda_2 > 0$).

We have employed the IGM model in this study to reveal the most important intermolecular interactions in the crystal structures discussed of this review, and compared them with those inferred from intermolecular geometries. The discussion below will illustrate how effective the IGM approach is compared to approaches that characterize intermolecular interactions based solely on the intermolecular geometries determined using X-ray diffraction measurements (as done for most of the systems discussed). The underlying mathematical details [255,256] and adequacy of the model in revealing both noncovalent and covalent interactions have been demonstrated on several occasions recently [257–260], which are therefore not repeated here. Both Multiwfn [261] and in-house codes, together with VMD [262], were utilized.

## 4. Prototypical Examples of Halogen-Centered Noncovalent Interactions

### *4.1. The Tetrafluoromethane ($CF_4$) System*

The geometry of tetrahedral $CF_4$ was reported by Greer and Meyer in 1969 (CSD ref. TFMETH01) [263], Bol'shutkin et al. in 1972 (CSD ref: TFMETH) [264], Pepe et al. in 1989 (CSD ref. TFMETH03) [265], and Fitch et al. in 1993 (CSD refs. TFMETH02 and TFMETH04) [266]. Of these, only the structures reported by Fitch et al. and Pepe et al. (TFMETH02 and TFMETH03, respectively) appear to be reliable because CSD refs. TFMETH01 and TFMETH04 do not contain coordinates of the system but only the cell parameters. CSD ref. TFMETH appears to be problematic as it reports $CF_4$ with a pseudo-square planar geometry.

The geometry shown in Figure 9 is taken from the study of Fitch et al. [266]. From the F···C and F···F intermolecular distances and the F···F–C and F···C–F angles summarized in a and b, respectively, it can be deduced that there are a variety of modes of interaction existing between the $CF_4$ molecules. Based solely on the arguments of the results of the MESP model, one might suggest [109,161,201,267] that the potentials of F in $CF_4$ are indicative of fluorine interacting only with electrophiles. From a later study reported elsewhere [158,268], it was found that that there are four positive σ-holes on the C atom directed along the outer extensions of the four F–C bonds, one would conclude that F···C(–F) in the crystal are genuine attractive contracts even though the $r$(F···C) are significantly longer—3.342 Å—than the sum of vdW radii of the C and F atoms (1.77 and 1.46 Å, respectively). While doing so, the importance of F···F interactions between the fluorine

atoms of the interacting $CF_4$ molecules has probably to be neglected, as was done in the experimental studies [263–266].

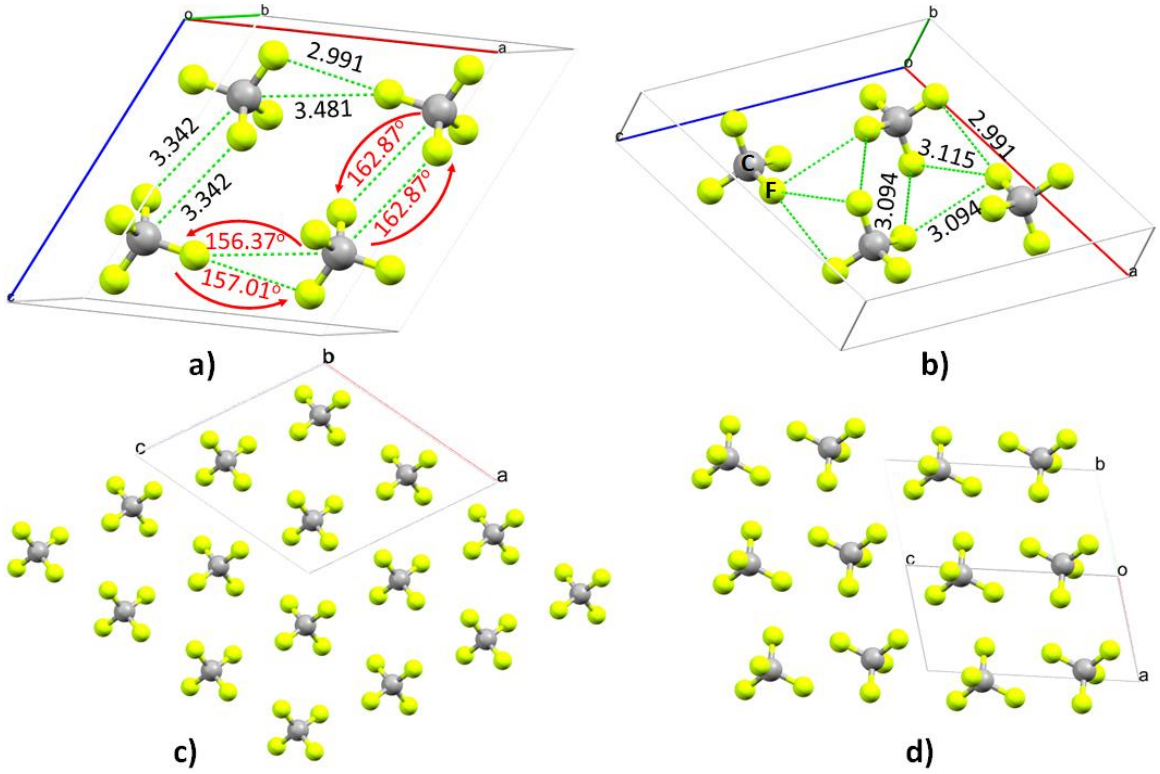


**Figure 9.** Various views of the ball-and-stick models of the unit cell of carbon tetrafluoride ($CF_4$) (CSD ref: TEMETH02): (**a**,**b**) unit cell and (**c**,**d**) 2 × 2 supercell. The F···F and F···C intermolecular bond distances and angles in (**a**,**b**) are in Å and degrees, respectively.

The *r*(F···F) intermolecular distances between the neighboring $CF_4$ molecules lie between 2.990 and 3.115 Å. These are slightly longer than twice the sum of the vdW radius of the F atom, 2.92 Å ($r_{vdW}$ = 1.46 Å). Even so, it does not prevent the F atoms from forming F···F contacts. In a theoretical study reported recently [158], it was shown that the outer axial portion of the F atom in $CF_4$ is weakly positive (mixed yellowish-green region on F in Figure 3e); it is therefore able to form F···F–C Type-II halogen bonds with the lateral F atom of the neighboring molecule. This interaction is weak, as shown by the interaction energies evaluated at various levels of theory [269]. Because many of them exist between the $CF_4$ molecules in the crystal, these must interplay for the development of the supramolecular structure in the solid-state.

As shown in Figure 9b, the F···F contacts between the $CF_4$ monomers in the crystal are also involved in forming the triangular-shaped windmill $F_3$ topology locally. There are two such topologies between the four monomers in the unit cell. The F···F···F angles between the fluorine atoms of the $F_3$ synthon are 59.82, 59.75, and 60.43°, respectively, which are close to the ideal value of 60°. From this, it is obvious that the windmill topology is a feature not just displayed by halogenated benzene derivatives on the metal surfaces [16,223]; it can also present in the crystal structure of perfluoromethane that does not feature an aromatic moiety. This observation is in-line with others who suggested that the windmill-type triangular topology can be formed in the gas phase and is not contingent on the existence of external forces [45].

The question that arises is whether the F···C and F···F contacts noted above in the solid-state structure of $CF_4$, which were characterized solely based on geometric and MESP arguments, are real. Although MESP adequately describes strong electrostatic interactions, such as halogen and hydrogen bonds in molecular complexes, it has been suggested that it lacks the sensitivity (and may even be

misleading) when attempting to interpret weaker interactions [270]. We provide evidence of this below by exploring the nature of the electron density isosurfaces that emerge from a promolecular IGM analysis. The results summarized in Figure 10a,b clarify that the F···F contacts between monomers in the crystal are genuine noncovalent interactions as indicated by the emergence of the electron density isosurfaces between the F atoms. At a higher isovalue of 0.0090 a.u., we found a few F···F interactions between the F atoms of the unit cell, and that there is no F···C(–F) contact between the $CF_4$ molecules in the crystal. The F···F contacts became more prominent when a lower isovalue, 0.0050 a.u., was used, which is generally expected when the attraction between interacting species is relatively weak as it typically appears in the low density region. The flatness of the isosurface that emerged from the low isovalue of 0.0050 a.u. gives some indication that there could be some van der Waals-type interaction between the C and F atoms. Even so, both the geometric and IGM results suggest that the F···F interactions are the key synthons responsible for the formation of the $CF_4$ crystal structure, and that our speculation, given above, about the presence of the windmill $F_3$ topology in the crystal, is also correct (see Figure 10b).

There are several reasons why the F···F weak contacts observed in the $CF_4$ crystal are not an artifact of the IGM analysis utilized. First, the fluorines in $CF_4$ have the capacity to form, not only 1:1 complexes with the Lewis bases $H_2O$, $NH_3$, $H_2CO$, HF, and HCN, but also 1:2, 1:3, and 1:4 clusters with the last three (randomly chosen) Lewis bases [158], with negative binding energies for all complexes. Second, the various topological and nontopological signatures obtained from applications of QTAIM, RDG, and NBO (natural bond orbital) analytical tools confirm that the N···F, O···F, and F···F long-ranged interactions developed between the interacting monomers in $H_3N\cdots FCF_3$, $H_2O\cdots FCF_3$, and $(Y–D)_{n=1–4}\cdots F_4C$ (Y–D = $H_2CO$, HCN, and HF) are real and are reminiscent of halogen bonding. Third, depending on the nature of the interacting monomers, it was shown that both nonadditive cooperative and anticooperative energetic effects are at play. Fourth, the dimers of fluorinated aromatic compounds we reported recently [49] provide QTAIM and SAPT evidence of the reliability of the F···F interactions formed by the entirely negative F in the monomers (see Figures 5g and 10c–f), though the origin of these interactions are not exactly same as those in $CF_4$. Although the F in $CF_4$ has a weak σ-hole that is positive, and is responsible for sustaining the directional interactions mentioned above in the gas phase, this argument is not strictly valid in the crystal as packing plays a crucial role that perturbs the atomic positions of $CF_4$ in the solid-state and hence affects the interaction type.

Another interesting case directly related to the above system was documented by Grabowski [271], a study that was criticized by Wick and Clark [124]. Grabowski found that the $H_3N\cdots CF_4$ binary complex has three electron density paths connecting N to nearby Fs, indicating the possibility of the formation of N···F interactions. The author seems to have overlooked the importance of these three bond paths, and claimed there is a tetrel bond between the C and N atoms in the complex even though there was no electron density path observed between them. This was not so for the other 1:1 $ZF_4$ (Z = Si, Se, Ge, As) complexes of $H_3N$ examined. One might link the reason for this missing bond path topology for the N···C interaction in $H_3N\cdots CF_4$ with that observed for some alcohol systems previously [240,241]. Although the possibility of a tetrel bond between the C and N in $H_3N\cdots CF_4$ may not be negligible, and the N···F interactions must be regarded as contributing to the stability of the entire complex. Their relative contributions to complex stability merits future study, which may include a discussion of results from a detailed analysis using an NBO second order hyperconjugative approach [272], SAPT analysis, and so on. The MESP concept of attraction between the positive tetrel center C and negative nitrogen base in $H_3N\cdots CF_4$ may not be the most suitable approach to quantitatively describe such interactions, nor it is universal so as to provide a standalone and unified argument in support of such interactions due to various reasons discussed above. It should also not be forgotten that it is also a model.

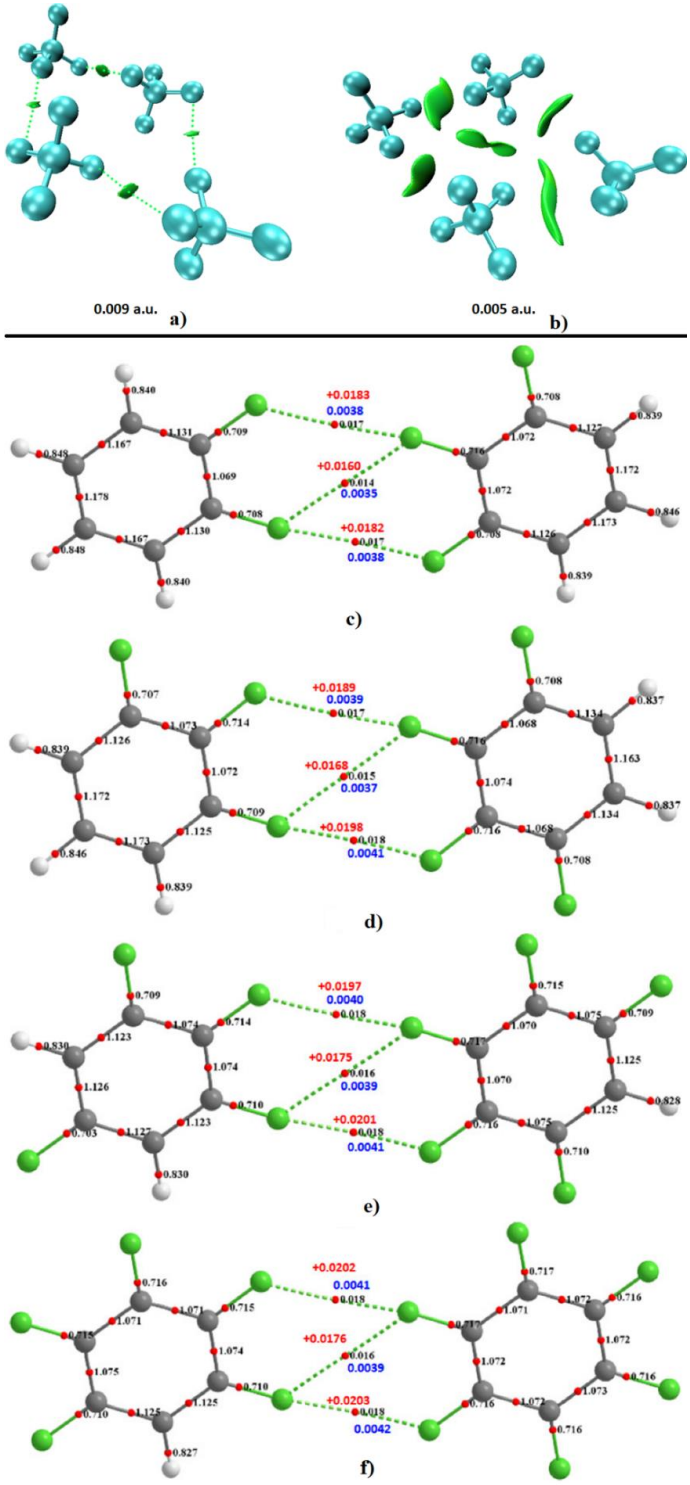


**Figure 10.** (**a**) 0.0090 a.u. (left) and (**b**) 0.0050 a.u. (right) isosurface plots of IGM analysis obtained from the unit cell of the $CF_4$ crystal (CSD Ref. TFMETH02). Included are the MP2/cc-pVTZ level QTAIM molecular graphs of some heteromolecular fluorine-substituted dimers [49] displaying Type-I and -III topologies of bonding (Scheme 1): (**c**) $H_4C_6F_2\cdots F_3C_6H_3$, (**d**) $H_3C_6F_3\cdots F_4C_6H_2$, (**e**) $H_2C_6F_4\cdots F_5C_6H$, and (**f**) $HC_6F_5\cdots F_6C_6$; formed even when the fluorine in the $C_6F_6$ monomer is entirely negative. The charge density ($\rho_b$/a.u., blue), the Laplacian of the charge density ($\nabla^2\rho_b$/a.u., red) at F$\cdots$F bcps and the delocalization indices for each atom–atom pair (black) are shown. bcps: tiny red spheres; bond paths: solid and dotted lines in atom color; solid and dotted lines represent the open- and closed-shell interactions, respectively. For simplicity, rcps (ring critical points) are not shown.

### *4.2. The Tetrachloromethane ($CCl_4$) System*

Of the eight hits in the CSD search (CSD refs. CARBTC and CARBTC01-07), two contain the geometry information for crystalline tetrachloromethane ($CCl_4$) (CARBTC, $P2_1/c$ [273], Figure 11, and CARBTC07, C2/c [274]). It is not a straightforward matter to infer the key bonding synthon responsible for the structure of the crystal from the arrangement between the monomers in the unit cell (Figure 11a,b). This is not surprising given that the Cl···Cl–C and Cl···C–C intermolecular bond angles are very nonlinear (∠Cl···Cl–C = 139.95° and ∠Cl···C–Cl = 156.49°, Figure 11b); the Cl···Cl and C···Cl bond lengths are 3.536 and 4.305 Å, respectively. These distances are slightly shorter than, and significantly larger than the sum of the van der Waals radii of the atoms, 3.57 and 3.64 Å, involved in these two contacts, respectively.

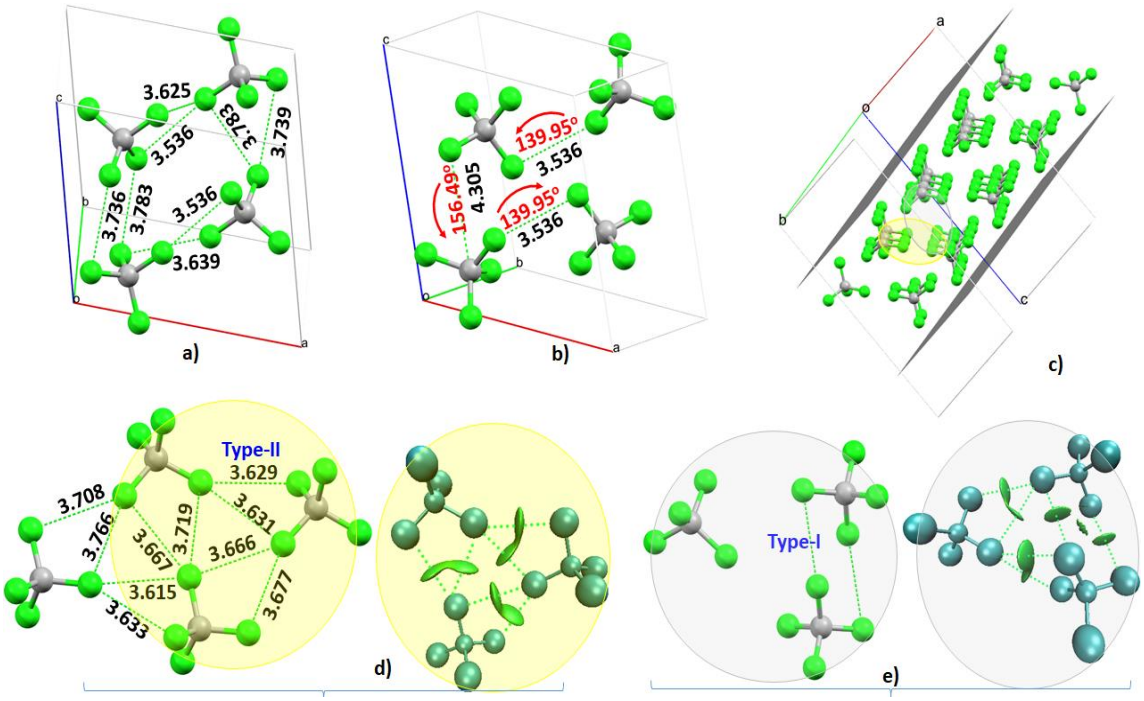


**Figure 11.** The ball-and-stick models of the (**a**,**b**) unit cell and (**c**) the (002) slicing pattern of the $CCl_4$ crystal (CSD ref code: CARBTC07). The triangular windmill-type intermolecular bonding topology is illustrated in (**d**), whereas the interlayer Type-I topology between the Cl atoms of the interacting monomers in the crystal is shown in (**e**). The 0.005 a.u. isosurface plots corresponding to the geometries (**d**,**e**) are illustrated, and were obtained with the IGM analysis.

Our MESP results show that the C and Cl atoms in $CCl_4$ conceive four and one positive σ-holes, respectively (Figure 3g). From this, it appears that the C···Cl interaction noted above could be a Coulomb-type interaction between the positive region on the carbon and the lateral negative site on the Cl. A similar conclusion might explain the origin of some of the Cl···Cl contacts, even though the ∠Cl···Cl–C are significantly nonlinear (Figure 11b).

An exploration of all types of intermolecular distances between the $CCl_4$ monomers in the unit cell (Figure 11a), as well those upon the enlargement of the unit cell in a specific orientation (Figure 11c), has enabled us to conclude that the geometry of crystal comprises both Type-I and -II topologies of bonding between the monomers. Although this sort of geometry based assignment could be superficial, the results of the IGM analysis in Figure 11d,e show that the chlorine atoms in the $CCl_4$ monomers in the crystal indeed feature both Type-I and -II contacts, which are characterized by the green IGM isosurfaces between the Cl atoms.

The layer marked by a yellow ellipse in Figure 11c involves several Type-I and -II Cl···Cl contacts. The triangular $Cl_3$ windmill topology, formed by the three Cl atoms of three $CCl_4$ monomers, is also

evident. The covalently bound Cl atom in each $CCl_4$ monomer forming this topology serves as a five-center noncovalent bond, yet each is engaged with two Type-II interactions with the interacting monomer. Clearly, and as found for $CF_4$, the nonlinearity of the type-II ∠Cl···Cl–C contacts in the crystal geometry is due to competition between several interactions, causing significant angular deviation from 180°. The Type-I contacts do predominantly occur between the layers (Figure 11e). These are all evident of the IGM isosurfaces illustrated in Figure 11d,e.

### *4.3. The Tetrabromomethane ($CBr_4$) System*

Although a CSD search for carbon tetrabromide ($CBr_4$) resulted in seven hits (CSD ref: CTBROM and CTBROM01-06), two of these single crystals (CSD ref: CTBROM and CTBROM06 with space group C2/c) contain the geometric information and were reported in 1977 [275] and 2003 [276], respectively. As for $CCl_4$, the geometry of the crystal of $CBr_4$, shown in Figure 12a,b, is also a consequence of both Type-I and -II bonding topologies. Each Br in the $CBr_4$ monomer is equipped with a positive σ-hole (Figure 3f), which shows the potential to attract the negative site, whereas the tetrahedral carbon presents with four σ-holes along the Br–C bond extensions. Even so, each Br in the $CBr_4$ monomer is seemingly involved in bonding with two similar atoms of a neighboring molecule, with Br···Br bond distances of 3.777 and 3.623 Å. The Br···C bond distance is significantly longer, 4.219 Å (Figure 12c), suggesting that these interactions are probably not the key bonding modes (*albeit* secondary) responsible for crystal formation.

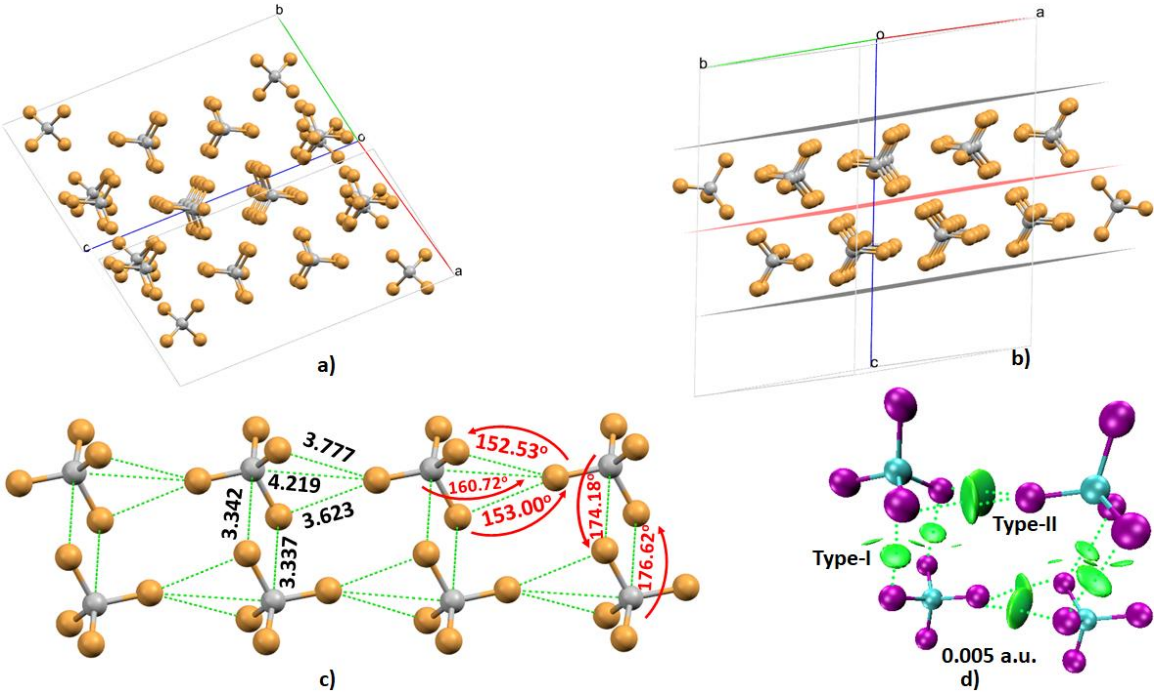


**Figure 12.** The ball-and-stick models of the (**a**,**b**) unit cell and (**b**) the (002) slicing pattern of the $CBr_4$ crystal (CSD ref code: CTBROM06). (**c**) Selected local distances between the $CBr_4$ monomers in the crystal. (**d**) The 0.005 a.u. isosurface plot corresponding to four $CBr_4$ monomer units is illustrated, and was obtained with the IGM analysis.

From an IGM analysis, as shown in Figure 12d, it seems that the Br···Br Type-I interactions are competing with the Type-II contacts, evident as single disc-like green circular volumes between the Br atoms. The Type-II contacts present as distorted dumbbells and round circular volumes in green. It is still difficult to conclude whether there is a triangular $Br_3$ windmill topology in the $CBr_4$ crystal since the Br···Br intermolecular distances between the Br atoms in a given layer are very long, and are significantly different from one another.

### *4.4. The Tetraiodomethane ($CI_4$) System*

The CSD search resulted in two hits for the tetraiodomethane ($CI_4$) in the solid-state. One was reported in 1937 (CSD ref: ZZZKDW) [277] (but no coordinates are available) and other was in 1982 (CSD ref. ZZZKDW01) [278]. The 2 × 2 supercell and slicing patterns of the latter is shown in Figure 13. There are nine $CI_4$ monomers in the unit cell (space group: I42m), of which eight occupy the four corners and one is at the center. From the geometry, it seems that the arrangement between the monomers is such that the carbon atom in the central monomer is linked with four I atoms of the nearest neighbors, probably forming an I···C–I topology (Figure 13d, top); this is comparable to what was inferred for the other three crystals of the family (discussed above). The electrophilic σ-hole region in the remaining four I atoms of each $CI_4$ monomer are linked with the neighboring species through an I···I–C topology. Because the I···I–C angles are all significantly nonlinear, one cannot demonstrate the exact nature of the various bonding interactions responsible for the formation of the crystal, as there are many of them and comprise both Type-I and -II I···I contacts. However, the results of an IGM analysis indeed permits us to conclude that there is no real I···C–I tetrel bonding topology observed in the crystal as might appear at first. There are I···I–C Type-I and -II interactions (Figure 13d,e) that cooperate each other in the development of the solid-state structure. There is no $I_3$-type windmill topology observed between the interacting $CI_4$ monomers forming the crystal.

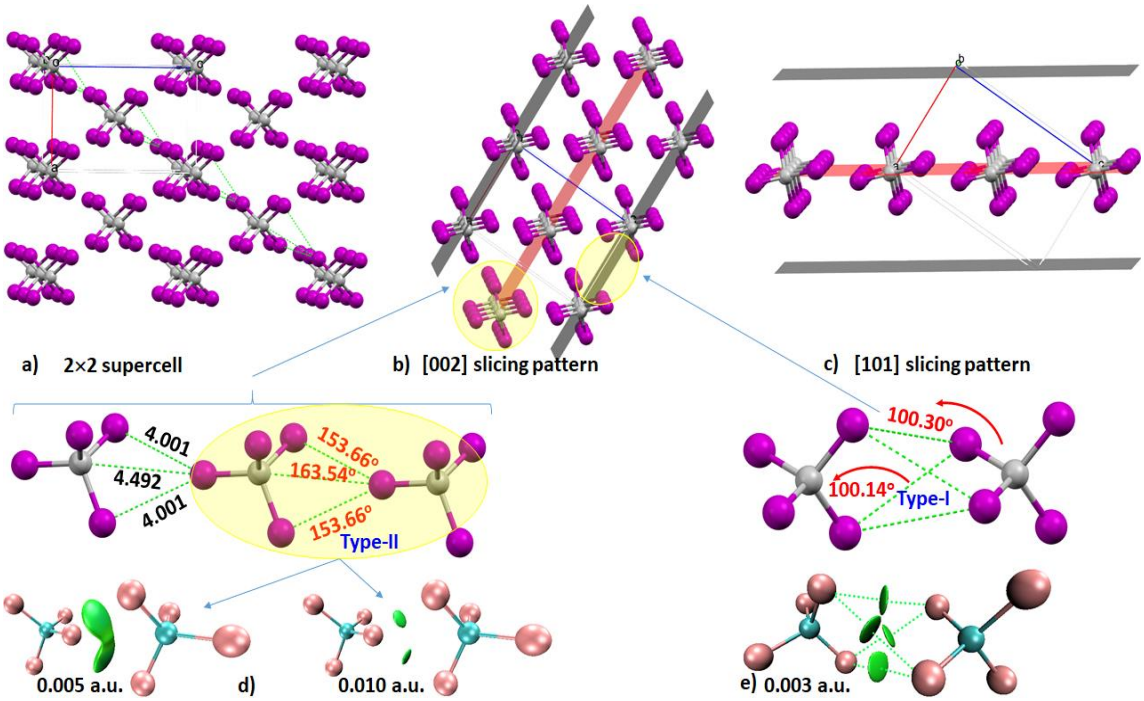


**Figure 13.** The ball-and-stick models of the $CI_4$ crystal (CSD ref. code: ZZZKDW01)). (**a**) Unit cell and 2 × 2 supercell and (**b**) [002] slicing pattern. (**c**) [101] Slicing pattern. Type-II and -I bonding patterns between interacting monomers in the crystal are shown in (**d**,**e**), respectively, with the IGM isosurfaces corresponding to these interactions in green volumes.

From a comparison of the Type-II interactions in the geometries of the $CX_4$ (X = F, Cl, Br, I) crystals discussed above, it is found that ∠F···F–C = 157.01°, ∠Cl···Cl–C = 155.26°, ∠Br···Br–C = 157.33°, and ∠I···I–C = 153.66°. This suggests that the widely held notion that iodine forms more directional interaction in molecules than the lighter halides is not necessarily always correct.

### *4.5. The Chlorine Monofluoride (ClF) Crystal System*

Another example, the crystal structure of chlorine monofluoride (ClF), is shown in Figure 14. From the geometric arrangement between the ClF monomers in the unit cell, both Type-I and -II F···F

contacts seem to play a role in self-assembly (Figure 14a). The F· · · F intermolecular distances—between 3.120 and 3.220 Å—are larger than twice the vdW radius of the F atom (2.92 Å). The angle associated with the Type-II F· · · F contacts is 145.30°, whereas for the Type-I contacts it varies between 82 and 86°. However, analysis of the supercell geometry of the crystal (Figure 14b) leads to the identification of the Cl· · · Cl–F contacts (Figure 14c). The contact is very directional, which is apparent from the Cl· · · Cl–F angle (∠Cl· · · Cl–F = 178.85°), in which the electrophilic σ-hole on the outer surface of the F–Cl bond in one molecule attracts the negative portion of the Cl atom in another similar molecule. These, together with the presence of various Type-I and -II F· · · F contacts, result in the formation of the ClF crystal structure. It is worth mentioning that the triangular $F_3$ windmill-type topology is also evident in the crystal. It is formed by the interacting F atoms of three neighboring ClF monomers for which the ∠F· · · F· · · F angle varies between 54.66 and 64.41° (Figure 14c, right). The significant distortion of the ∠F· · · F· · · F from ideal values is perhaps a result of the competition between the Type-I and -II F· · · F contacts.

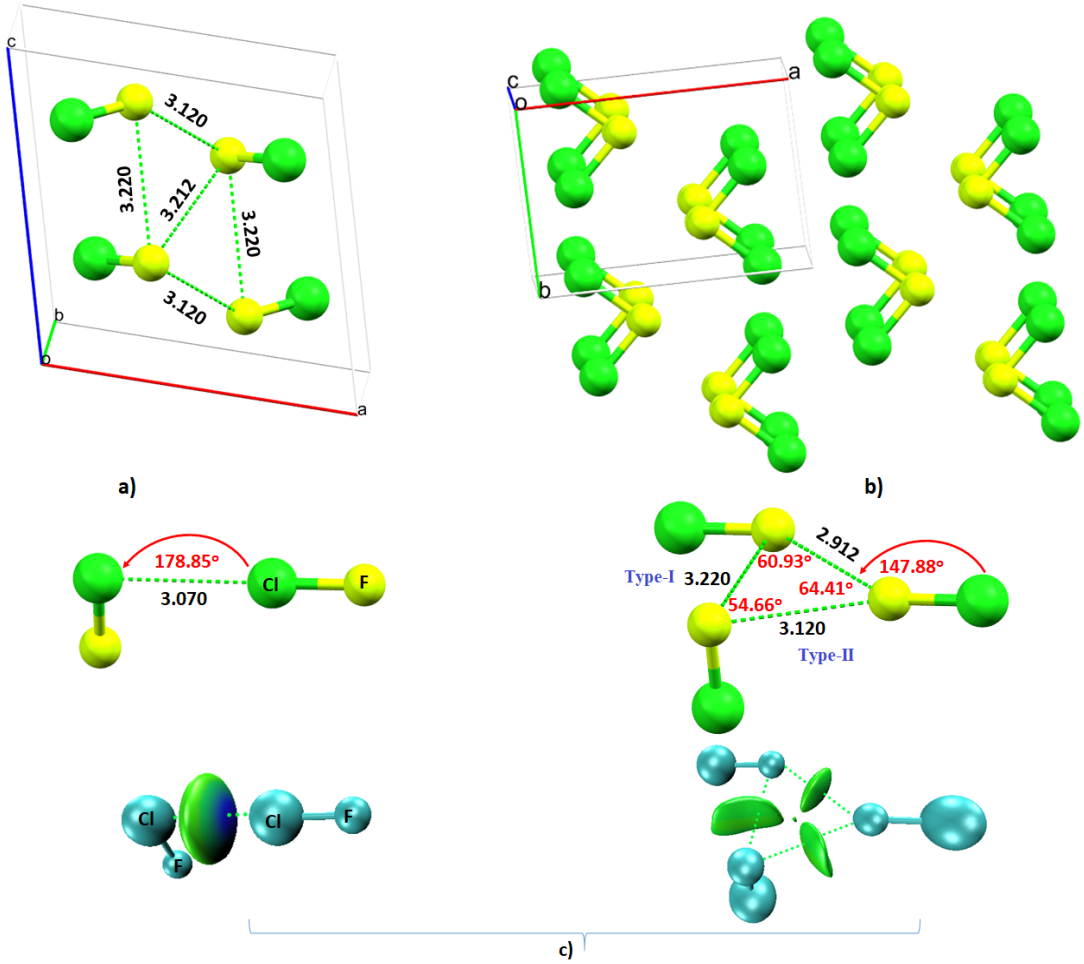


**Figure 14.** The ball-and-stick models of chlorine monofluoride (ClF) crystal (CSD ref: YATKOV): (**a**) Unit cell and (**b**) 2 × 2 supercell. (**c**) Possible bonding modes identified between halogen that emerged from an IGM analysis atoms are illustrated as isosurfaces in green and mixed blue-green.

The results of an IGM analysis (Figure 14c, left) show that the Cl· · · Cl–F contacts are indeed very strong. This is reminiscent of the coloring scheme associated with the IGM isosurface, appearing between the Cl atoms; in this case the central portion of the circular IGM volume is bluish and the peripheral portions are greenish. By contrast, the green IGM isosurfaces between the F atoms of the F· · · F contacts are, relatively speaking, thinner and flat (Figure 14c, right), suggesting a relatively large charge density depletion in the bonding region compared to that observed in the bonding region of

the Cl···Cl contacts. From Figure 14c (right), it is obvious that the F atoms in two ClF monomers responsible for the formation of both Type-I and -II F···F contacts are simultaneously engaged in more than two contacts. The fluorine in the monomer forming the Type-I contact is disposed such that it is actually interacting with the mid portion of the bond in the other monomer. This is reminiscent of the bonding scenario discussed by Murray et al. [26]. According to these authors, noncovalent bonding does not always occur between atoms, that is, the interactions within crystal lattices are Coulombic, and the strongest positive and/or negative regions do not always correspond to the positions of atoms: they are sometimes located between atoms.

### *4.6. Examples of Some Crystal Systems Stabilized by Type-I and -II Contacts*

#### 4.6.1. Some Halogen-Substituted Fullerene Systems

As for the ClF and other systems discussed above, a similar conclusion might be arrived at in the case of the bromine-assisted chlorinated fullerene, $(C_{60}Cl_{30})_2{\cdot}3Br_2$ crystal (CSD ref: FIKHAJ), Figure 15 [279]. In it, the chlorine-terminated $C_{60}$ fullerenes are linked to each other by $Br_2$ and in which both Type-I and -II Cl···Br and Cl···Cl contacts are evident. The intermolecular distances associated with many of these contacts are in the 3.50 to 3.69 Å range (Figure 15a). These are close to, or marginally less than, the sum of the vdW radii of the Cl and Br atoms, 3.68 Å, or twice the van der Waals radius of the Cl atom: 3.64 Å ($r_{vdW}$(Cl) = 1.82 Å and $r_{vdW}$(Br) = 1.86 Å).

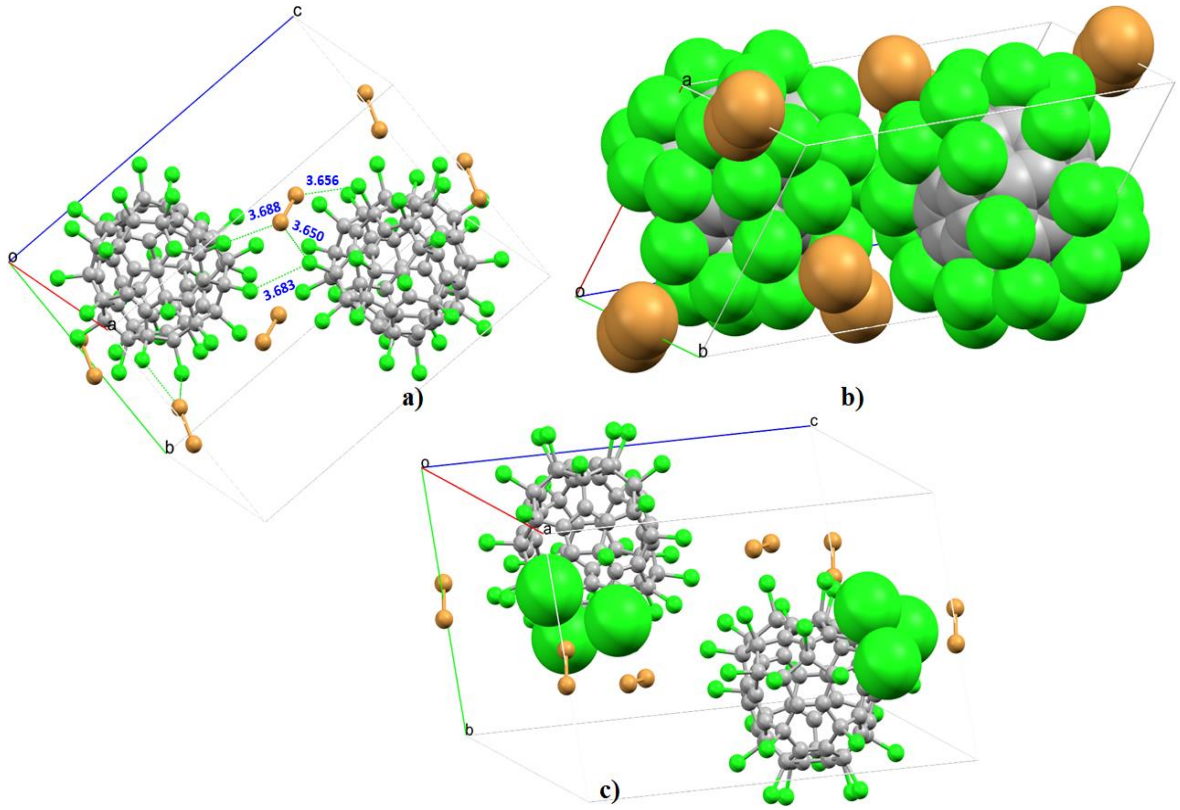


**Figure 15.** The (**a**) ball-and-stick and (**b**) space-filling models of unit cell of the crystal structure of $(C_{60}Cl_{30})_2{\cdot}3Br_2$ crystal (CSD ref: FIKHAJ). (**c**) Illustration of space-filling local regions that can be used as an exemplar to understand the development of halogen···halogen bonding between the Br atoms in $Br_2$ and the midpoint region between the Cl atoms.

For the formation of some of the contacts noted above, the junction region between the two, or three Cl atoms of the $C_{60}$ system, serves as an interacting site for Br (Figure 15c). Also, there are significant Type-I halogen···halogen intramolecular interactions between the Cl atoms of $C_{60}Cl_{30}$

with distances between 3.0 and 3.3 Å. These are in part responsible for providing local stability to the entire solid-state assembly. A similar bonding scenario was discussed by Johansson and Swart in the perhalogenated ethanes, $X_3C–CY_3$ (X, Y = F, Cl) [210]. According to these authors, the halogen$\cdots$halogen bond character in these systems is quite different from standard halogen bonds and hydrogen bonds as no bond critical points were found between the halogens (from a QTAIM analysis) in these systems, and the underlying concept of the σ-holes on the halogens could not be used to describe the bonding interactions. It was suggested that the intramolecular halogen$\cdots$halogen bonding interactions they examined in the $X_3C–CY_3$ systems were of an unusually strong van der Waals type.

Figure 16 illustrates the crystal structure of hexabromofullerene carbon disulfide [280], yet another example of halogen-substituted fullerene system. The packing between the hexabromofullerene monomers in the crystal is driven by the $CS_2$ molecules, as well as by the noncovalent interactions formed between the terminal Br atoms in one $C_{60}$ fullerene monomer and the outer π surfaces of a second similar monomer. The $CS_2$ molecules serve as the spacer, enforcing the fullerene molecules to engage in $S_2C_\pi\cdots\pi(C_{60})$ and $S\cdots\pi(C_{60})$ interactions, in which the lateral negative sites of the S atoms involved in the latter interactions act as electron density donors. In addition, the electrophilic region on the S atom along the outer extension of the C–S bonds in $CS_2$ forms Br$\cdots$S(C) Type-II chalcogen bonds that are markedly longer ($r$(Br$\cdots$S) = 4.087 Å) than the sum of the van der Waals radii of the Br and S atoms—3.75 Å—and are quasilinear (∠Br$\cdots$S–C = 168.68°, Figure 16b). There are also Br$\cdots$Br Type-I and -II contacts that are formed between some of the close-lying terminal Br atoms of each fullerene molecule (Figure 16a), which are shorter than twice the vdW radius of the Br atom—3.72 Å. Note that it is quite difficult to separate out individual contacts in the crystal. Many of these are secondary and the interplay between them provides the stability to overall crystal geometry of the system. This also explains the nonlinearity of the Br$\cdots$S–C chalcogen bonds. That the $S\cdots\pi(C_{60})$ and Br$\cdots$S–C bonds in the crystal lattice are real is confirmed by our IGM analysis (see Figure 16c). Although the latter are weaker, the former, which occur between the lateral sides of S and $(C{=}C)_\pi$, are the dominant interactions; they are very dispersed and are assumed to be relatively stronger.

Our observations about the mixed nature Type-I and Type-II interactions in the fullerene crystals discussed above are supportive of the recent results of Bauzá and Frontera [157], who reported the dimerization energies of analogous systems, $(C_{60}F_{36})_2$, $(C_{60}Br_{24}Cl_{24})_2$, and $(C_{60}Br_{24})_2$, using density functional theory with BP86-D3/def2-SVP. The authors found that these crystal systems were stabilized by extensive halogen$\cdots$halogen contacts. The stabilization (binding) energies for the F$\cdots$F, Cl$\cdots$Br and Br$\cdots$Br contacts in the corresponding crystals were −7.7, −11.8, and −10.6 kcal mol$^{-1}$, respectively (single points were carried out on the X-ray structures to obtain these energies without geometry minimization).

We note further that the sulfur quadrupole moment in $CS_2$ is positive and, and, there is negative π-electron density around the S atom but a positive σ-hole along the axis. The carbon quadrupole moment is negative, reflecting a reduced π-electron density around the C atom [196]. Because of this nature of the molecule, Singh et al. [281] found that the molecule displays versatile coordination modes, and has ability to feature crossed, parallel-stacked, T-shaped, and L-shaped geometries in its clusters. This ability of the molecule explains why $CS_2$ could displays a number of coordination modes to form the hexabromofullerene carbon disulfide crystal.

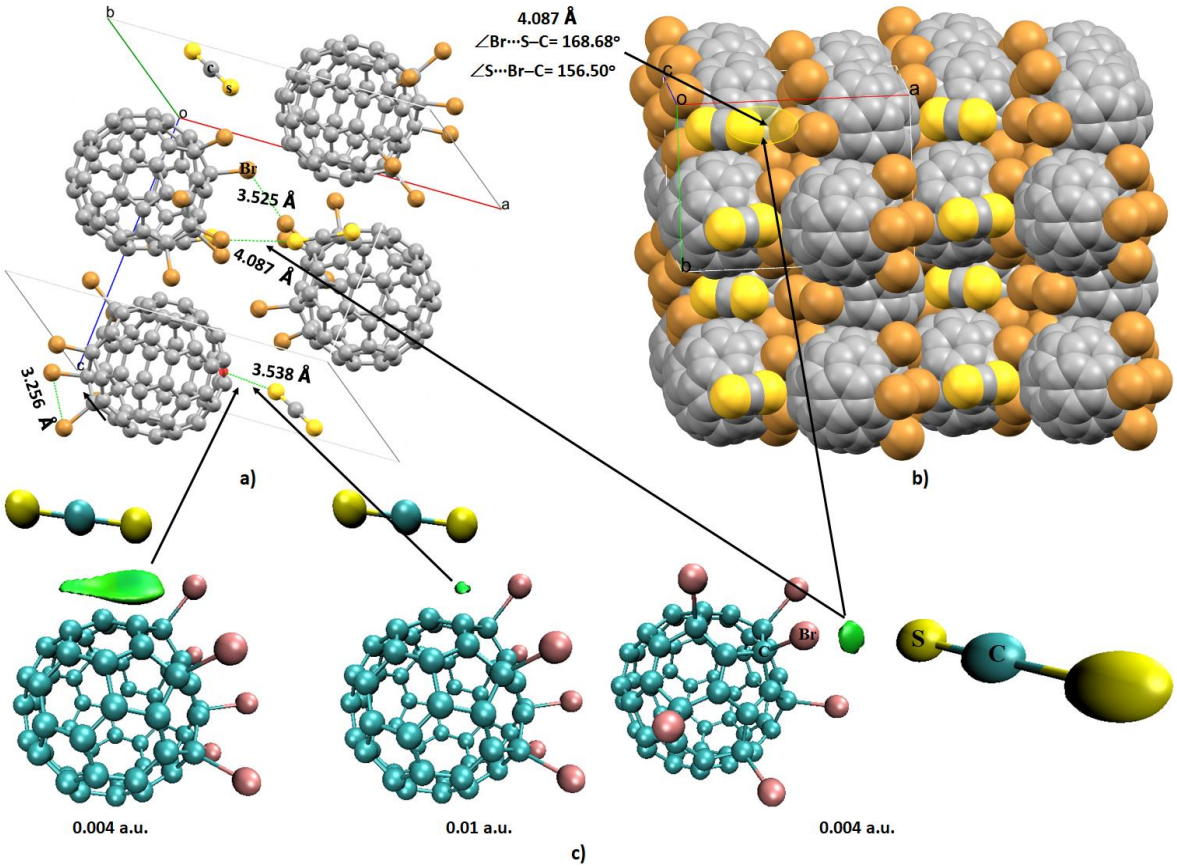


**Figure 16.** The (**a**) unit cell ball-and-stick and (**b**) 2 × 2 supercell space-filling models of hexabromofullerene carbon disulfide crystal (CSD ref: YAYNOC). (**c**) Specific IGM representation of bonding interactions between the S atom in $CS_2$ and the Br and $(C=C)_\pi$ (and $C_6$ ring) of the hexabromo-substituted $C_{60}$, obtained with different isovalues. Selected intra- and intermolecular distances (and angles) are shown in (**a**).

### 4.6.2. Some Halogen-Substituted Borane Systems

Using halogenated carboranes as counterions, fluorinated benzyl-type carbocations, such as $(\rho\text{-}FC_6H_4)_2CF^+$, $(\rho\text{-}FC_6H_4)(CH_3)CF^+$, and fluorinated trityl ions, were shown to be readily isolated. Figures 17 and 18 represent two such examples, showing the crystals of 1-fluoro-1-(4-fluorophenyl) ethylium 1-carba-2,3,4,5,6,7,8,9,10,11,12-undecaiododododecaborate [282] and fluoro (bis(4-fluorophenyl))methylium 1-carba-2,3,4,5,6,7,8,9,10,11,12-undecaiododododecaborate fluorobenzene [282]. The stability of these crystals are driven by halogen bonding and several other noncovalent interactions, wherein the Coulombic interaction between the cation and anion in the ion pair system plays the leading role in effecting stabilization. The shortest I···$C^+$(F) distance in $[(p\text{-}F\text{-}C_6H_4)_2CF][CHB_{11}I_{11}]\cdot C_6H_5F$ is 4.22 Å (Figure 17a), and that in $[(p\text{-}F\text{-}C_6H_4)(CH_3)CF]^+[CHB_{11}I_{11}]^-$ is 3.90 Å (Figure 18a); both of these are greater than sum of the vdW radii of the I and C atoms—3.81 Å. Although these were expected to be the important bonding modes in the study, this is not so for the crystals shown in Figures 17 and 18.

There are several other interactions in these systems that are revealed by an IGM analysis; in addition to the $C^+$···I contact found in Figure 17a, there are also I···F, I···H(methyl) and π···I contacts. Whereas the latter one is presumably weak, the other two are predominantly stabilizing. The closest approach of the anion to the cation in Figure 17a is evidenced by the two I atom contacts that are at 3.074 and 3.394 Å with H atoms of the $–CH_3$ group. The methyl group in the carbocation is unusually acidic, as inferred from the very broad nature of the infrared band observed centered at a very low wavenumber of 2750 $cm^{-1}$. Both the I···$C^+$ and I···F contacts in the crystal are very nonlinear (∠I···C–F = 71.53° and ∠I···F–C = 88.99°), suggesting a Type-I bonding pattern.

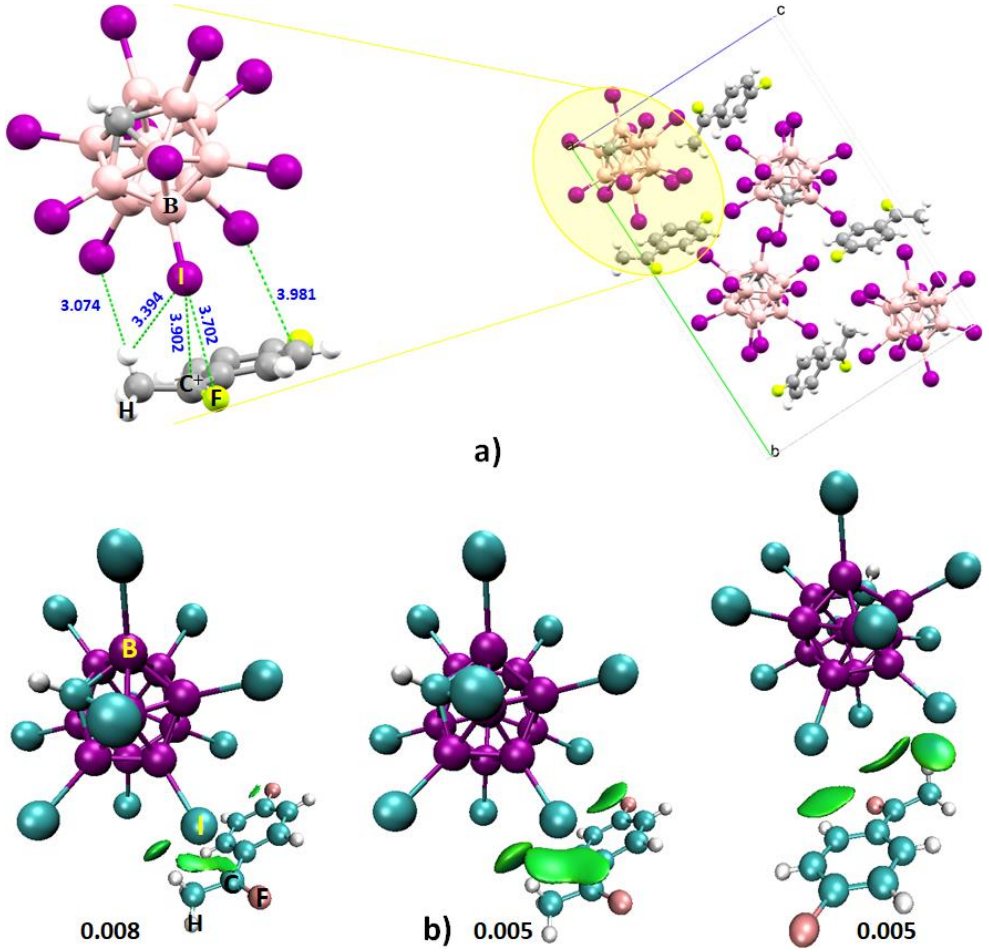


**Figure 17.** (**a**) The unit cell (right) of the crystal structure of 1-fluoro-1-(4-fluorophenyl)ethylium 1-carba-2,3,4,5,6,7,8,9,10,11,12-undecaiododododecaborate (CSD ref. DEZDIW). (**b**) The IGM isosurface plot, obtained with two different isovalues: 0.0080 and 0.0050 a.u. Intermolecular distances are shown in (**a**) are in Å.

By contrast, one of the primary intermolecular bonding modes shown in Figure 18a is presumably I···F(C), in which F acts as an electrophilic center; this is not surprising as the cation is entirely electropositive. The *r*(I···F) and ∠I···F–C values associated with this interaction are 3.480 Å and 157.50°, respectively, showing significant nonlinearly of the halogen bond. The Type-II topology is evident in this contact; so the traditional requirement that the presence of a positive σ-hole on the F atom is essential for the formation of the halogen bond is found not always to be true. The halogen atom interacting with the nucleophile is entirely positive, but its σ-hole, which is expected along the outer extension of the C–F bond, is not involved in forming the halogen bond. The significant nonlinearity of the halogen bond is not only due to the involvement of the F atom in other, secondary interactions, but also because it is interacting with the central region of the surface formed by the three I atoms of the anion (see the space-filling model in Figure 18b). The two I···F secondary interactions are significantly nonlinear: the upper one has ∠I···F–C = 133.37° and the lower one has ∠I···F–C = 112.26°. In addition to the interactions noted above, other interactions between the cation and the anion, the I···H(C) contacts, appear feasible. The space-filling model also suggests the possibility of a $C_\pi$···I interaction between the interacting species.

Our analysis did not enable us to identify such a I···$C^+$ contact in the structure illustrated in Figure 18, as it is very long (4.22 Å), although this was not so for the geometry illustrated in Figure 17. The results of the IGM analysis, however, suggest that the predominant interaction mode is indeed the $C_\pi$···I interaction, characterized by a blue-green isosurface at low density (Figure 18c, left), with the

I· · · H(C) interaction seemingly strengthening the interaction. The I· · · F–C motif characterized by a weak isosurface in the high density region (Figure 18c, right) is very much sharp (circular disc-like) at low density ((Figure 18c, left), and is in agreement with the speculations arising from the intermolecular distance (*vide supra*). There is no I· · · $C^+$ contact in the crystal structure, however, in contrast to the interpretation of the experimental data [282].

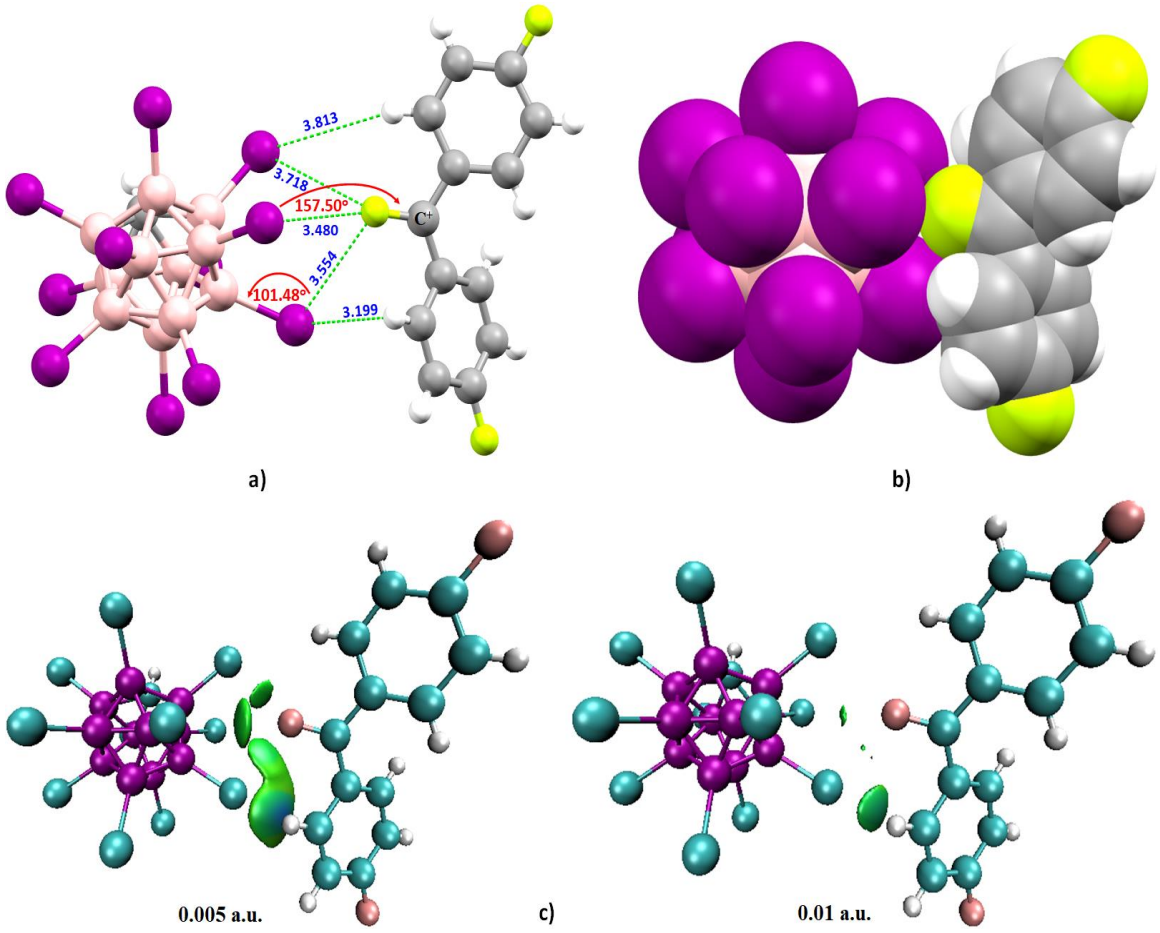


**Figure 18.** The crystal structure of fluoro(bis(4-fluorophenyl))methylium 1-carba-2,3,4,5,6,7,8,9,10, 11,12-undecaiodododecaborate fluorobenzene (CSD ref: DEZFAQ). (**a**) Ball-and-stick and (**b**) space-filling models. A $C_6H_5F$ solvate molecule has been omitted for clarity. Shown in (**c**) are the specific IGM representations of bonding interactions between interacting monomers, obtained with two different isovalues.

#### 4.6.3. Some Halogen-Substituted Aromatic and Nonaromatic Systems

Decabromodiphenyl ether (DecaBDE) is a brominated flame retardant for which there is a high annual worldwide demand (several thousand tons per annum). The crystal structure of the compound is illustrated in Figure 19a. Apart from the $\pi\cdots\pi$ and $\pi\cdots$Br contacts, the DecaBDE monomers in the crystal are linked with each other through Br· · · Br Type-I and -II contacts, leading to the formation of pore-like topologies locally. The formation of Br· · · Br Type-I and -II contacts is exemplified in the IGM isosurface plot (Figure 19b). The supposedly electrophilic region on the Br atom of the C–Br bond attracts the lateral sites of the Br atoms of the interacting monomer (Figure 19b, left) forming Type-II contacts. These are typically shorter than the Type-I contacts. For instance, and as shown in Figure 19b, the Type-II contacts have $r$(Br· · · Br) values of 3.625 and 3.621 Å, respectively, which are accompanied with ∠Br· · · Br–C values of 158.10° and 150.77°, respectively. On the other hand, the Type-I contacts have $r$(Br· · · Br) values $\geq$ 3.830 Å and are associated with ∠Br· · · Br–C angles of 115.7° and 118°, respectively (not shown).

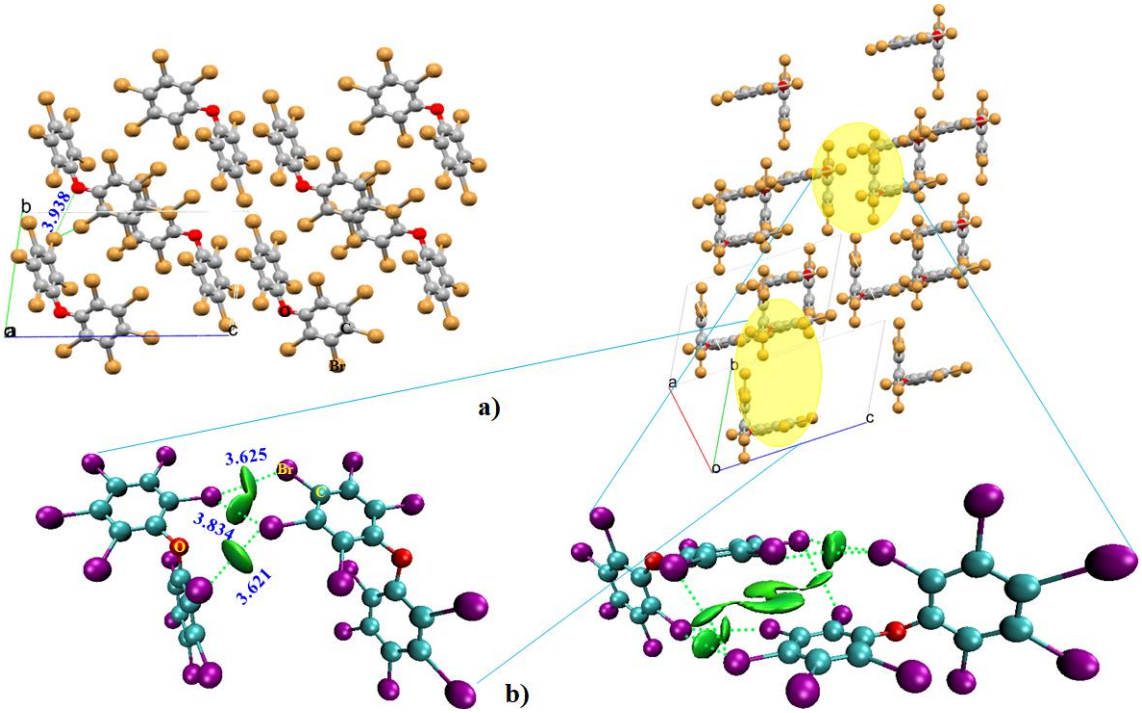


**Figure 19.** (**a**) Two views of the ball-and-stick model of the crystal structure of 1-(2,3,4,5,6-pentabromophenoxy)-2,3,4,5,6-pentabromobenzene (CSD ref: COCDED). (**b**) IGM isosurface plot (isovalue = 0.005 a.u.) illustrating possible halogen-center intermolecular bonding scenarios. Selected bond distances are shown in Å.

It might appear that the Br and O atoms are linked in the crystal structure. However, the intermolecular distance between these atoms is very long—3.938 Å (substantially larger than the sum of the vdW radii of Br and O, 3.36 Å)—and the ∠O···Br–C is 153.41° (Figure 19a). IGM analysis does not predict any interaction between these atoms when an isovalue of 0.0050 a.u. was used in our analysis; however, when a smaller isovalue—0.003 a.u.—was used (not shown), a very weak interaction, probably of van der Waals type, was identified. These results show that an examination of intermolecular geometries alone would miss many Type-I interactions between the DecaBDE monomers in the crystal, and the conclusion arrived in the absence of electron density based models could be misleading.

Figure 20 illustrates another set of crystal geometries which, it has been suggested, are driven by N···X–C (X = Br, I) halogen bonds [283–285]. These are examples of adducts from a series of di-bromo-perfluoro-alkyl compounds formed between $BrCF_2(CF_2)_nCF_2Br$ ($n$ = 2, 4, 6) and several nitrogen base halogen bond acceptors. The intermolecular interactions N···Br and N···I halogen bonds vary between 2.746 and 3.046 Å. The ∠N···X–C (X = Br, I) lies between 172.58 and 177.00°, indicative of Type-II halogen bonding in these crystals. There is no secondary interaction between the I atom of the C–I bond and the N atom for geometries in Figure 20b,c. The reason for the deviation of the ∠N···I–C from 180° for the halogen bonds in these crystal structures is unclear as one would expect an almost linear interaction between the interacting atoms given that the σ-hole on the I atom is perfectly along the outer extension of the C–I bond. The angular deviation in Figure 20a,d is the consequence of interference from neighboring H atoms of the nitrogen containing donors, with the lateral negative halogen derivative forming secondary interactions, indicated by the flat isosurface domains between the interacting atomic basins.

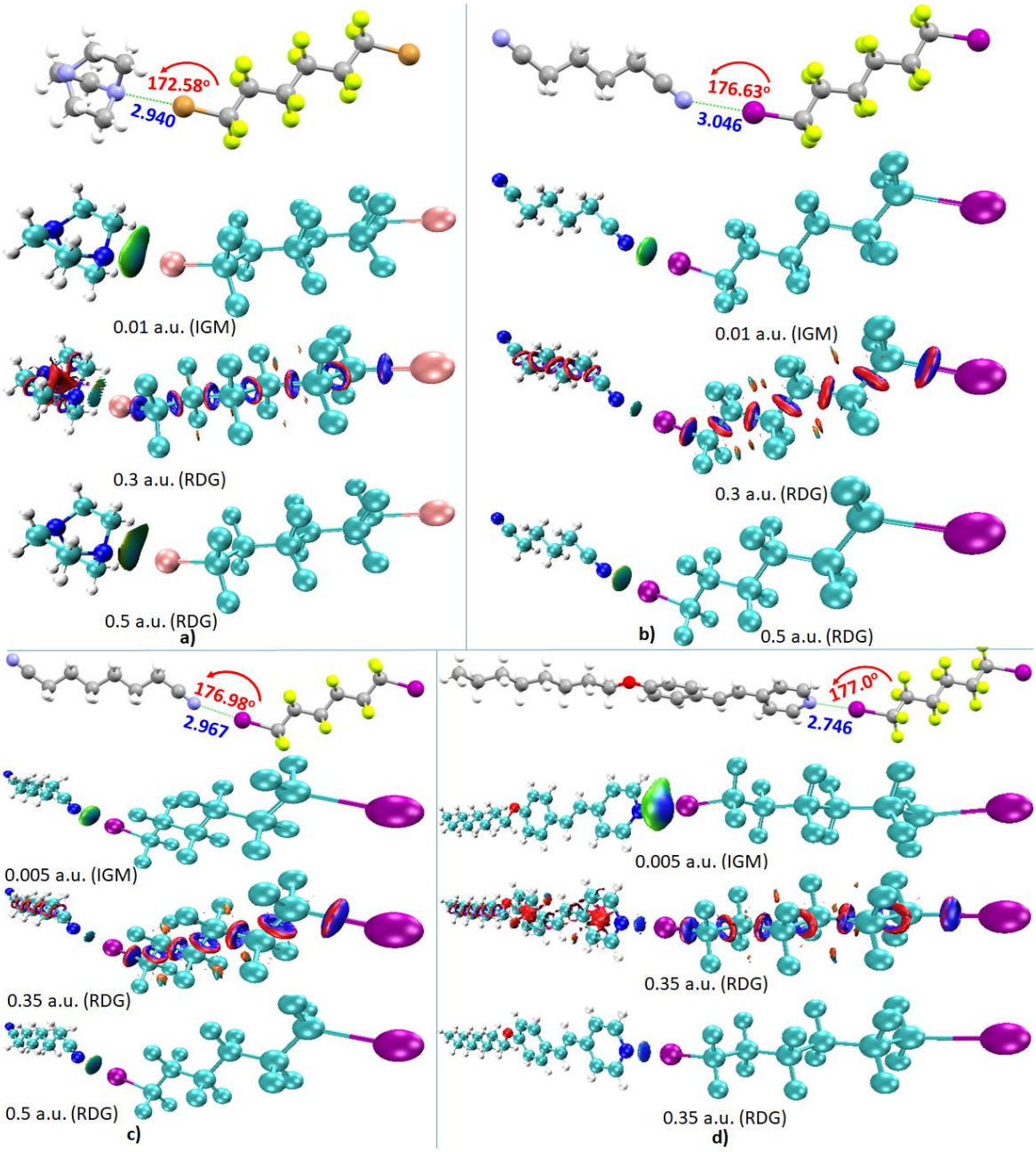


**Figure 20.** (First entry) Topology of Type-II halogen bonding in the crystal of (**a**) 1,4-diazabicyclo [2.2.2]octane 1,6-dibromo-1,1,2,2,3,3,4,4,5,5,6,6-dodecafluorohexane (CSD ref: CEMGEJ), (**b**) 1,4-Dicyanobutane 1,6-di-iodo-1,1,2,2,3,3,4,4,5,5,6,6-dodecafluorohexan (CSD ref: EBIJAB), (**c**) 1,6-Dicyanohexane 1,6-di-iodo-1,1,2,2,3,3,4,4,5,5,6,6-dodecafluorohexane (CSD ref: EBIJIJ), and (**d**) bis(4-(2-(4-pyridyl)ethenyl)-1-(octyloxy)benzene) 1,6-diiodo-1,1,2,2,3,3,4,4,5,5,6, 6-dodecafluorohexane (CSD ref: DENMIT). Included in all cases are the isosurface plots emerged from promolecular IGM and Reduced Density Gradient (RDG) analyses: the second entry represents the IGM isosurface plot, the second entry represents the RDG isosurface plot, and the third entry represents the RDG isosurface plot; in which case only the N and I atoms were considered and the midpoint between them was defined as center. The blue and green parts of the isosurface are indicative of attraction, whereas the reddish part of the isosurface is a consequence of steric repulsion.

From the magnitude of the intermolecular distances, it is clear that the strength of the N···I interaction would follow the order Figure 20d > Figure 20c > Figure 20b. This is in perfect agreement

with the coloring scheme associated with the isosurfaces, emerged from either RDG or IGM, in which the isosurface between N and I in Figure 20d has a more bluish hue than those in Figure 20b,c.

Although the majority of XB donors are known to be iodine-containing compounds, Brisdon and coworkers [285] reported a small number of crystals in which the bromine serves as the halogen bond donor. Single-crystal X-ray diffraction studies revealed that each of these crystals comprises one-dimensional halogen-bonded networks formed through N···Br connectivity. The N···Br halogen-bond distances were between 2.809 and 2.818 Å, respectively, and are about 0.58 and 0.59 Å shorter than the sum of the van der Waals radii of the N and Br atoms, respectively, potentially indicative of strong halogen bonds. Although these studies have constricted the nature of intermolecular interaction within the framework of the crystal to N···Br, the importance of many other inter- and intramolecular interactions responsible for the stability of the entire crystal was not seriously taken into account.

Figure 21a illustrates one such system formed between a dibromo-dodecadfluorohexane, $BrCF_2(CF_2)_4CF_2Br$ and 1,4-di-aza-bicyclo-[2.2.2]octane. Figure 21b shows its extended crystal structure. In addition to the N···Br halogen bond forming the 1D network, the fluorine atoms of the dibromo-dodecadfluorohexane participate in F···F contacts with a similar neighboring molecule. That the F···F contacts are real is clear from the space-filling model (Figure 21a). The terminal Br atoms and a few F atoms of $–CF_2–$ fragments of the dibromo-dodecadfluorohexane are also involved in F···H and Br···H intermolecular interactions with the 1,4-diazabicyclo[2.2.2]octane moiety. These latter interactions are not very weak, which is understandable given the lateral sites of the Br and F atoms engage with the entirely positive sites delocalized over the H atoms of the interacting molecule. All these interactions are clear in the IGM plot emanated using the molecules in the unit cell of the crystal, in which the shapes of the green isosurfaces between the interacting atomic basins are broad and well spread out (Figure 21c).

Similarly, for the formation of the crystal structure of 1,4-dicyanobutane and the diiodo-dodecadfluorohexane, $ICF_2(CF_2)_4CF_2I$, the terminal I atoms of the latter form N···I interactions with the nitrogen base of 1,4-dicyanobutane, with $r$(N···I) = 3.046 Å and ∠N···I–C = 176.63°. Additionally, the dibromo-dodecadfluorohexane molecules are linked to each other by a significant number of F···F Type-I and -II interactions. There are also I···H(C) and I···F interactions between the two types of interacting monomers. These interactions are reminiscent of the IGM plot (c) of Figure 22.

As with Br-containing XB donors in crystals, perfluorionated chains with sulfonyl chloride ($SO_2Cl$) ends have some significance in the formation of crystals since the 4- and 6-membered α,ω-dihaloperfluoroalkanes have been cocrystallized with other molecules. The X-ray crystallographic measurements of two nonhydrogen-containing $ClSO_2(CF_2)_4SO_2Cl$ (octafluorobutane-1,4-disulfonyl dichloride) and $ClSO_2(CF_2)_6SO_2Cl$ (dodecafluorohexane-1,6-disulfonyl dichloride) crystals were recently reported [286] as the first examples of O···Cl–S halogen bonding complemented by short F···F contacts between neighboring chains. The nature and type of these intermolecular interactions were assigned based on the crystallographic geometry only. This identification of F···F and O···Cl interactions is in agreement with our results that emanate from the geometric and IGM based charge density analyses (Figures 23 and 24). In particular, our geometric analysis suggests that there are at least four F···F and two F···O contacts between the two $ClSO_2(CF_2)_6SO_2Cl$ monomers in the unit cell that are roughly in a slip-parallel arrangement (Figure 23a). The intermolecular distances associated with the F···F vary between 3.016 and 3.312 Å; the angles associated with these are 176.3 and 174.1°, respectively, illustrating a Type-II bonding topology. The F···O contacts have comparable intermolecular distances, 3.080 Å, that are slightly shorter than the sum of the vdW radii of O and F atoms (2.96 Å), with ∠F···O–S (=167.6°) signifying a Type-II bonding pattern.

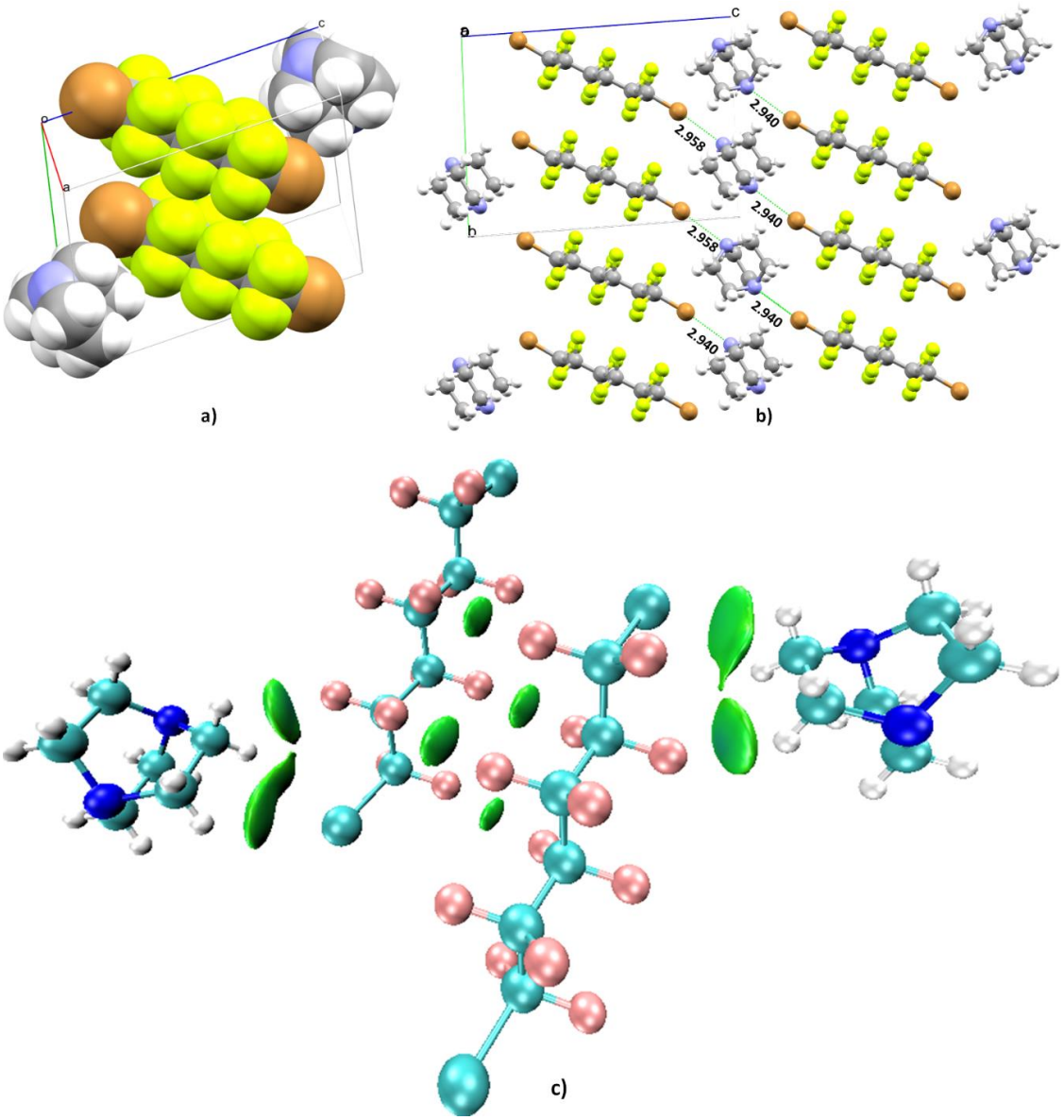


**Figure 21.** (**a**) The (**a**) space-filling model of the unit cell and (**b**) the ball-and-stick model of the 2 × 2 supercell structure of the crystal of 1,4-diazabicyclo[2.2.2]octane 1,6-dibromo-1,1,2,2,3,3,4,4,5,5,6,6-dodecafluorohexane (CSD ref: CEMGEJ). (**c**) IGM isosurface plot (isovalue = 0.0050 a.u.) for molecular domains in the unit cell, illustrating possible halogen-center intermolecular bonding scenarios. Selected bond distances are shown in Å.

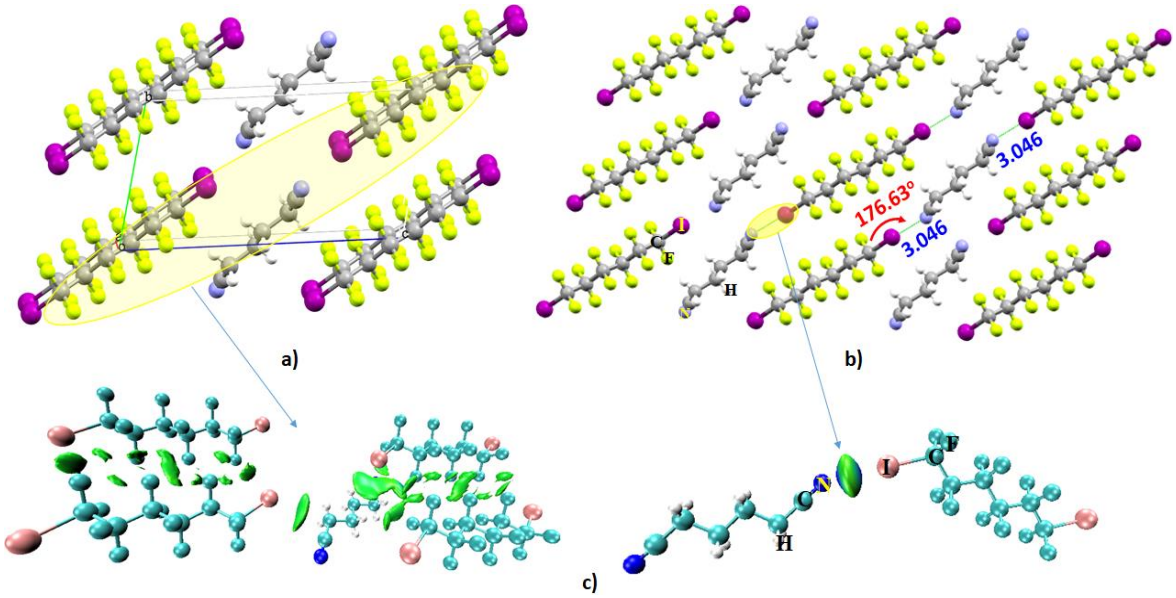


**Figure 22.** (**a**) The unit cell and (**b**) 2 × 2 supercell representations of the crystal structure of 1,4-dicyanobutane and $ICF_2(CF_2)_4CF_2I$ (CSD ref: EBIJAB). (**c**) The results of the IGM isosurface plot (isovalue = 0.004 a.u.) are illustrated for some specific regions. Selected bond distances and bond angles are given in Å and degree, respectively.

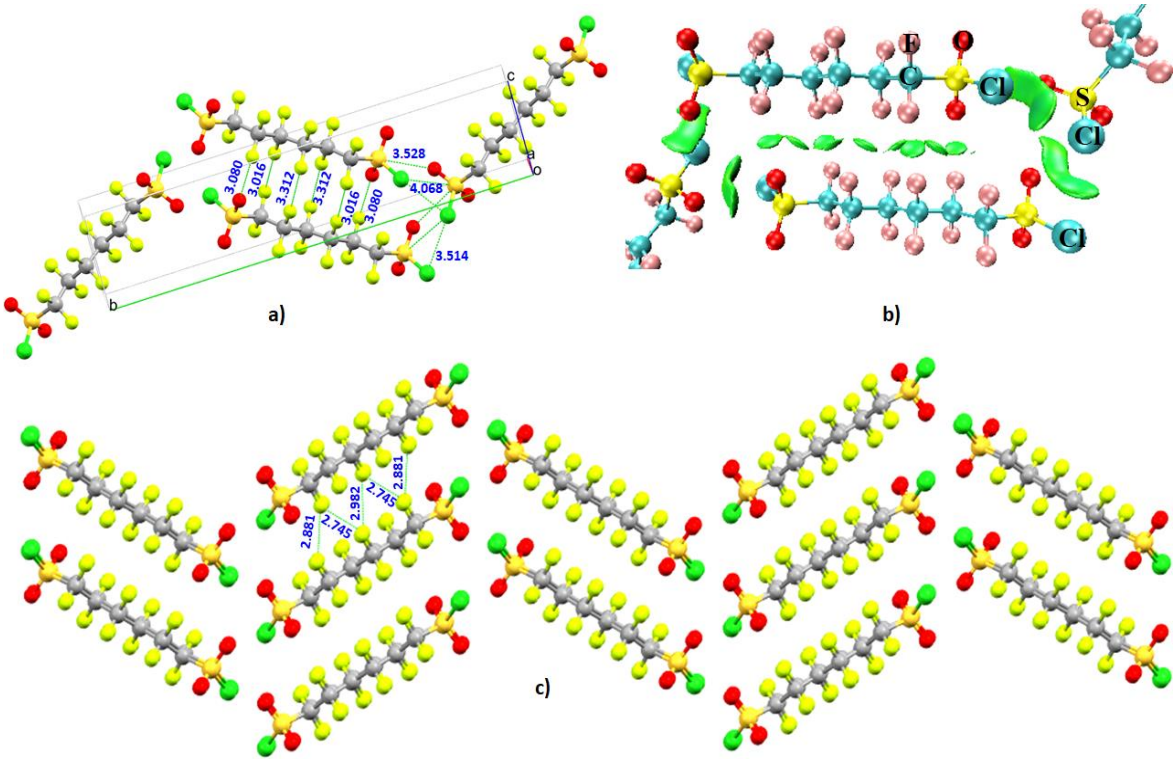


**Figure 23.** (**a**) The ball-and-stick model of the crystal structure of dodecafluorohexane-1,6-disulfonyl dichloride (CSD ref: TEWNUH). (**b**) IGM isosurface plot (isovalue = 0.005 a.u.), illustrating possible halogen-center intermolecular bonding scenarios. Selected bond distances are shown in Å. (**c**) An extended model of the crystal, showing the zigzag array in 3D.

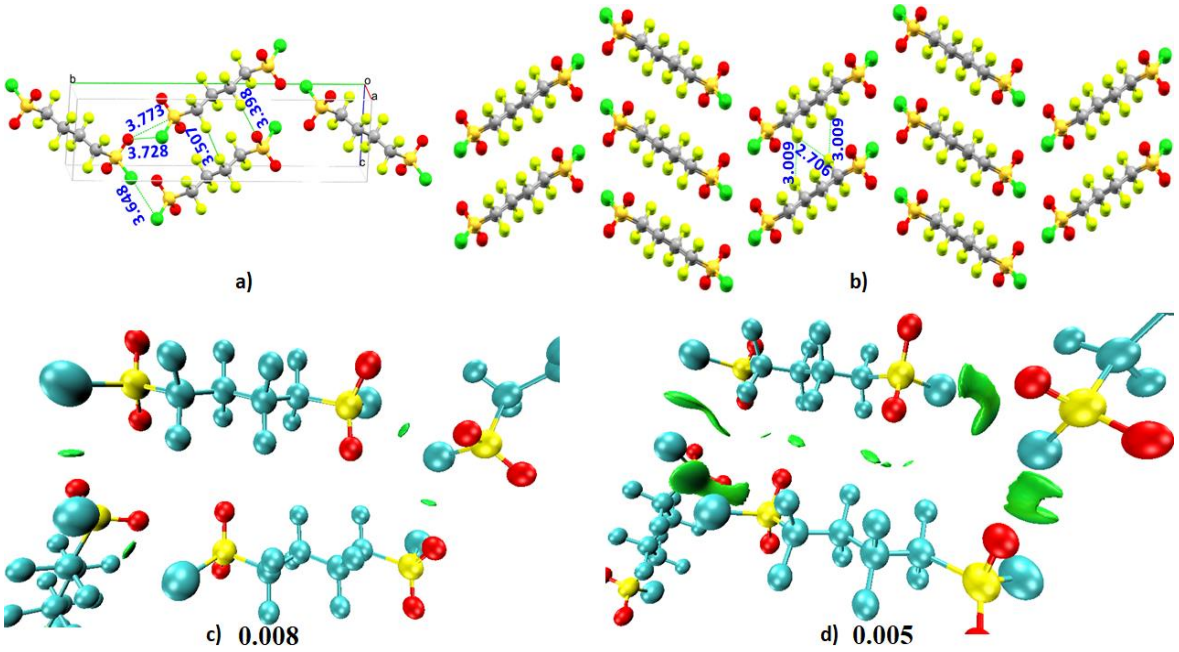


**Figure 24.** (**a**) The ball-and-stick model of the crystal structure of octafluorobutane-1,4-disulfonyl dichloride (CSD ref: TEWNOB). (**b**) An extended model of the crystal, showing the zigzag array in 3D. (**c**) The IGM isosurface plot, with isovalues of 0.0080 and 0.0050 a.u., illustrating possible halogen-center intermolecular bonding scenarios. Selected bond distances are shown in Å.

There are other interactions in the crystal as well; the remaining two $ClSO_2(CF_2)_6SO_2Cl$ monomers in the unit cell are involved in Cl···Cl, Cl···S, O···Cl, and O···S attractive interactions (Figure 23a,b). Of these, the first is most dominant, and appears both at high and low isovalues in the IGM analyses. Together with this are the Cl···S and O···Cl contacts that collectively appear as a broad and elongated isosurface in green, in which the latter two are not very apparent at a higher isovalue of 0.008 a.u., indicating that these are weakly bound contacts. The IGM analysis suggests that there could be four Type-II and one Type-I F···F contacts between a pair of two $ClSO_2(CF_2)_6SO_2Cl$ monomers (Figure 23c). There are other such contacts, in which the associated intermolecular distances are very short. These interlayer contacts lie between 2.881 and 2.982 Å (not shown), and the ∠F···F–C associated with these vary between 144.9 and 152.7°, suggesting the presence of both Type-I and -II contacts. Clearly, these constitute a rich variety of cooperative interactions that are responsible for the solid-state structure and the development of the zigzag array in 3D (Figure 23c).

For the $ClSO_2(CF_2)_4SO_2Cl$ crystal (Figure 24a) however, the Cl···Cl Type-I contact is significant in the high density region (Figure 24c), indicating that it is one of the key driving forces in the formation of the crystal. There are other interactions between the monomers, such as the O···S Type-II chalcogen bond and O···F Type-I contacts, which are weak and appear only when a low isovalue of 0.0050 a.u. was used in the IGM analysis.

The Cl···Cl contact distances in the unit cells of $ClSO_2(CF_2)_4SO_2Cl$ and $ClSO_2(CF_2)_6SO_2Cl$ are 3.648 and 3.514 Å, respectively, with ∠Cl···Cl–S od 113.2 and 117.1°, respectively. The O···S distances in the corresponding crystals are 3.773 and 3.528 Å, respectively. Similarly, the shortest F···F distances are 3.507 and 3.016 Å, respectively. Whereas the bond angles associated with these interactions significantly deviate from 180°, it seems that enlargement of the perfluoroalkane chains by the $–CF_2$ fragment causes many fluorine atoms to become involved in a larger number of F···F contacts, making the larger system, $ClSO_2(CF_2)_6SO_2Cl$, relatively more stable than the $ClSO_2(CF_2)_4SO_2Cl$ system. Similarly, as found for $ClSO_2(CF_2)_6SO_2Cl$ (Figure 23b), there are three short F···F contacts between layers, two equivalent (3.009 Å) and one potentially shorter (2.705 Å), bridging the $–CF_2$ fragments of neighboring molecules along the (101) direction.

Finally, we note that there have been hundreds of thousands of crystal structures deposited in CSD in which the chemical bonding is either unknown or only partially explored. The main interest in such studies probably lies in the exploration of their materials or chemical properties, such as their catalytic behavior. One such example may be the dichloro-bis((henicosafluorodecyl)(diphenyl)-phosphine)-palladium(II) crystal system, Figure 25a [287]. The unit cell contains two molecules in which the fluorinated fragments are linked to each other by F···F contacts. Figure 25b shows that these contacts within the building bulk that vary from 2.719 to 3.081 Å. The ∠F···F–F associated with these contacts varies between 166.33 and 172.78°, showing a Type-II pattern. There are several such contacts feasible in the expanded crystal with Type-I topology, which can be evidence of the space-filling unit cell model of the crystal (Figure 25c), as well from the IGM isosurface plots shown in Figure 26. Clearly, from the local geometries of the crystal structure alone, it is difficult to speculate what causes the occurrence of the attractive interaction between the F atoms within the monomer, although many of these could be typified as of lump-hole type (or of Type-III type). Even so, it is impossible to comment on the actual nature of the surface reactivity of the fluorine atoms of the fluorinated chains as in the entire monomer the fluorine atoms are at least overlapped and hence providing a view on the exact origin of the F···F interactions in this system would be ambiguous.

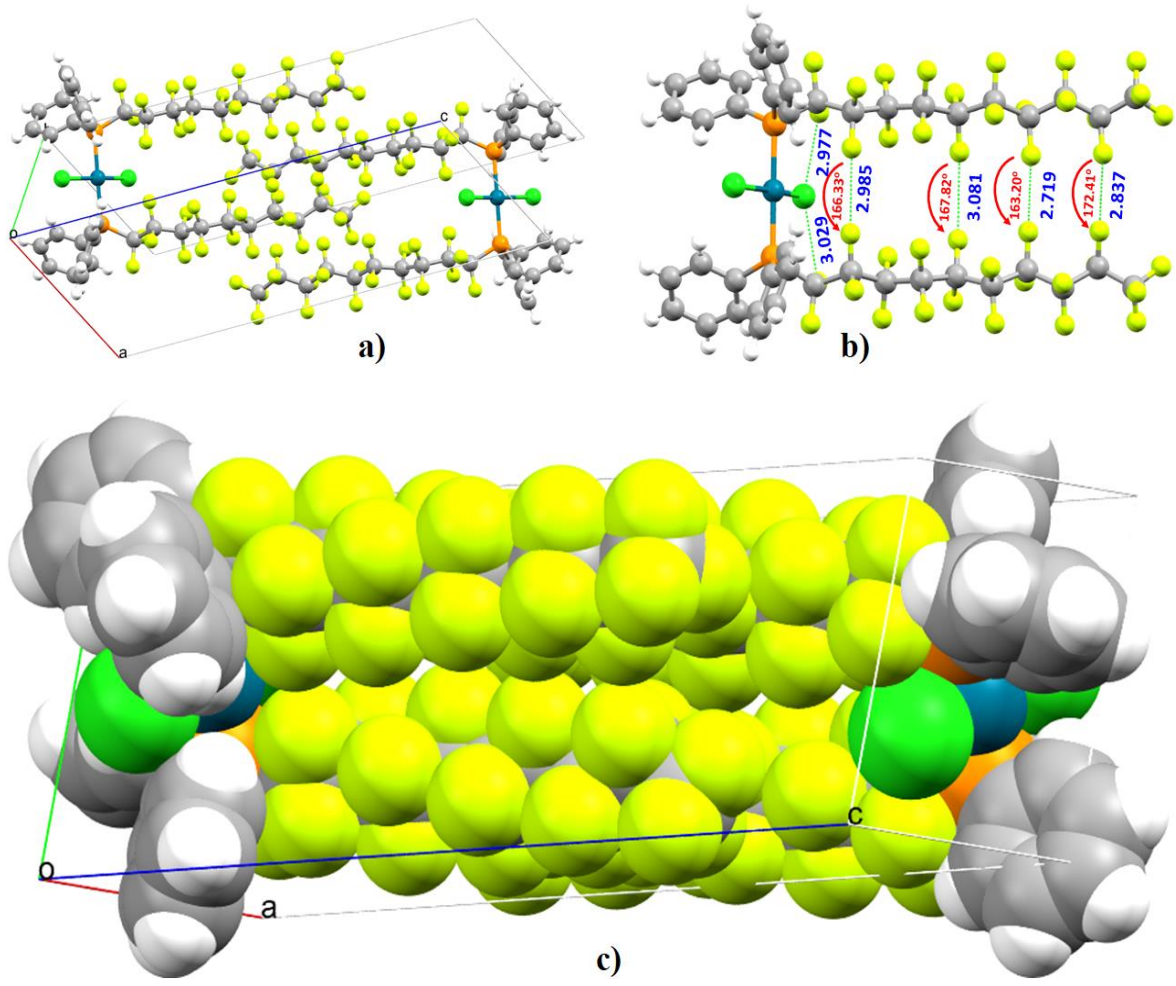


**Figure 25.** (**a**) The unit cell of the dichloro-bis((henicosafluorodecyl)(diphenyl)-phosphine)-palladium(II) crystal (CSD ref: ZETSIC). (**b**) Selected intramolecular contacts within the framework of the monomer. Intermolecular distances and angles are in Å and degrees, respectively. (**c**) The space-filling model of the unit cell of the crystal, showing potential overlap between the vdW spheres associated with the F atoms.

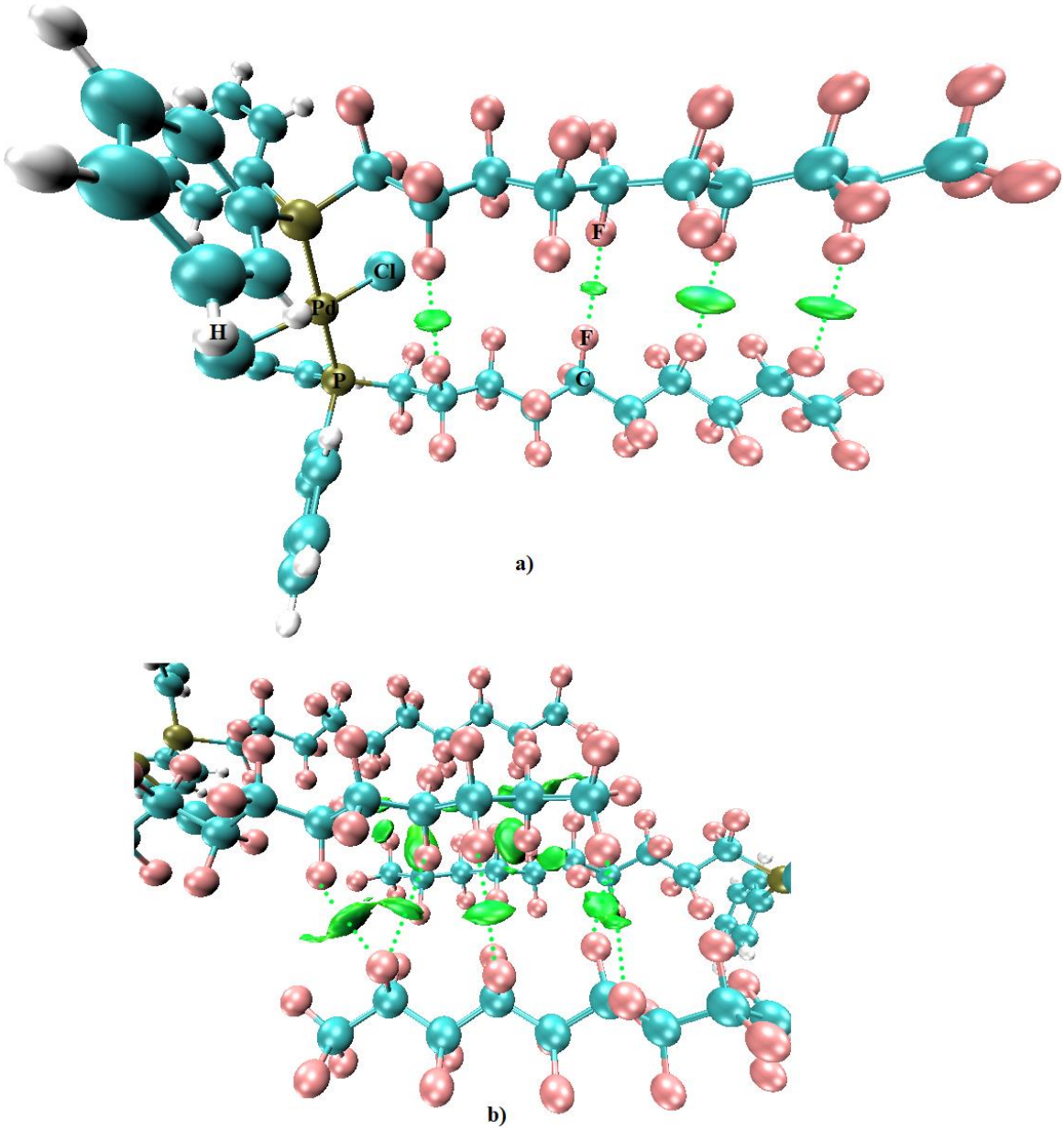


**Figure 26.** The IGM isosurface (0.005 a.u.) plot of the (**a**) dichloro-bis((henicosafluorodecyl)-(diphenyl) phosphine)-palladium(II) monomer and (**b**) that between the two monomers in the unit cell, showing potential F···F intra- and intermolecular interactions. The atom labeling is shown in (**a**).

## 5. Conclusions and Outlook

In this short review we have summarized the viewpoints currently being advanced, from theoretical and experimental studies, about the nature of halogen bonding and halogen-centered noncovalent interactions. These discussions and the disagreement evident in them, including the appropriate application of current state-of-the-art theoretical tools on specific systems of interest (e.g., MESP, RDG, NBO, SAPT, and QTAIM), seem likely to continue until a consensus is eventually reached on an appropriate unified and standalone approach to identify halogen-centered noncovalent interactions. Many structures catalogued in structure databases have not been fully understood; consequently, the chemistry discussed is incomplete, and in many instances, misleading. These require significant systematic exploration.

We have provided several examples of crystals involving halogen-centered noncovalent interactions, taken from the Cambridge Structure Database. We endeavored to show that it is very

difficult to gain insight into the presence and the actual nature of these interactions based solely on the concept of σ-hole theory or the geometry of the solid-state structure. In particular, we have shown that Type-I halogen···halogen bonding is a versatile interaction that does not obey any strict bonding rule. Close proximity and significant geometrical nonlinearity between bonded atoms are the only descriptor that could be utilized for their characterization. The utilization of space-filling models is informative to some extent, especially when there is an overlap between the interacting atomic basins, but is of little use when the interacting atoms are beyond the sum of their van der Waals radii. The Type-I halogen bond topology appears especially when there is crowding of heavier halogen atoms in the molecular framework. It also appears when two monomers are in close proximity. Its appearance is also dependent on whether other secondary interactions play a role in the interactions between the monomers, cooperating with each other to form the crystals; examples of this, for instance, are the crystals of halogen-terminated fullerene derivatives, as well as halogen-substituted borane and transition metal complexes (a few of these are illustrated in this study).

Many studies suggest that the appearance of the Type-I interaction is a consequence of dispersion, and is of the van der Waals type. In our view, this is a poor terminology to describe this interaction provided that one accepts the pressing argument that the nature of inter- or intramolecular interactions between atoms forming complexes is purely Coulombic. On the other hand, if dispersion is distinct from electrostatics, polarization, and charge transfer interactions, then it does certainly have its own place in the description of these interactions. This means that the description of a Type-I topology of bonding as "dispersion driven" is valid, as are the energy partitioning approaches and the mathematical models developed for exploring real effects, in which case, the "pure Coulombic" view is meaningless. The same argument is transferable to the Type-III interactions. We further note that there is no feasible way to quantify and infer exactly the energetic and orbital origins of Type-I interactions as these do not always appear as isolated, single interactions between molecules. Even within the single molecule itself, for example, in $C_{60}Cl_{30}$ (Figure 15), it is not a straightforward matter to quantify the energetic and orbital origins of the individual Cl···Cl intramolecular interactions as there are many of them simultaneously occurring. It is therefore difficult to provide a realistic account of the origin of Type-I interactions in many chemical systems.

We have also shown that the concept of "less than the sum of the van der Waals radii" is not always a valid criterion to be invoked when studying Type-I and -II interactions, especially on occasions where intermolecular interactions are weakly bound. We have shown that depending on the chemical environment the halogen bond (and even the chalcogen bond) distances can be significantly larger than the sum of the van der Waals radii of the bonded atomic basins. This is also applicable to chalcogen bonding and other noncovalent interactions.

Although the aforesaid van der Waals type long-ranged interactions are weak, they contribute in part to the packing and the stability of the overall crystal structure (as in $ClSO_2(CF_2)_6SO_2Cl$ and palladium(II) complex discussed above, for example), and cannot be neglected when the focus is on the stability of the entire crystal structure.

There are instances where the bonding does not occur between atoms but rather between the midpoint of a bond, or the junction (facial) region formed by several atoms (as in fluoro(bis(4-fluorophenyl)) methylium-1-carba-2,3,4,5,6,7,8,9,10,11,12-undecaiododododecaborate fluorobenzene) and the electrophile. In such cases, it is misleading to call the resulting contact a bond; it would be preferable to refer to it as an "interaction", which could be primary or secondary in nature if it is the forced consequence of the primary interaction(s).

Without significant exploration of the MESP of a wide variety of fluorinated compounds, it is misleading to assume or claim that the fluorine is generally negative (just by examining mere di- and polyatomic molecules). The nature of the F atoms in some examples of the crystal structures of fluorine-substituted compounds shown in this study are not known; thus it is hard to determine whether these do have negative (or positive) σ-holes on their surfaces or on bond extensions. These, and many others, could be the fruitful focus for theoretical modeling in future studies.

Though informative, the MESP model is certainly not the tool to correctly predict the complete nature of reactive sites on the surface of monomers if appropriate isodensity envelopes are not chosen for mapping of the potential. Even if such sites are correctly predicted, it is not always true that a site with a given polarity will attract a site of an opposite polarity of the interacting species and could then be utilized to reveal the chemistry of a noncovalent interaction between them.

We have also shown that Type-II interactions are not always representatives of halogen bonding. This is so because such a geometrical topology can occur between atoms that are either both positive, or both negative (as in dichloro-bis((henicosafluorodecyl)(diphenyl)-phosphine)-palladium(II)). Many of these interactions may be regarded as lump-hole (or even charge transfer) interactions, in which case dispersion plays a critical role. Examples of this type have been discussed recently in a number of theoretical studies [12,17,45,46,49,51,52,142,157,212–217]; putative interactions of a similar type apparent in many crystals need significant exploration to arrive at definitive conclusions as to their nature. We suggested calling them Type-III interactions.

As mentioned above, it is not always possible to quantify individual interactions in a system, especially when there are many interactions involving the same electrophilic center and in which some are Type-I and others Type-II (as illustrated for some crystal structures of this study). Even so, on such occasions, the IGM isosurface plot analysis is very useful in providing a reasonably reliable insight into the chemistry of these interactions; the approach assists in displaying the possible atomic or fragmental origin of interacting sites forming the local interactions.

Many weak interactions in the examples chosen in this study were made apparent only with IGM-based lower isovalues—~0.0050 a.u.—and were difficult to identify solely from an exploration of the intermolecular geometries. Without exploring a significant number of such interactions in many chemical systems it is difficult, at this stage, to firmly claim whether the IGM method is robust compared to other topological approaches since the results of IGM for the $CF_4$ crystal did not match with those inferred from the MESP model. However, it should not be forgotten that these different results emerge because packing plays a very critical role in determining the crystal structures, and that it is absent between molecules in the gas phase. In addition to new insights, IGM gave the expected (and counterintuitive) isosurface features associated with various interactions in crystals that have been known experimentally.

The highlights provided in this study, firstly, could be taken as challenges for theoretical chemists, and secondly, show that the application of charge density based approaches, including charge transfer and energy decomposition models, would be exceptionally useful in revealing the exciting chemistry of halogen-centered noncovalent interactions and far beyond.

**Author Contributions:** Conceptualization and Project Design, P.R.V. and A.V.; Investigation, P.R.V. and A.V.; Supervision, P.R.V.; Writing—Original Draft, P.R.V. and A.V.; Writing—Review & Editing, P.R.V., A.V., and H.M.M.

**Funding:** This research received no external funding.

**Acknowledgments:** A.V. and P.R.V. thank Koichi Yamashita for support. This work was entirely conducted using the facilities provided by the University of Tokyo, and P.R.V. and A.V. are currently affiliated with AIST. H.M.M. thanks the National Research Foundation, Pretoria, South Africa, and the University of the Witwatersrand for funding. We thank both the reviewers for their very useful comments and suggestions that have greatly assisted us to improve the quality of the manuscript.

**Conflicts of Interest:** The authors declare no conflict of interest.

## References

1. Chan, Y.-C.; Yeung, Y.-Y. Halogen Bond Catalyzed Bromocarbocyclization. *Angew. Chem. Int. Ed.* **2018**, *57*, 3483–3487. [CrossRef] [PubMed]
2. Robertson, C.C.; Wright, J.S.; Carrington, E.J.; Perutz, R.N.; Hunter, C.A.; Brammer, L. Hydrogen bonding vs. halogen bonding: The solvent decides. *Chem. Sci.* **2017**, *8*, 5392–5398. [CrossRef] [PubMed]

3. Wang, Y.; Wang, J.; Li, G.-X.; He, G.; Chen, G. Halogen-Bond-Promoted Photoactivation of Perfluoroalkyl Iodides: A Photochemical Protocol for Perfluoroalkylation Reactions. *Org. Lett.* **2017**, *19*, 1442–1445. [CrossRef] [PubMed]
4. Wang, H.; Wang, W.; Jin, W.J. σ-Hole Bond vs. π-Hole Bond: A Comparison Based on Halogen Bond. *Chem. Rev.* **2016**, *116*, 5072–5104. [CrossRef] [PubMed]
5. Brammer, L. Halogen bonding, chalcogen bonding, pnictogen bonding, tetrel bonding: Origins, current status and discussion. *Faraday Discuss.* **2017**, *203*, 485–507. [CrossRef] [PubMed]
6. Wolters, L.P.; Schyman, P.; Pavan, M.J.; Jorgensen, W.L.; Bickelhaupt, F.M.; Kozuch, S. The many faces of halogen bonding: A review of theoretical models and methods. *Wiley Interdiscip. Rev. Comput. Mol. Sci.* **2014**, *4*, 523–540. [CrossRef]
7. Murray, J.S.; Politzer, P. Molecular electrostatic potentials and noncovalent interactions. *WIREs Comput. Mol. Sci.* **2017**, *7*, e1326. [CrossRef]
8. Riley, K.E.; Hobza, P. Strength and Character of Halogen Bonds in Protein–Ligand Complexes. *Cryst. Growth Des.* **2011**, *11*, 4272–4278. [CrossRef]
9. Auffinger, P.; Hays, F.A.; Westhof, E.; Ho, P.S. Halogen bonds in biological molecules. *Proc. Natl. Acad. Sci. USA* **2004**, *101*, 16789–16794. [CrossRef]
10. Cavallo, G.; Metrangolo, P.; Milani, R.; Pilati, T.; Priimagi, A.; Resnati, G.; Terraneo, G. The halogen bond. *Chem. Rev.* **2016**, *116*, 2478–2601. [CrossRef]
11. Saha, A.; Rather, S.A.; Sharada, D.; Saha, B.K. C–X···X–C vs. C–H···X–C, Which One Is the More Dominant Interaction in Crystal Packing (X = Halogen)? *Cryst. Growth Des.* **2018**, *18*, 6084–6090. [CrossRef]
12. Varadwaj, A.; Varadwaj, P.R.; Marques, H.M.; Yamashita, K. Revealing Factors Influencing the Fluorine-Centered Non-Covalent Interactions in Some Fluorine-Substituted Molecular Complexes: Insights from First-Principles Studies. *ChemPhysChem* **2018**, *19*, 1486–1499. [CrossRef]
13. Stone, A.J. Are Halogen Bonded Structures Electrostatically Driven? *J. Am. Chem. Soc.* **2013**, *135*, 7005–7009. [CrossRef]
14. Bayse, C.A. Halogen bonding from the bonding perspective with considerations for mechanisms of thyroid hormone activation and inhibition. *New J. Chem.* **2018**, *42*, 10623–10632. [CrossRef]
15. Ding, X.; Tuikka, M.; Haukka, M. Halogen Bonding in Crystal Engineering. In *Recent Advances in Crystallography*; Benedict, J.B., Ed.; IntechOpen: London, UK, 2012.
16. Kawai, S.; Sadeghi, A.; Xu, F.; Peng, L.; Orita, A.; Otera, J.; Goedecker, S.; Meyer, E. Extended halogen bonding between fully fluorinated aromatic molecules. *ACS Nano* **2015**, *9*, 2574–2583. [CrossRef]
17. Varadwaj, A.; Varadwaj, P.R.; Marques, H.M.; Yamashita, K. CondMat Public Archive. Comment on "Extended Halogen Bonding between Fully Fluorinated Aromatic Molecules; Kawai et al., ACS Nano, **2015**, *9*, 2574–2583". Available online: https://arxiv.org/ftp/arxiv/papers/1802/1802.09995.pdf (accessed on 7 February 2019).
18. Lu, Y.; Liu, Y.; Xu, Z.; Li, H.; Liu, H.; Zhu, W. Halogen bonding for rational drug design and new drug discovery. *Expert Opin. Drug Discov.* **2012**, *7*, 375–383. [CrossRef]
19. Mukherjee, A.; Tothadi, S.; Desiraju, G.R. Halogen Bonds in Crystal Engineering: Like Hydrogen Bonds yet Different. *Acc. Chem. Res.* **2014**, *47*, 2514–2524. [CrossRef]
20. Gilday, L.C.; Robinson, S.W.; Barendt, T.A.; Langton, M.J.; Mullaney, B.R.; Beer, P.D. Halogen Bonding in Supramolecular Chemistry. *Chem. Rev.* **2015**, *115*, 7118–7195. [CrossRef]
21. Jungbauer, S.H.; Bulfield, D.; Kniep, F.; Lehmann, C.W.; Herdtweck, E.; Huber, S.M. Toward Molecular Recognition: Three-Point Halogen Bonding in the Solid State and in Solution. *J. Am. Chem. Soc.* **2014**, *136*, 16740–16743. [CrossRef]
22. Hostaš, J.; Řezáč, J. Accurate DFT-D3 Calculations in a Small Basis Set. *J. Chem. Theory Comput.* **2017**, *13*, 3575–3585. [CrossRef]
23. Otero-de-la-Roza, A.; Johnson, E.R.; DiLabio, G.A. Halogen Bonding from Dispersion-Corrected Density-Functional Theory: The Role of Delocalization Error. *J. Chem. Theory Comput.* **2014**, *10*, 5436–5447. [CrossRef] [PubMed]
24. Kozuch, S.; Martin, J.M.L. Halogen Bonds: Benchmarks and Theoretical Analysis. *J. Chem. Theory Comput.* **2013**, *9*, 1918–1931. [CrossRef] [PubMed]
25. Politzer, P.; Murray, J.S.; Clark, T.; Resnati, G. The σ-hole revisited. *Phys. Chem. Chem. Phys.* **2017**, *19*, 32166–32178. [CrossRef] [PubMed]

26. Murray, J.S.; Resnati, G.; Politzer, P. Close contacts and noncovalent interactions in crystals. *Faraday Discuss.* **2017**, *203*, 113–130. [CrossRef] [PubMed]
27. Politzer, P.; Murray, J.S.; Clark, T. Mathematical modeling and physical reality in noncovalent interactions. *J. Mol. Model.* **2015**, *21*, 52. [CrossRef] [PubMed]
28. Zhao, Y.; Truhlar, D.G. The M06 suite of density functionals for main group thermochemistry, thermochemical kinetics, noncovalent interactions, excited states, and transition elements: Two new functionals and systematic testing of four M06-class functionals and 12 other functionals. *Theor. Chem. Acc.* **2008**, *120*, 215–241.
29. Walker, M.; Harvey, A.J.A.; Sen, A.; Dessent, C.E.H. Performance of M06, M06-2X, and M06-HF Density Functionals for Conformationally Flexible Anionic Clusters: M06 Functionals Perform Better than B3LYP for a Model System with Dispersion and Ionic Hydrogen-Bonding Interactions. *J. Phys. Chem. A* **2013**, *117*, 12590–12600. [CrossRef]
30. Varadwaj, A.; Varadwaj, P.R.; Marques, H.M.; Yamashita, K. A DFT assessment of some physical properties of iodine-centered halogen bonding and other non-covalent interactions in some experimentally reported crystal geometries. *Phys. Chem. Chem. Phys.* **2018**, *20*, 15316–15329. [CrossRef]
31. Angarov, V.; Kozuch, S. On the σ, π and δ hole interactions: A molecular orbital overview. *New J. Chem.* **2018**, *42*, 1413–1422. [CrossRef]
32. Koohi, A.M.; Mahdavifar, Z.; Noorizadeh, S. Can Fluorine form Halogen Bond? Investigation of Halogen Bonds through Steric Charge. *ChemistrySelect* **2017**, *2*, 2713–2717. [CrossRef]
33. Roy, D.; Marianski, M.; Maitra, N.T.; Dannenberg, J.J. Comparison of some dispersion-corrected and traditional functionals with CCSD(T) and MP2 ab initio methods: Dispersion, induction, and basis set superposition error. *J. Chem. Phys.* **2012**, *137*, 134109. [CrossRef]
34. Wang, Y.; Jin, X.; Yu, H.S.; Truhlar, D.G.; He, X. Revised M06-L functional for improved accuracy on chemical reaction barrier heights, noncovalent interactions, and solid-state physics. *Proc. Natl. Acad. Sci. USA* **2017**, *114*, 8487–8492. [CrossRef] [PubMed]
35. Paranthaman, S. Assessment of DFT Functionals in Predicting Bond Length and Atomization Energy of Catalytically Important Metal Dimer. *Croat. Chem. Acta* **2017**, *90*, 17–26. [CrossRef]
36. Vydrov, O.A.; Van Voorhis, T. Benchmark Assessment of the Accuracy of Several van der Waals Density Functionals. *J. Chem. Theory Comput.* **2012**, *8*, 1929–1934. [CrossRef]
37. Kovács, A.; Dobrowolski, J.C.; Ostrowski, S.; Rode, J.E. Benchmarking density functionals in conjunction with Grimme's dispersion correction for noble gas dimers ($Ne_2$, $Ar_2$, $Kr_2$, $Xe_2$, $Rn_2$). *Int. J. Quantum Chem.* **2017**, *117*, e25358. [CrossRef]
38. Ayers, P.W.; Parr, R.G. Is it impossible to find the universal density functional? Or is it just well-hidden? *Ind. J. Chem.* **2014**, *53A*, 929–931.
39. Desiraju, G.R.; Shing Ho, P.; Kloo, L.; Legon, A.C.; Marquardt, R.; Metrangolo, P.; Politzer, P.; Resnati, G.; Rissanen, K. Definition of the halogen bond (IUPAC Recommendations 2013). *Pure Appl. Chem.* **2013**, *85*, 1711–1713. [CrossRef]
40. Thirman, J.; Engelage, E.; Huber, S.M.; Head-Gordon, M. Characterizing the interplay of Pauli repulsion, electrostatics, dispersion and charge transfer in halogen bonding with energy decomposition analysis. *Phys. Chem. Chem. Phys.* **2018**, *20*, 905–915. [CrossRef]
41. Huber, S.M.; Jimenez-Izal, E.; Ugalde, J.M.; Infante, I. Unexpected Trends in Halogen-Bond Based Noncovalent Adducts. *Chem. Commun.* **2012**, *48*, 7708–7710. [CrossRef]
42. Tawfik, M.; Donald, K.J. Halogen Bonding: Unifying Perspectives on Organic and Inorganic Cases. *J. Phys. Chem. A* **2014**, *118*, 10090–10100. [CrossRef]
43. Scheiner, S. Systematic Elucidation of Factors That Influence the Strength of Tetrel Bonds. *J. Phys. Chem. A* **2017**, *121*, 5561–5568. [CrossRef]
44. Dong, W.; Li, Q.; Scheiner, S. Comparative Strengths of Tetrel, Pnicogen, Chalcogen, and Halogen Bonds and Contributing Factors. *Molecules* **2018**, *23*, 1681. [CrossRef] [PubMed]
45. Varadwaj, P.R.; Varadwaj, A.; Jin, B.-Y. Unusual bonding modes of perfluorobenzene in its polymeric (dimeric, trimeric and tetrameric) forms: Entirely negative fluorine interacting cooperatively with entirely negative fluorine. *Phys. Chem. Chem. Phys.* **2015**, *17*, 31624–31645. [CrossRef] [PubMed]

46. Varadwaj, A.; Varadwaj, P.R.; Jin, B.-Y. Can an entirely negative fluorine in a molecule, viz. perfluorobenzene, interact attractively with the entirely negative site(s) on another molecule(s)? Like liking like! *RSC Adv.* **2016**, *6*, 19098–19110. [CrossRef]
47. Varadwaj, A.; Varadwaj, P.R.; Yamashita, K. Do surfaces of positive electrostatic potential on different halogen derivatives in molecules attract? Like attracting like! *J. Comput. Chem.* **2018**, *39*, 343–350. [CrossRef] [PubMed]
48. Schneider, H.-J. Hydrogen bonds with fluorine. Studies in solution, in gas phase and by computations, conflicting conclusions from crystallographic analyses. *Chem. Sci.* **2012**, *3*, 1381–1394. [CrossRef]
49. Varadwaj, P.; Varadwaj, A.; Marques, H.; Yamashita, K. Can Combined Electrostatic and Polarization Effects Alone Explain the F$\cdots$F Negative-Negative Bonding in Simple Fluoro-Substituted Benzene Derivatives? A First-Principles Perspective. *Computation* **2018**, *6*, 51. [CrossRef]
50. Tantardini, C. When does a hydrogen bond become a van der Waals interaction? A topological answer. *J. Comput. Chem.* **2019**, *40*, 937–943. [CrossRef]
51. Wang, C.; Danovich, D.; Shaik, S.; Wu, W.; Mo, Y. Attraction between electrophilic caps: A counterintuitive case of noncovalent interactions. *J. Comput. Chem* **2019**, *40*, 1015–1022. [CrossRef]
52. Varadwaj, P.R.; Varadwaj, A.; Jin, B.-Y. Halogen bonding interaction of chloromethane withseveral nitrogen donating molecules: Addressing thenature of the chlorine surface σ-hole. *Phys. Chem. Chem. Phys.* **2014**, *16*, 19573–19589. [CrossRef]
53. Riley, K.E.; Vazquez, M.; Umemura, C.; Miller, C.; Tran, K.-A. Exploring the (Very Flat) Potential Energy Landscape of R–Br$\cdots\pi$ Interactions with Accurate CCSD(T) and SAPT Techniques. *Chem. Eur. J.* **2016**, *22*, 17690–17695. [CrossRef]
54. Arunan, E.; Desiraju, G.R.; Klein, R.A.; Sadlej, J.; Scheiner, S.; Alkorta, I.; Clary, D.C.; Crabtree, R.H.; Dannenberg, J.J.; Hobza, P.; et al. Definition of the hydrogen bond (IUPAC Recommendations 2011). *Pure Appl. Chem.* **2011**, *83*, 1637–1641. [CrossRef]
55. Clark, T. Halogen bonds and σ-holes. *Faraday Discuss.* **2017**, *203*, 9–27. [CrossRef] [PubMed]
56. Arunan, E. Hydrogen bond seen, halogen bond defined and carbon bond proposed: Intermolecular bonding, a field that is maturing! *Curr. Sci.* **2013**, *105*, 892–894.
57. Zhang, J.; Chen, P.; Yuan, B.; Ji, W.; Cheng, Z.; Qiu, X. Real-Space Identification of Intermolecular Bonding with Atomic Force Microscopy. *Science* **2013**, *342*, 611–614. [CrossRef]
58. Ritter, S.K. The Cheimcal Bond. *C E News Arch.* **2007**, *85*, 37–40. [CrossRef]
59. Bader, R.W.F. Bond paths are not chemical bonds. *J. Phys. Chem. A* **2009**, *113*, 10391–10396. [CrossRef] [PubMed]
60. De Oteyza, D.G.; Gorman, P.; Chen, Y.-C.; Wickenburg, S.; Riss, A.; Mowbray, D.J.; Etkin, G.; Pedramrazi, Z.; Tsai, H.-Z.; Rubio, A.; et al. Direct Imaging of Covalent Bond Structure in Single-Molecule Chemical Reactions. *Science* **2013**. [CrossRef]
61. Itatani, J.; Levesque, J.; Zeidler, D.; Spanner, M.; Corkum, P.B.; Villeneuve, D.M. Tomographic imaging of molecular orbitals with high harmonic generation. In Proceedings of the 14th International Conference on Ultrafast Phenomena, Niigata, Japan, 25–30 July 2004; p. M3.
62. Itatani, J.; Levesque, J.; Zeidler, D.; Niikura, H.; Pépin, H.; Kieffer, J.C.; Corkum, P.B.; Villeneuve, D.M. Tomographic imaging of molecular orbitals. *Nature* **2004**, *432*, 867. [CrossRef] [PubMed]
63. Mulder, P. Are Orbitals Observable? *HYLE Int. J. Philos. Chem.* **2011**, *17*, 24–35.
64. Schwarz, W.H.E. Measuring Orbitals: Provocation or Reality? *Angew Chem. Int. Ed.* **2006**, *45*, 1508–1517. [CrossRef]
65. Scerri, E.R. Have Orbitals Really Been Observed? *J. Chem. Ed.* **2000**, *77*, 1492. [CrossRef]
66. Ivanov, M.V.; Reid, S.A.; Rathore, R. Game of Frontier Orbitals: A View on the Rational Design of Novel Charge-Transfer Materials. *J. Phys. Chem. Lett.* **2018**, *9*, 3978–3986. [CrossRef] [PubMed]
67. Ito, O.; D'Souza, F. Recent Advances in Photoinduced Electron Transfer Processes of Fullerene-Based Molecular Assemblies and Nanocomposites. *Molecules* **2012**, *17*, 5816. [CrossRef] [PubMed]
68. Torrente, I.F.; Franke, K.J.; Pascual, J.I. Spectroscopy of $C_{60}$ single molecules: The role of screening on energy level alignment. *J. Phys. Condens. Matter* **2008**, *20*, 184001. [CrossRef]
69. Wu, Q.; Zhao, D.; Goldey, M.B.; Filatov, A.S.; Sharapov, V.; Colón, Y.J.; Cai, Z.; Chen, W.; de Pablo, J.; Galli, G.; et al. Intra-molecular Charge Transfer and Electron Delocalization in Non-fullerene Organic Solar Cells. *ACS Appl. Mater. Interfaces* **2018**, *10*, 10043–10052. [CrossRef] [PubMed]

70. Lee, K.J.; Woo, J.H.; Xiao, Y.; Kim, E.; Mazur, L.M.; Kreher, D.; Attias, A.-J.; Matczyszyn, K.; Samoc, M.; Heinrich, B.; et al. Structure–charge transfer property relationship in self-assembled discotic liquid-crystalline donor–acceptor dyad and triad thin films. *RSC Adv.* **2016**, *6*, 57811–57819. [CrossRef]
71. Tishchenko, O.; Truhlar, D.G. Atom-Cage Charge Transfer in Endohedral Metallofullerenes: Trapping Atoms within a Sphere-Like Ridge of Avoided Crossings. *J. Chem. Phys. Lett.* **2013**, *4*, 422–425. [CrossRef]
72. Campanera, J.M.; Bo, C.; Olmstead, M.M.; Balch, A.L.; Poblet, J.M. Bonding within the Endohedral Fullerenes $Sc_3N@C_{78}$ and $Sc_3N@C_{80}$ as Determined by Density Functional Calculations and Reexamination of the Crystal Structure of $\{Sc_3N@C_{78}\}\cdot Co(OEP)\}\cdot 1.5(C_6H_6)\cdot 0.3(CHCl_3)$. *J. Phys Chem. A* **2002**, *106*, 12356–12364. [CrossRef]
73. Popov, A.A.; Yang, S.; Dunsch, L. Endohedral fullerenes. *Chem. Rev.* **2013**, *113*, 5989–6113. [CrossRef]
74. Wang, B.; Zheng, S.; Saha, A.; Bao, L.; Lu, X.; Guldi, D.M. Understanding Charge-Transfer Characteristics in Crystalline Nanosheets of Fullerene/(Metallo)porphyrin Cocrystals. *J. Am. Chem. Soc.* **2017**, *139*, 10578–10584. [CrossRef] [PubMed]
75. Alhameedi, K.; Karton, A.; Jayatilaka, D.; Thomas, S.P. Bond orders for intermolecular interactions in crystals: Charge transfer, ionicity and the effect on intramolecular bonds. *IUCrJ* **2018**, *5*, 635–646. [CrossRef] [PubMed]
76. Davey, J.B.; Legon, A.C.; Waclawik, E.R. Inter- and intramolecular electron transfer in the complex OC···ICl determined from iodine and chlorine nuclear quadrupole hyperfine structure in its rotational spectrum. *Phys. Chem. Chem. Phys.* **1999**, *1*, 3097–3101. [CrossRef]
77. Legon, A.C. Angular and radial geometries, charge transfer and binding strength in isolated complexes B···ICl: Some generalisations. *Chem. Phys. Lett.* **1999**, *314*, 472–480. [CrossRef]
78. Legon, A.C. Tetrel, pnictogen and chalcogen bonds identified in the gas phase before they had names: A systematic look at non-covalent interactions. *Phys. Chem. Chem. Phys.* **2017**, *19*, 14884–14896. [CrossRef] [PubMed]
79. Davey, J.B.; Legon, A.C.; Waclawik, E.R. Measurement of inter- and intramolecular charge transfer in the complex $N_2$···ICl from analysis of halogen nuclear quadrupole hyperfine structure in the rotational spectrum. *J. Mol. Struct. THEOCHEM* **2000**, *500*, 403–411. [CrossRef]
80. Legon, A.C.; Thumwood, J.M.A.; Waclawik, E.R. Rotational spectroscopy of $H_3P$···BrCl and the systematics of intermolecular electron transfer in the series B···BrCl, where B=CO, HCN, $H_2O$, $C_2H_2$, $C_2H_4$, $H_2S$, $NH_3$, and $PH_3$. *J. Chem. Phys.* **2000**, *113*, 5278. [CrossRef]
81. Davey, J.B.; Legon, A.C. A gas phase complex of acetylene and bromine: Geometry, binding strength and charge transfer from rotational spectroscopy. *Chem. Phys. Lett.* **2001**, *350*, 39–50. [CrossRef]
82. Legon, A.C.; Waclawik, E.R. Angular geometry, binding strength and charge transfer for the complex $H_2S$···ICl determined by rotational spectroscopy. *Chem. Phys. Lett.* **1999**, *312*, 385–393. [CrossRef]
83. Legon, A.C. Prereactive Complexes of Dihalogens XY with Lewis Bases B in the Gas Phase: A Systematic Case for the Halogen Analogue B···XY of the Hydrogen Bond B···HX. *Angew. Chem. Int. Ed.* **1999**, *38*, 2686–2714. [CrossRef]
84. Herrebout, W.A.; Legon, A.C.; Waclawik, E.R. Is there significant intermolecular charge transfer in the ground state of the HCN···ICI complex? An answer from rotational spectroscopy. *Phys. Chem. Chem. Phys.* **1999**, *1*, 4961–4966. [CrossRef]
85. Legon, A.C.; Millen, D.J.; Rogers, S.C. Microwave spectrum of a gas-phase charge-transfer complex. *J. Chem. Soc. Chem. Commun.* **1975**, 580–581. [CrossRef]
86. Bloemink, H.I.; Legon, A.C.; Thorn, J.C. 'Charge-transfer' complexes of ammonia with halogens. Nature of the binding in $H_3N$···BrCl from its rotational spectrum. *J. Chem. Soc. Faraday Trans.* **1995**, *91*, 781–787. [CrossRef]
87. Campbell, E.J.; Keenan, M.R.; Buxton, L.W.; Balle, T.J.; Soper, P.O.; Legon, A.C.; Flygare, W.H. $^{83}$Kr Nuclear quadrupole coupling in KrHF: Evidence for charge transfer. *Chem. Phys. Lett.* **1980**, *70*, 420–424. [CrossRef]
88. Legon, A.C. π-Electron "Donor–Acceptor" Complexes B···ClF and the Existence of the "Chlorine Bond". *Chem. Eur. J.* **1998**, *4*, 1890–1897. [CrossRef]
89. Clark, T.; Politzer, P.; Murray, J.S. Correct electrostatic treatment of noncovalent interactions: The importance of polarization. *WIRES Comput. Mol. Sci.* **2015**, *5*, 169–177. [CrossRef]
90. Oliveira, V.; Kraka, E.; Cremer, D. Quantitative Assessment of Halogen Bonding Utilizing Vibrational Spectroscopy. *Inorg. Chem.* **2017**, *56*, 488–502. [CrossRef]

91. Sexton, T.; Kraka, E.; Cremer, D. Extraordinary Mechanism of the Diels–Alder Reaction: Investigation of Stereochemistry, Charge Transfer, Charge Polarization, and Biradicaloid Formation. *J. Phys Chem. A* **2016**, *120*, 1097–1111. [CrossRef]
92. Zhao, Z.; Rogers, D.M.; Beck, T.L. Polarization and charge transfer in the hydration of chloride ions. *J. Chem. Phys.* **2010**, *132*, 014502. [CrossRef]
93. Oliveira, V.; Kraka, E.; Cremer, D. The intrinsic strength of the halogen bond: Electrostatic and covalent contributions described by coupled cluster theory. *Phys. Chem. Chem. Phys.* **2016**, *18*, 33031–33046. [CrossRef]
94. Oliveira, V.; Kraka, E. Systematic Coupled Cluster Study of Noncovalent Interactions Involving Halogens, Chalcogens, and Pnicogens. *J. Phys. Chem. A* **2017**, *121*, 9544–9556. [CrossRef] [PubMed]
95. Řezáč, J.; de la Lande, A. On the role of charge transfer in halogen bonding. *Phys. Chem. Chem. Phys.* **2017**, *19*, 791–803. [CrossRef] [PubMed]
96. Varadwaj, P.R.; Varadwaj, A.; Jin, B.Y. Ligand(s)-to-metal charge transfer as a factor controlling the equilibrium constants of late first-row transition metal complexes: Revealing the Irving-Williams thermodynamical series. *Phys. Chem. Chem. Phys.* **2015**, *17*, 805–811. [CrossRef] [PubMed]
97. Varadwaj, P.R. Methylammonium Lead Trihalide Perovskite Solar Cell Semiconductors Are Not Organometallic: A Perspective. *Helv. Chim. Acta* **2017**, *100*, e1700090. [CrossRef]
98. Varadwaj, A.; Varadwaj, P.R.; Yamashita, K. Revealing the Cooperative Chemistry of the Organic Cation in the Methylammonium Lead Triiodide Perovskite Semiconductor System. *ChemistrySelect* **2018**, *3*, 7269–7282. [CrossRef]
99. Varadwaj, A.; Varadwaj, P.R.; Yamashita, K. Hybrid organic–inorganic $CH_3NH_3PbI_3$ perovskite building blocks: Revealing ultra-strong hydrogen bonding and mulliken inner complexes and their implications in materials design. *J. Comput. Chem.* **2017**, *38*, 2802–2818. [CrossRef]
100. Zieleniewska, A.; Lodermeyer, F.; Roth, A.; Guldi, D.M. Fullerenes—How 25 years of charge transfer chemistry have shaped our understanding of (interfacial) interactions. *Chem. Soc. Rev.* **2018**, *47*, 702–714. [CrossRef] [PubMed]
101. Mollahosseini, M.; Karunaratne, E.; Gibson, G.N.; Gascón, J.A.; Papadimitrakopoulos, F. Fullerene-Assisted Photoinduced Charge Transfer of Single-Walled Carbon Nanotubes through a Flavin Helix. *J. Am. Chem. Soc.* **2016**, *138*, 5904–5915. [CrossRef] [PubMed]
102. Meng, Y.-S.; Sato, O.; Liu, T. Manipulating Metal-to-Metal Charge Transfer for Materials with Switchable Functionality. *Angew Chem. Int. Ed.* **2018**, *57*, 12216–12226. [CrossRef]
103. Dunsch, L.; Yang, S. The Recent State of Endohedral Fullerene Research. The Electrochemical Society: Interface. 2006, pp. 34–39. Available online: https://www.electrochem.org/dl/interface/sum/sum06/sum06_p34.pdf (accessed on 7 February 2019).
104. Stasyuk, A.J.; Solà, M.; Voityuk, A.A. Reliable charge assessment on encapsulated fragment for endohedral systems. *Sci. Rep.* **2018**, *8*, 2882. [CrossRef]
105. Robinson, S.W.; Mustoe, C.L.; White, N.G.; Brown, A.; Thompson, A.L.; Kennepohl, P.; Beer, P.D. Evidence for Halogen Bond Covalency in Acyclic and Interlocked Halogen-Bonding Receptor Anion Recognition. *J. Am. Chem. Soc.* **2015**, *137*, 499–507. [CrossRef] [PubMed]
106. Mustoe, C.L.; Gunabalasingam, M.; Yu, D.; Patrick, B.O.; Kennepohl, P. Probing covalency in halogen bonds through donor K-edge X-ray absorption spectroscopy: Polyhalides as coordination complexes. *Faraday Discuss.* **2017**, *203*, 79–91. [CrossRef] [PubMed]
107. Puttreddy, R.; Topić, F.; Valkonen, A.; Rissanen, K. Halogen-Bonded Co-Crystals of Aromatic N-oxides: Polydentate Acceptors for Halogen and Hydrogen Bonds. *Crystals* **2017**, *7*, 214. [CrossRef]
108. Ruedenberg, K. The Physical Nature of the Chemical Bond. *Rev. Mod. Phys.* **1962**, *34*, 326–376. [CrossRef]
109. Clark, T.; Hennemann, M.; Murray, J.S.; Politzer, P. Halogen bonding: The σ-hole. *J. Mol. Model.* **2007**, *13*, 291–296. [CrossRef] [PubMed]
110. Bader, R.F.W. Molecular fragments or chemical bonds. *Acc. Chem. Res.* **1975**, *8*, 34–40. [CrossRef]
111. Bader, R.F.W.; Nguyen-Dang, T.T. Quantum Theory of Atoms in Molecules–Dalton Revisited. In *Advances in Quantum Chemistry*; Löwdin, P.-O., Ed.; Academic Press: New York, NY, USA, 1981; Volume 14, pp. 63–124.
112. Bader, R.F.W.; Nguyen-Dang, T.T.; Tai, Y. A topological theory of molecular structure. *Rep. Prog. Phys.* **1981**, *44*, 893–947. [CrossRef]
113. Bader, R.F.W. Atoms in molecules. *Acc. Chem. Res.* **1985**, *18*, 9–15. [CrossRef]
114. Grabowski, S.J. What is the covalency of hydrogen bonding? *Chem. Rev.* **2011**, *111*, 2597–2625. [CrossRef]

115. Quiñonero, D.; Alkorta, I.; Elguero, J. Cation–cation and anion–anion complexes stabilized by halogen bonds. *Phys. Chem. Chem. Phys.* **2016**, *18*, 27939–27950. [CrossRef]
116. Politzer, P.; Huheey, J.E.; Murray, J.S.; Grodzicki, M. Electronegativity and the concept of charge capacity. *J. Mol. Struct. THEOCHEM* **1992**, *259*, 99–120. [CrossRef]
117. Clark, T.; Murray, J.S.; Politzer, P. The σ-Hole Coulombic Interpretation of Trihalide Anion Formation. *ChemPhysChem* **2018**, *19*, 1–7. [CrossRef] [PubMed]
118. Politzer, P.; Riley, K.E.; Bulat, F.A.; Murray, J.S. Perspectives on Halogen Bonding and Other σ-Hole Interactions: Lex Parsimoniae (Occam's Razor). *Comput. Theor. Chem.* **2012**, *998*, 2–8. [CrossRef]
119. Politzer, P.; Murray, J.S.; Clark, T. σ-Hole Bonding: A Physical Interpretation. In *Halogen Bonding I: Impact on Materials Chemistry and Life Science*; Metrangolo, P., Resnati, G., Eds.; Springer International Publishing: Cham, Switzerland, 2015.
120. Clark, T. σ-Holes. *Wiley Interdiscip. Rev. Comput. Mol. Sci.* **2013**, *3*, 13–20. [CrossRef]
121. Cremer, D.; Wu, A.; Larsson, A.; Kraka, E. Some Thoughts about Bond Energies, Bond Lengths, and Force Constants. *J. Mol. Model.* **2000**, *6*, 396–412. [CrossRef]
122. Cremer, D.; Kraka, E. From Molecular Vibrations to Bonding, Chemical Reactions, and Reaction Mechanism. *Curr. Org. Chem.* **2010**, *14*, 1524–1560. [CrossRef]
123. Zhu, T.; de Silva, P.; Van Voorhis, T. Self-Attractive Hartree Decomposition: Partitioning Electron Density into Smooth Localized Fragments. *J. Chem. Theory Comput.* **2018**, *14*, 92–103. [CrossRef]
124. Wick, C.R.; Clark, T. On bond-critical points in QTAIM and weak interactions. *J. Mol. Model.* **2018**, *24*, 142. [CrossRef]
125. Jansen, G. Symmetry-adapted perturbation theory based on density functional theory for noncovalent interactions. *Wiley Interdiscip. Rev. Comput. Mol. Sci.* **2014**, *4*, 127–144. [CrossRef]
126. Esterhuysen, C.; Heßelmann, A.; Clark, T. Trifluoromethyl: An Amphiphilic Noncovalent Bonding Partner. *ChemPhysChem* **2017**, *18*, 772–784. [CrossRef]
127. Sharapa, D.I.; Margraf, J.T.; Hesselmann, A.; Clark, T. Accurate Intermolecular Potential for the $C_{60}$ Dimer: The Performance of Different Levels of Quantum Theory. *J. Chem. Theory Comput.* **2017**, *13*, 274–285. [CrossRef] [PubMed]
128. Vandenbrande, S.; Waroquier, M.; Speybroeck, V.V.; Verstraelen, T. The Monomer Electron Density Force Field (MEDFF): A Physically Inspired Model for Noncovalent Interactions. *J. Chem. Theory Comput.* **2017**, *13*, 161–179. [CrossRef] [PubMed]
129. Heidar-Zadeh, F.; Ayers, P.W.; Verstraelen, T.; Vinogradov, I.; Vöhringer-Martinez, E.; Bultinck, P. Information-Theoretic Approaches to Atoms-in-Molecules: Hirshfeld Family of Partitioning Schemes. *J. Phys. Chem. A* **2018**, *122*, 4219–4245. [CrossRef] [PubMed]
130. Verstraelen, T.; Ayers, P.W.; Van Speybroeck, V.; Waroquier, M. Hirshfeld-E Partitioning: AIM Charges with an Improved Trade-off between Robustness and Accurate Electrostatics. *J. Chem. Theory Comput.* **2013**, *9*, 2221–2225. [CrossRef] [PubMed]
131. Szalewicz, K. Symmetry-adapted perturbation theory of intermolecular forces. *WIREs Comput. Mol. Sci.* **2012**, *2*, 254–272. [CrossRef]
132. Fanfrlík, J.; Pecina, A.; Řezáč, J.; Sedlak, R.; Hnyk, D.; Lepšík, M.; Hobza, P. B–H$\cdots\pi$: A nonclassical hydrogen bond or dispersion contact? *Phys. Chem. Chem. Phys.* **2017**, *19*, 18194–18200. [CrossRef]
133. Zou, W.; Zhang, X.; Dai, H.; Yan, H.; Cremer, D.; Kraka, E. Description of an unusual hydrogen bond between carborane and a phenyl group. *J. Organomet. Chem.* **2018**, *865*, 114–127. [CrossRef]
134. Zhang, X.; Dai, H.; Yan, H.; Zou, W.; Cremer, D. B–H$\cdots\pi$ Interaction: A New Type of Nonclassical Hydrogen Bonding. *J. Am. Chem. Soc.* **2016**, *138*, 4334–4337. [CrossRef]
135. *CSD 5.38*; Cambridge Crystallographic Data Centre (CCDC): Cambridge, UK, 2016.
136. Mackenzie, C.F.; Spackman, P.R.; Jayatilaka, D.; Spackman, M.A. CrystalExplorer model energies and energy frameworks: Extension to metal coordination compounds, organic salts, solvates and open-shell systems. *IUCrJ* **2017**, *4*, 575–587. [CrossRef]
137. Varadwaj, P.R.; Varadwaj, A.; Jin, B.Y. Significant evidence of C$\cdots$O and C$\cdots$C long-range contacts in several heterodimeric complexes of CO with $CH_3$–X, should one refer to them as carbon and dicarbon bonds! *Phys. Chem. Chem. Phys.* **2014**, *16*, 17238–17252. [CrossRef]
138. Bauzá, A.; Frontera, A. Aerogen Bonding Interaction: A New Supramolecular Force? *Angew Chem. Int. Ed.* **2015**, *54*, 7340–7343. [CrossRef] [PubMed]

139. Mitra, M.; Manna, P.; Bauzá, A.; Ballester, P.; Seth, S.K.; Ray Choudhury, S.; Frontera, A.; Mukhopadhyay, S. 3-Picoline Mediated Self-Assembly of M(II)–Malonate Complexes (M = Ni/Co/Mn/Mg/Zn/Cu) Assisted by Various Weak Forces Involving Lone Pair–π, π–π, and Anion···π–Hole Interactions. *J. Phys. Chem. B* **2014**, *118*, 14713–14726. [CrossRef] [PubMed]
140. Shahi, A.; Arunan, E. Hydrogen bonding, halogen bonding and lithium bonding: An atoms in molecules and natural bond orbital perspective towards conservation of total bond order, inter- and intra-molecular bonding. *Phys. Chem. Chem. Phys.* **2014**, *16*, 22935–22952. [CrossRef] [PubMed]
141. Varadwaj, A.; Marques, H.M.; Varadwaj, P.R. Is the Fluorine in Molecules Dispersive? Is Molecular Electrostatic Potential a Valid Property to Explore Fluorine-Centered Non-Covalent Interactions? *Molecules* **2019**, *24*, 379. [CrossRef]
142. Eskandari, K.; Lesani, M. Does fluorine participate in halogen bonding? *Chem. Eur. J.* **2015**, *21*, 4739–4746. [CrossRef]
143. Huggins, M.L. 50 Years of Hydrogen Bond Theory. *Angew. Chem. Int. Ed. Engl.* **1971**, *10*, 147–152. [CrossRef]
144. Huggins, M.L. Hydrogen bridges in organic compounds. *J. Org. Chem.* **1936**, *01*, 407–456. [CrossRef]
145. Pauling, L. The Structure and Entropy of Ice and of Other Crystals with Some Randomness of Atomic Arrangement. *J. Am. Chem. Soc.* **1935**, *57*, 2680–2684. [CrossRef]
146. Colin, M.M.; Gaultier de Claubry, H. Sur Le Combinaisons de L'iode Avec Les Substances Végétales et Animales. *Ann. Chim.* **1814**, *90*, 87–100.
147. Colin, M. Note Sur Quelques Combinaisons de L'iode. *Ann. Chim.* **1814**, *91*, 252–272.
148. Guthrie, F. On the Iodide of Diammonium *J. Chem. Soc.* **1863**, *16*, 239–244. [CrossRef]
149. Hassel, O. Structural Aspects on Interatomic Charge-Transfer Bonding. *Science* **1970**, *170*, 497–502. [CrossRef] [PubMed]
150. Strømme, K.O. An X-Ray Analysis of the 1:1 Compound Trimethylamine-Iodine. *Acta Chem. Scand.* **1959**, *13*, 268–274. [CrossRef]
151. Hassel, O.; Strømme, K.O. Crystal Structure of the Addition Compound 1,4-Dioxan-Chlorine. *Acta Chem. Scand.* **1959**, *13*, 1775–1780. [CrossRef]
152. Hassel, O.; Strømme, K.O. Crystal Structure of the 1:1 Addition Compound Formed by Acetone and Bromine. *Acta Chem. Scand.* **1959**, *13*, 275–280. [CrossRef]
153. Hassel, O. Structural Aspects of Interatomic Charge-Transfer Bonding. In *Nobel Lectures, Chemistry 1963–1970*; Elsevier Publishing Company: Amsterdam, The Netherlands, 1972; pp. 314–329.
154. Dumas, J.-M.; Peurichard, H.; Gomel, M. $CX_4$···Base Interactions as Models of Weak Charge-transfer Interactions: Comparison with Strong Charge-transfer and Hydrogen-bond Interactions. *J. Chem. Res. S* **1978**, *2*, 54–57.
155. Jones, R.H.; Knight, K.S.; Marshall, W.G.; Coles, S.J.; Horton, P.N.; Pitak, M.B. The competition between halogen bonds (Br···O) and C–H···O hydrogen bonds: The structure of the acetone–bromine complex revisited. *CrystEngComm* **2013**, *15*, 8572–8577. [CrossRef]
156. Marshall, W.G.; Jones, R.H.; Knight, K.S. Negative 2D thermal expansion in the halogen bonded acetone bromine complex. *CrystEngComm* **2018**, *20*, 3246–3250. [CrossRef]
157. Bauzá, A.; Frontera, A. On the Importance of Halogen–Halogen Interactions in the Solid State of Fullerene Halides: A Combined Theoretical and Crystallographic Study. *Crystals* **2017**, *7*, 191. [CrossRef]
158. Varadwaj, A.; Varadwaj, P.R.; Jin, B.-Y. Fluorines in tetrafluoromethane as halogen bond donors: Revisiting address the nature of the fluorine's σ-hole. *Int. J. Quantum Chem.* **2015**, *115*, 453–470. [CrossRef]
159. Bader, R.F.W.; Carroll, M.T.; Cheeseman, J.R.; Chang, C. Properties of atoms in molecules: Atomic volumes. *J. Am. Chem. Soc.* **1987**, *109*, 7968–7979. [CrossRef]
160. Lange, A.; Heidrich, J.; Zimmermann, M.O.; Exner, T.E.; Boeckler, F.M. Scaffold Effects on Halogen Bonding Strength. *J. Chem. Inf. Model.* **2019**. [CrossRef] [PubMed]
161. Brinck, T.; Murray, J.S.; Politzer, P. Surface electrostatic potentials of halogenated methanes as indicators of directional intermolecular interactions. *Int. J. Quantum Chem.* **1992**, *44*, 57–64. [CrossRef]
162. Groenewald, F.; Esterhuysen, C.; Dillen, J. Extensive theoretical investigation: Influence of the electrostatic environment on the $I_3^-$···$I_3^-$ anion–anion interaction. *Theor. Chem. Acc.* **2012**, *131*, 1281. [CrossRef]
163. Pedireddi, V.R.; Reddy, D.S.; Goud, B.S.; Craig, D.C.; Rae, A.D.; Desiraju, G.R. The nature of halogen···halogen interactions and the crystal structure of 1,3,5,7-tetraiodoadamantane. *J. Chem. Soc. Perkin Trans. 2* **1994**, 2353–2360. [CrossRef]

164. Saha, B.K.; Nangia, A.; Nicoud, J.-F. Using Halogen···Halogen Interactions to Direct Noncentrosymmetric Crystal Packing in Dipolar Organic Molecules. *Cryst. Growth Des.* **2006**, *6*, 1278–1281. [CrossRef]
165. Saha, B.K.; Saha, A.; Rather, S.A. Shape and Geometry Corrected Statistical Analysis on Halogen···Halogen Interactions. *Cryst. Growth Des.* **2017**, *17*, 2314–2318. [CrossRef]
166. Saha, B.K.; Rather, S.A.; Saha, A. Interhalogen Interactions in the Light of Geometrical Correction. *Cryst. Growth Des.* **2016**, *16*, 3059–3062. [CrossRef]
167. Bosch, E.; Barnes, C.L. Triangular Halogen-Halogen-Halogen Interactions as a Cohesive Force in the Structures of Trihalomesitylenes. *Cryst. Growth Des.* **2002**, *2*, 299–302. [CrossRef]
168. Foi, A.; Corrêa, R.S.; Ellena, J.; Doctorovich, F.; Di Salvo, F. Halogen···halogen contacts for the stabilization of a new polymorph of 9,10-dichloroanthracene. *J. Mol. Struct.* **2014**, *1059*, 1–7. [CrossRef]
169. Metrangolo, P.; Resnati, G. Type II halogen···halogen contacts are halogen bonds. *IUCrJ* **2014**, *1*, 5–7. [CrossRef]
170. Dunitz, J.D. Intermolecular atom–atom bonds in crystals? *IUCrJ* **2015**, *2*, 157–158. [CrossRef]
171. Lecomte, C.; Espinosa, E.; Matta, C.F. On atom-atom "short contact" bonding interactions in crystals. *IUCrJ* **2015**, *2*, 161–163. [CrossRef]
172. Tejender, S.; Thakur, T.S.; Dubeyb, R.; Desirajub, G.R. Intermolecular atom–atom bonds in crystals—A chemical perspective. *IUCrJ* **2015**, *2*, 159–160.
173. Desiraju, G.R. Crystal engineering and IUCrJ. *IUCrJ* **2016**, *3*, 1–2. [CrossRef]
174. Ayers, P.L.; Boyd, R.J.; Bultinck, P.; Caffarel, M.; Carbó-Dorca, R.; Causá, M.; Cioslowski, J.; Contreras-Garcia, J.; Cooper, D.L.; Coppens, P.; et al. Six questions on topology in theoretical chemistry. *Comput. Theor. Chem.* **2015**, *1051*, 2–16. [CrossRef]
175. Huber, S.M.; Scanlon, J.D.; Jimenez-Izal, E.; Ugalde, J.M.; Infante, I. On the directionality of halogen bonding. *Phys. Chem. Chem. Phys.* **2013**, *15*, 10350–10357. [CrossRef]
176. Grant Hill, J.; Legon, A.C. On the directionality and non-linearity of halogen and hydrogen bonds. *Phys. Chem. Chem. Phys.* **2015**, *17*, 858–867. [CrossRef]
177. Desiraju, G.R. A bond by any other name. *Angew. Chem. Int. Ed.* **2011**, *50*, 52–59. [CrossRef]
178. McAllister, L. Experimental and Theoretical Studies of the Halogen Bond and the Electrophilic Bromination Reaction. Ph.D. Thesis, The University of York, York, UK, 2014.
179. Bader, R.F.W. Definition of Molecular Structure: By Choice or by Appeal to Observation? *J. Phys. Chem. A* **2010**, *114*, 7431–7444. [CrossRef]
180. Meister, J.; Schwarz, W.H.E. Principal Components of Ionicity. *J. Phys. Chem.* **1994**, *98*, 8245–8252. [CrossRef]
181. Matczak, P. A Test of Various Partial Atomic Charge Models for Computations on Diheteroaryl Ketones and Thioketones. *Computation* **2016**, *4*, 3. [CrossRef]
182. Volkov, A.; Gatti, C.; Abramov, Y.; Coppens, P. Evaluation of net atomic charges and atomic and molecular electrostatic moments through topo-logical analysis of the experimental charge density. *Acta Cryst. A* **2000**, *56*, 252–258. [CrossRef]
183. Bader, R.F.W.; Matta, C.F. Atomic charges are measurable quantum expectation values: A rebuttal of criticisms of QTAIM charges. *J. Phys. Chem. A* **2004**, *108*, 8385–8394. [CrossRef]
184. Politzer, P.; Murray, J.S.; Concha, M.C. σ-hole bonding between like atoms; a fallacy of atomic charges. *J. Mol. Model.* **2008**, *14*, 659–665. [CrossRef]
185. Murray, J.S.; Politzer, P. The electrostatic potential: An overview. *WIREs Comput. Mol. Sci.* **2011**, *1*, 153–163. [CrossRef]
186. Politzer, P.; Murray, J.S.; Clark, T. Halogen bonding and other σ-hole interactions: A perspective. *Phys. Chem. Chem. Phys.* **2013**, *15*, 11178–11189. [CrossRef] [PubMed]
187. Murray, J.S.; Zadeh, D.H.; Lane, P.; Politzer, P. The role of "excluded" electronic charge in noncovalent interactions. *Mol. Phys.* **2018**. [CrossRef]
188. Politzer, P.; Murray, J.S. The Hellmann-Feynman theorem: A perspective. *J. Mol. Model.* **2018**, *24*, 266. [CrossRef] [PubMed]
189. Bultinck, P.; Cardenas, C.; Fuentealba, P.; Johnson, P.A.; Ayers, P.W. Atomic Charges and the Electrostatic Potential Are Ill-Defined in Degenerate Ground States. *J. Chem. Theory Comput.* **2013**, *9*, 4779–4788. [CrossRef]
190. Ionescu, C.-M.; Sehnal, D.; Falginella, F.L.; Pant, P.; Pravda, L.; Boucha, T.; Vařeková, R.S.; Geidl, S.; Koča, J. Atomic Charge Calculator: Interactive web-based calculation of atomic charges in large biomolecular complexes and drug-like molecules. *J. Cheminform.* **2015**, *7*, 50. [CrossRef] [PubMed]

191. Hamad, S.; Balestra, S.R.G.; Bueno-Perez, R.; Calero, S.; Ruiz-Salvador, A.R. Atomic charges for modeling metal–organic frameworks: Why and how. *J. Solid State Chem.* **2015**, *223*, 144–151. [CrossRef]
192. Xu, Q.; Zhong, C. A General Approach for Estimating Framework Charges in Metal-Organic Frameworks. *J. Phys. Chem. C* **2010**, *114*, 5035–5042. [CrossRef]
193. Mobley, D.L.; Dumont, E.; Chodera, J.D.; Dill, K.A. Comparison of Charge Models for Fixed-Charge Force Fields: Small-Molecule Hydration Free Energies in Explicit Solvent. *J. Phys. Chem. B* **2007**, *111*, 2242–2254. [CrossRef]
194. Riniker, S. Fixed-Charge Atomistic Force Fields for Molecular Dynamics Simulations in the Condensed Phase: An Overview. *J. Chem. Inf. Model.* **2018**, *58*, 565–578. [CrossRef] [PubMed]
195. Martin-Noble, G.C.; Reilley, D.; Rivas, L.M.; Smith, M.D.; Schrier, J. EQeq+C: An Empirical Bond-Order Corrected Extended Charge Equilibration Method. *J. Chem. Theory Comput.* **2015**, *11*, 3364–3374. [CrossRef] [PubMed]
196. Lynden-Bell, R.M.; Stone, A.J. A model with charges and polarizability for $CS_2$ in an ionic liquid. *J. Chem. Sci.* **2017**, *129*, 883–890. [CrossRef]
197. Scholfield, M.R.; Ford, M.C.; Carlsson, A.-C.C.; Butta, H.; Mehl, R.A.; Ho, P.S. Structure–Energy Relationships of Halogen Bonds in Proteins. *Biochemistry* **2017**, *56*, 2794–2802. [CrossRef]
198. Scholfield, M.R.; Zanden, C.M.V.; Carter, M.; Shing Ho, P. Halogen bonding (X-bonding): A biological perspective. *Protein Sci.* **2013**, *22*, 139–152. [CrossRef]
199. Politzer, P.; Murray, J.S.; Lane, P.; Concha, M.C. Electrostatically driven complexes of $SiF_4$ with amines. *Int. J. Quant. Chem.* **2009**, *109*, 3773–3780. [CrossRef]
200. Politzer, P.; Murray, J.S.; Clark, T. Halogen bonding: An electrostatically-driven highly directional noncovalent interaction. *Phys. Chem. Chem. Phys.* **2010**, *12*, 7748–7757. [CrossRef] [PubMed]
201. Politzer, P.; Lane, P.; Concha, M.C.; Ma, Y.; Murray, J.S. An Overview of Halogen Bonding. *J. Mol. Model.* **2007**, *13*, 305–311. [CrossRef] [PubMed]
202. Murray, J.S.; Riley, R.E.; Politzer, P.; Clark, T. Directional weak intermolecular interactions: σ-hole bonding. *Aust. J. Chem.* **2010**, *63*, 1598–1607. [CrossRef]
203. Riley, K.E.; Tran, K.-A. Strength, character, and directionality of halogen bonds involving cationic halogen bond donors. *Faraday Discuss.* **2017**, *203*, 47–60. [CrossRef] [PubMed]
204. Yahia-Ouahmed, M.; Tognetti, V.; Joubert, L. Intramolecular halogen bonding: An interacting quantum atoms study. *Theor. Chem. Acc.* **2016**, *135*, 45. [CrossRef]
205. Lin, F.-Y.; MacKerell, A.D. Do Halogen–Hydrogen Bond Donor Interactions Dominate the Favorable Contribution of Halogens to Ligand–Protein Binding? *J. Phys. Chem. B* **2017**, *121*, 6813–6821. [CrossRef]
206. Neaton, J.B. A direct look at halogen bonds. *Science* **2017**, *358*, 167–168. [CrossRef]
207. Riley, K.E.; Hobza, P. Investigations into the Nature of Halogen Bonding Including Symmetry Adapted Perturbation Theory Analyses. *J. Chem. Theory Comput.* **2008**, *4*, 232–242. [CrossRef]
208. Mu, X.; Wang, Q.; Wang, L.-P.; Fried, S.D.; Piquemal, J.-P.; Dalby, K.N.; Ren, P. Modeling Organochlorine Compounds and the σ-Hole Effect Using a Polarizable Multipole Force Field. *J. Phys. Chem. B* **2014**, *118*, 6456–6465. [CrossRef]
209. Kolář, M.H.; Hobza, P. Computer Modeling of Halogen Bonds and Other σ-Hole Interactions. *Chem. Rev.* **2016**, *116*, 5155–5187. [CrossRef]
210. Johansson, M.P.; Swart, M. Intramolecular halogen–halogen bonds? *Phys. Chem. Chem. Phys.* **2013**, *15*, 11543–11553. [CrossRef] [PubMed]
211. Mo, Y.; Bao, P.; Gao, J. Energy decomposition analysis based on a block-localized wavefunction and multistate density functional theory. *Phys. Chem. Chem. Phys.* **2011**, *13*, 6760–6775. [CrossRef] [PubMed]
212. Bauzá, A.; Frontera, A. Electrostatically enhanced F···F interactions through hydrogen bonding, halogen bonding and metal coordination: An ab initio study. *Phys. Chem. Chem. Phys.* **2016**, *18*, 20381–20388. [CrossRef] [PubMed]
213. Bauzá, A.; Frontera, A. Theoretical study on σ- and π-hole carbon···carbon bonding interactions: Implications in CFC chemistry. *Phys. Chem. Chem. Phys.* **2016**, *18*, 32155–32159. [CrossRef] [PubMed]
214. Metrangolo, P.; Murray, J.S.; Pilati, T.; Politzer, P.; Resnati, G.; Terraneo, G. The fluorine atom as a halogen bond donor, viz. a positive site. *Cryst. Eng. Commun.* **2011**, *13*, 6593–6596. [CrossRef]
215. Metrangolo, P.; Murray, J.S.; Pilati, T.; Politzer, P.; Resnati, G.; Terraneo, G. Fluorine-centered halogen bonding: A factor in recognition phenomena and reactivity. *Cryst. Growth Des.* **2011**, *11*, 4238–4246. [CrossRef]

216. Panini, P.; Chopra, D. Understanding of Noncovalent Interactions Involving Organic Fluorine. In *Hydrogen Bonded Supramolecular Structures. Lecture Notes in Chemistry*; Li, Z.T., Wu, L.Z., Eds.; Springer: Berlin/Heidelberg, Germany, 2015; Volume 87.
217. Chaplot, S.L.; McIntyre, G.J.; Mierzejewski, A.; Pawley, G.S. Structure of 1,3,5-trichloro-2,4,6-trifluorobenzene. *Acta Crystallogr. B* **1981**, *37*, 1896–1900. [CrossRef]
218. Desiraju, G.R. Supramolecular Synthons in Crystal Engineering—A New Organic Synthesis. *Angew. Chem. Int. Ed.* **1995**, *34*, 2311–2327. [CrossRef]
219. Legon, A.C.; Walker, N.R. What's in a name? "Coinage-metal" non-covalent bonds and their definition. *Phys. Chem. Chem. Phys.* **2018**, *20*, 19332–19338. [CrossRef]
220. Ghosh, S.; Reddy, C.M.; Desiraju, G.R. Hexaiodobenzene: A redetermination at 100 K. *Acta Crystallogr. E* **2007**, *63*, o910–o911. [CrossRef]
221. Khotsyanova, T.L.; Smirnova, V.I. Crystal and Molecular Structure of hexaiodobenzene. *Kristallografiya* **1968**, *13*, 787–790.
222. Steer, R.J.; Watkins, S.F.; Woodward, P. Crystal and molecular structure of hexaiodobenzene. *J. Chem. Soc. C* **1970**, 403–408. [CrossRef]
223. Han, Z.; Czap, G.; Chiang, C.; Xu, C.; Wagner, P.J.; Wei, X.; Zhang, Y.; Wu, R.; Ho, W. Imaging the halogen bond in self-assembled halogenbenzenes on silver. *Science* **2017**, *358*, 206–210. [CrossRef]
224. Liu, M.; Zeng, Y.; Sun, Z.; Meng, L. Predicting the halogen-*n* (*n* = 3–6) synthons to form the "windmill" pattern bonding based on the halogen-bonded interactions. *J. Comput. Chem.* **2019**. [CrossRef]
225. Bader, R.F. *Atoms in Molecules: A Quantum Theory*; Oxford University Press: Oxford, UK, 1990.
226. Johnson, E.R.; Keinan, S.; Mori-Sánchez, P.; Contreras-García, J.; Cohen, A.J.; Yang, W. Revealing Noncovalent Interactions. *J. Am. Chem. Soc.* **2010**, *132*, 6498–6506. [CrossRef]
227. De Silva, P.; Corminboeuf, C. Simultaneous Visualization of Covalent and Noncovalent Interactions Using Regions of Density Overlap. *J. Chem. Theory Comput.* **2014**, *10*, 3745–3756. [CrossRef]
228. Becke, A.D.; Edgecombe, K.E. A simple measure of electron localization in atomic and molecular systems. *J. Chem. Phys.* **1990**, *92*, 5397–5403. [CrossRef]
229. Silvi, B.; Savin, A. Classification of chemical bonds based on topological analysis of electron localization functions. *Nature* **1994**, *371*, 683. [CrossRef]
230. Yu, M.; Trinkle, D.R. Accurate and efficient algorithm for Bader charge integration. *J. Chem. Phys.* **2011**, *134*, 064111. [CrossRef]
231. Parr, R.G.; Weitao, Y. *Density-Functional Theory of Atoms and Molecules*; Oxford University Press: Oxford, UK, 1995.
232. Keith, T.A. *AIMAll, version 17.01.25*; TK Gristmill Software: Overland Park, KS, USA, 2016; Available online: http://aim.tkgristmill.com (accessed on 7 February 2019).
233. Bader, R.F.W. A Bond Path: A Universal Indicator of Bonded Interactions. *J. Phys. Chem. A* **1998**, *102*, 7314–7323. [CrossRef]
234. Panini, P.; Gonnade, R.G.; Chopra, D. Experimental and computational analysis of supramolecular motifs involving $Csp_2$(aromatic)–F and $CF_3$ groups in organic solids. *New J. Chem.* **2016**, *40*, 4981–5001. [CrossRef]
235. Bankiewicz, B.; Matczak, P.; Palusiak, M. Electron Density Characteristics in Bond Critical Point (QTAIM) versus Interaction Energy Components (SAPT): The Case of Charge-Assisted Hydrogen Bonding. *J. Phys. Chem. A* **2012**, *116*, 452–459. [CrossRef] [PubMed]
236. Checinska, L.; Grabowsky, S.; Malecka, M.; Rybarczyk-Pirek, A.J.; Józwiak, A.; Paulmann, C.; Luger, P. Experimental and theoretical electron-density study of three isoindole derivatives: Topological and Hirshfeld surface analysis of weak intermolecular interactions. *Acta Crystallogr. B* **2011**, *67*, 569–581. [CrossRef] [PubMed]
237. Varadwaj, A.; Varadwaj, P.R.; Marques, H.M.; Yamashita, K. Halogen in materials design: Revealing the nature of hydrogen bonding and other non-covalent interactions in the polymorphic transformations of methylammonium lead tribromide perovskite. *Mater. Today Chem.* **2018**, *9*, 1–16. [CrossRef]
238. Varadwaj, P.R.; Varadwaj, A.; Marques, H.M.; Yamashita, K. Significance of hydrogen bonding and other noncovalent interactions in determining octahedral tilting in the $CH_3NH_3PbI_3$ hybrid organic–inorganic halide perovskite solar cell semiconductor. *Sci. Rep.* **2019**, *9*, 50. [CrossRef] [PubMed]
239. Escudero-Adán, E.C.; Bauzá, A.; Lecomte, C.; Frontera, A.; Ballester, P. Boron triel bonding: A weak electrostatic interaction lacking electron-density descriptors. *Phys. Chem. Chem. Phys.* **2018**, *20*, 24192–24200. [CrossRef] [PubMed]

240. Lane, J.R.; Schrøder, S.D.; Saunders, G.C.; Kjaergaard, H.G. Intramolecular Hydrogen Bonding in Substituted Aminoalcohols. *J. Phys. Chem. A* **2016**, *120*, 6371–6378. [CrossRef] [PubMed]
241. Lane, J.R.; Contreras-García, J.; Piquemal, J.-P.; Miller, B.J.; Kjaergaard, H.G. Are Bond Critical Points Really Critical for Hydrogen Bonding? *J. Chem. Theory Comput.* **2013**, *9*, 3263–3266. [CrossRef]
242. Outeiral, C.; Vincent, M.A.; Martín Pendás, Á.; Popelier, P.L.A. Revitalizing the concept of bond order through delocalization measures in real space. *Chem. Sci.* **2018**, *9*, 5517–5529. [CrossRef]
243. Poater, J.; Duran, M.; Solà, M.; Silvi, B. Theoretical Evaluation of Electron Delocalization in Aromatic Molecules by Means of Atoms in Molecules (AIM) and Electron Localization Function (ELF) Topological Approaches. *Chem. Rev.* **2005**, *105*, 3911–3947. [CrossRef]
244. Poater, J.; Fradera, X.; Duran, M.; Solá, M. The delocalization index as an electronic aromaticity criterion: Application to a series of planar polycyclic aromatic hydrocarbons. *Chem. Eur. J.* **2003**, *9*, 400–406. [CrossRef] [PubMed]
245. Firme, C.L.; Antunes, O.A.C.; Esteves, P.M. Relation between bond order and delocalization index of QTAIM. *Chem. Phys. Lett.* **2009**, *468*, 129–133. [CrossRef]
246. Farrugia, L.J.; Evans, C.; Lentz, D.; Roemer, M. The QTAIM Approach to Chemical Bonding Between Transition Metals and Carbocyclic Rings: A Combined Experimental and Theoretical Study of $(\eta^5\text{-}C_5H_5)Mn(CO)_3$, $(\eta^6\text{-}C_6H_6)Cr(CO)_3$, and (E)-$((\eta^5\text{-}C_5H_4)CF{=}CF(\eta^5\text{-}C_5H_4))(\eta^5\text{-}C_5H_5)_2Fe_2$. *J. Am. Chem. Soc.* **2009**, *131*, 1251–1268. [CrossRef] [PubMed]
247. Monza, E.; Gatti, C.; Lo Presti, L.; Ortoleva, E. Revealing Electron Delocalization through the Source Function. *J. Phys. Chem. A* **2011**, *115*, 12864–12878. [CrossRef] [PubMed]
248. Bader, R.F.W.; MacDougall, P.J. Toward a theory of chemical reactivity based on the charge density. *J. Am. Chem. Soc.* **1985**, *107*, 6788–6795. [CrossRef]
249. Cremer, D.; Kraka, E. A Description of the Chemical Bond in Terms of Local Properties of Electron Density and Energy. *Croat. Chem. Acta* **1984**, *57*, 1259–1281.
250. Cremer, D.; Kraka, E. Chemical Bonds without Bonding Electron Density—Does the Difference Electron-Density Analysis Suffice for a Description of the Chemical Bond? *Angew. Chem. Int. Ed. Engl.* **1984**, *23*, 627–628. [CrossRef]
251. Kraka, E.; Cremer, D. *Chemical Implications of Local Features of the Electron Density Distribution*; Springer-Verlag: Heidelberg, Germany, 1990; Volume 2.
252. Lane, J.R.; Hansen, A.S.; Mackeprang, K.; Kjaergaard, H.G. Kinetic Energy Density as a Predictor of Hydrogen-Bonded OH-Stretching Frequencies. *J. Phys. Chem. A* **2017**, *121*, 3452–3460. [CrossRef] [PubMed]
253. Varadwaj, P.R.; Marques, H.M. The physical chemistry of coordinated aqua-, ammine-, and mixed-ligand $Co^{2+}$ complexes: DFT studies on the structure, energetics, and topological properties of the electron density. *Phys. Chem. Chem. Phys.* **2010**, *12*, 2126–2138. [CrossRef]
254. Varadwaj, P.R.; Marques, H.M. The physical chemistry of $[M(H_2O)_4(NO_3)_2]$ (M = $Mn^{2+}$, $Co^{2+}$, $Ni^{2+}$, $Cu^{2+}$, $Zn^{2+}$) complexes: Computational studies of their structure, energetics and the topological properties of the electron density. *Theor. Chem. Acc.* **2010**, *127*, 711–725. [CrossRef]
255. Lefebvre, C.; Rubez, G.; Khartabil, H.; Boisson, J.-C.; Contreras-García, J.; Hénon, E. Accurately extracting the signature of intermolecular interactions present in the NCI plot of the reduced density gradient versus electron density. *Phys. Chem. Chem. Phys.* **2017**, *19*, 17928–17936. [CrossRef] [PubMed]
256. Lefebvre, C.; Khartabil, H.; Boisson, J.-C.; Contreras-García, J.; Piquemal, J.-P.; Hénon, E. The Independent Gradient Model: A New Approach for Probing Strong and Weak Interactions in Molecules from Wave Function Calculations. *ChemPhysChem* **2018**, *19*, 724–735. [CrossRef] [PubMed]
257. An, X.; Kang, Y.; Li, G. The interaction between chitosan and tannic acid calculated based on the density functional theory. *Chem. Phys.* **2019**, *520*, 100–107. [CrossRef]
258. Kyzyma, O.; Bashmakova, N.; Gorshkova, Y.; Ivankov, O.; Mikheev, I.; Kuzmenko, M.; Kutovyy, S.; Nikolaienko, T. Interaction between the plant alkaloid berberine and fullerene $C_{70}$: Experimental and quantum-chemical study. *J. Mol. Liquids* **2019**, *278*, 452–459. [CrossRef]
259. Venkataramanan, N.S.; Suvitha, A. Nature of bonding and cooperativity in linear DMSO clusters: A DFT, AIM and NCI analysis. *J. Mol. Graph. Model.* **2018**, *81*, 50–59. [CrossRef]
260. Zhao, X.; Huang, S.; Liu, Y.; Li, J.; Zhu, W. Effects of Noncovalent Interactions on the Impact Sensitivity of HNS-Based Cocrystals: A DFT Study. *Cryst. Growth Des.* **2019**, *19*, 756–767. [CrossRef]
261. Lu, T.; Chen, F. A multifunctional wavefunction analyzer. *J. Comput. Chem.* **2012**, *33*, 580–592. [CrossRef]

262. Humphrey, W.; Dalke, A.; Schulten, K. VMD—Visual Molecular Dynamics. *J. Mol. Graph.* **1996**, *14*, 33–38. [CrossRef]
263. Greer, S.C.; Meyer, L. $CF_4$: Crystal Structure and Solid Phase Diagram with Ar. *J. Chem. Phys.* **1969**, *51*, 4583–4586. [CrossRef]
264. Bol'shutkin, D.N.; Gasan, V.M.; Prokhvatilov, A.I.; Erenburg, A.I. The crystal structure of α-$CF_4$. *Acta Cryst. B* **1972**, *28*, 3542–3547. [CrossRef]
265. Pepè, G.; Gay, J.-M. Structure of α-$CF_4$ at low temperature. *J. Chem. Phys.* **1989**, *90*, 5735–5737. [CrossRef]
266. Fitch, A.N. The structure of solid carbon tetrafluoride. *Z. Krist. Cryst. Mater.* **1993**, *203*, 29–40.
267. Metrangolo, P.; Resnati, G. Halogen Versus Hydrogen. *Science* **2008**, *321*, 918–919. [CrossRef] [PubMed]
268. Donald, K.J.; Tawfik, M. The Weak Helps the Strong: σ-Holes and the Stability of $MF_4$·Base Complexes. *J. Phys. Chem. A* **2013**, *117*, 14176–14183. [CrossRef]
269. Osuna, R.M.; Hernández, V.; Navarrete, J.T.L.; D'Oria, E.; Novoa, J.J. Theoretical evaluation of the nature and strength of the F···F intermolecular interactions present in fluorinated hydrocarbons. *Theor. Chem. Acc.* **2011**, *128*, 541–553. [CrossRef]
270. Wheeler, S.E.; Bloom, J.W.G. Toward a More Complete Understanding of Noncovalent Interactions Involving Aromatic Rings. *J. Phys. Chem. A* **2014**, *118*, 6133–6147. [CrossRef]
271. Grabowski, S. Lewis Acid Properties of Tetrel Tetrafluorides—The Coincidence of the σ-Hole Concept with the QTAIM Approach. *Crystals* **2017**, *7*, 43. [CrossRef]
272. Alabugin, I.V.; Gilmore, K.M.; Peterson, P.W. Hyperconjugation. *WIREs Comput. Mol. Sci.* **2011**, *1*, 109–141. [CrossRef]
273. Piermarini, G.J.; Braun, A.B. Crystal and molecular structure of CCl4 III: A high pressure polymorph at 10 kbar. *J. Chem. Phys.* **1973**, *58*, 1974–1982. [CrossRef]
274. Cohen, S.; Powers, R.; Rudman, R. Polymorphism of the crystalline methylchloromethane compounds. VI. The crystal and molecular structure of ordered carbon tetrachloride. *Acta Cryst. B* **1979**, *35*, 1670–1674. [CrossRef]
275. More, M.; Baert, F.; Lefebvre, J. Solid-state phase transition in carbon tetrabromide $CBr_4$. I. The crystal structure of phase II at room temperature. *Acta Cryst. B* **1977**, *33*, 3681–3684. [CrossRef]
276. Lindeman, S.V.; Hecht, J.; Kochi, J.K. The Charge-Transfer Motif in Crystal Engineering. Self-Assembly of Acentric (Diamondoid) Networks from Halide Salts and Carbon Tetrabromide as Electron-Donor/Acceptor Synthons. *J. Am. Chem. Soc.* **2003**, *125*, 11597–11606. [CrossRef]
277. Eucken, A. Rotation von Molekeln und Iongruppen in Kristallen. *Z. Elektrochem. Angew. Phys. Chem.* **1939**, *45*, 126–150.
278. Pohl, S. Die Kristallstruktur von $CI_4$. *Z. Krisattlogr.* **1982**, *159*, 211. [CrossRef]
279. Troyanov, S.I.; Shustova, N.B.; Popov, A.A.; Sidorov, L.N.; Kemnitz, E. Preparation and Structural Characterization of Two Kinetically Stable Chlorofullerenes, $C_{60}Cl_{28}$ and $C_{60}Cl_{30}$. *Angew. Chem.* **2005**, *117*, 436–439. [CrossRef]
280. Troshin, P.A.; Kemnitz, E.; Troyanov, S.I. *CCDC 230207: Experimental Crystal Structure Determination*; Cambridge Crystallographic Data Centre: Cambridge, UK, 2004; p. 2675.
281. Singh, G.; Verma, R.; Gadre, S.R. Understanding Packing Patterns in Crystals by Analysis of Small Aggregates: A Case Study of CS2. *J. Phys. Chem. A* **2015**, *119*, 13055–13063. [CrossRef] [PubMed]
282. Douvris, C.; Stoyanov, E.S.; Tham, F.S.; Reed, C.A. Isolating fluorinated carbocations. *Chem. Commun.* **2007**, 1145–1147. [CrossRef] [PubMed]
283. Metrangolo, P.; Pilati, T.; Resnati, G.; Stevenazzi, A. Metric engineering of perfluorocarbon–hydrocarbon layered solids driven by the halogen bonding. *Chem. Commun.* **2004**, 1492–1493. [CrossRef]
284. Metrangolo, P.; Präsang, C.; Resnati, G.; Liantonio, R.; Whitwood, A.C.; Bruce, D.W. Fluorinated liquid crystals formed by halogen bonding. *Chem. Commun.* **2006**, 3290–3292. [CrossRef]
285. Brisdon, A.K.; Muneer, A.M.T.; Pritchard, R.G. Halogen bonding in a series of $Br(CF_2)_nBr$–DABCO adducts ($n$ = 4, 6, 8). *Acta Crystallogr. C* **2017**, *73*, 874–879. [CrossRef]

286. Liu, X.; McMillen, C.D.; Thrasher, J.S. Cooperative intermolecular S–Cl···O and F···F associations in the crystal packing of α,ω-di(sulfonyl chloride) perfluoroalkanes, $ClSO_2(CF_2)_nSO_2Cl$, where $n$ = 4, 6. *New J. Chem.* **2018**, *42*, 10484–10488. [CrossRef]
287. Kawaguchi, S.-I.; Minamida, Y.; Ohe, T.; Nomoto, A.; Sonoda, M.; Ogawa, A. Synthesis and Properties of Perfluoroalkyl Phosphine Ligands: Photoinduced Reaction of Diphosphines with Perfluoroalkyl Iodides. *Angew. Chem. Int. Ed.* **2013**, *52*, 1748–1752. [CrossRef] [PubMed]